CHARLES PANKOW
FOUNDATION
Building Innovation through Research

Setting Bar-Bending Requirements for High-Strength Steel Bars

Stephen D. Zhao
Wassim M. Ghannoum

Sponsored by:
The Charles Pankow Foundation
The Concrete Reinforcing Steel Institute
The American Concrete Institute's Foundation, Concrete Research Council

June 30, 2016

Setting Bar-Bending Requirements for High-Strength Steel Bars

CPF Research Grant Agreement #01-15

Funded by

CHARLES PANKOW FOUNDATION
P.O. Box 820631
Vancouver, Washington 98682
Co-funded by
The Concrete Reinforcing Steel Institute's, and
The American Concrete Institute's Foundation

Principal Investigator: Dr. Wassim M. Ghannoum

Graduate Research Assistant: Stephen Zhao

Industry Support:

Industry Champions: Mike Mota, VP Engineering, CRSI

Advisory Panel: Salem Faza, MMFX

Denis Hunter, Gerdau

Erik Nissen, NUCOR Steel Seattle

Jacob Seltzer, CMC

Acknowledgements

This project was made possible by funding from the Charles Pankow Foundation, the Concrete Reinforcing Steel Institute, and the American Concrete Institute's Foundation. The steel donations of CMC, Gerdau, MMFX, and NUCOR Steel Inc. Seattle are gratefully acknowledged. The bending was performed at no cost to this project by the fabrication facility at Harris Rebar in New Braunfels. The technical contributions of Mike Mota, the project's industry champion, David McDonald, CRSI President and CEO, and the advisory panel is gratefully acknowledged.

Abstract

Setting Bar-Bending Requirements for High-Strength Steel Bars

The reinforcing steel industry is currently developing high-strength reinforcing bars with specified yield strengths of 80 and 100 ksi due to increased demand for such grades in concrete construction. However, none of the higher steel grades are able to match the benchmark mechanical properties of grade 60 steel; with each high-strength variant diverging from benchmark behavior in different ways. There is concern that the less ductile higher grade reinforcing bars may fracture at the bends and may require larger bend diameters. Limited tests are available that investigate the relation between bend diameter and the ductility, or conversely the brittleness, of reinforcing bars at bends. No such tests exist for the newly developed high-strength reinforcement having yield strengths exceeding 80 ksi. Bend/re-bend (or re-straightening) tests were conducted on grade 60 and higher grade reinforcing bars to investigate relations between bend diameters and bend performance. The tests were monitored using digital image correlation technology from which never-before recorded comparative measures were obtained. Test results indicated significant differences in bend performance between bars of varying grades, such that wider bend diameters may be necessary for certain higher grade bars.

Table of Contents

List of Tables

List of Figures

CHAPTER 1: Introduction

1.1 Motivation

There is an increasing need for higher strength reinforcing steel in seismic and non-seismic applications. A main driver for higher strengths is the need to reduce bar congestion in seismic designs and reduce material quantities generally. Steel manufacturers in the United States are currently developing reinforcing bars with yield strengths reaching 120 ksi and with varying mechanical and chemical properties. The new high-strength bars are being produced using varying methods, the most common of which are quenching and tempering, and micro-alloying. However, none of the higher steel grades in production are able to match the benchmark mechanical properties of grade 60 steel; with each high-strength variant diverging from benchmark behavior in different ways. There is concern that the less ductile higher steel grades may fracture at the bends and may require larger bend diameters. Anecdotal evidence has been reported of high-strength bars (HSRB) fracturing at the bends when dropped at a construction site (particularly in cold weather).

In this report, high-strength reinforcing bars (HSRB) are defined as steel reinforcing bars with yield strengths of 80 ksi or higher (i.e., grade 80 or higher).

1.2 Objectives and Scope

Efforts are underway to produce new ASTM specifications for HSRB to give steel mills a clear target to aim for in their production of HSRB. To complete the ASTM specifications for HSRB, bar bending requirements need to be revisited given recent evidence of HSRB fracturing at bends. Limited tests are available that investigate the relation between bend diameter and the ductility, or conversely the brittleness, of

reinforcing bars at bends. No such tests exist for the newly developed high-strength reinforcement having yield strengths exceeding 80 ksi.

The main objectives of this study are to evaluate the performance under load of bends satisfying ACI 318-14 (2014) in HSRB, and compare that performance with the benchmark performance of grade 60 bars bent in the same way and to same diameters.

To achieve project objectives, bend and re-bend tests, such as those specified in New-Zealand and United-Kingdom standards (AS/NZS 4761:2001; BS 4449:2005+A2:2009), were conducted on HSRB and grade 60 bars. The tests provided a measure of the reserve strength and ductility of bar bends, which cannot be obtained using visual inspection of bend cracking, as described in ASTM standards for reinforcing bars (ASTM A615, A706, A1035). HSRB with varying manufacturing processes, grades, diameters, and bend diameters were tested. The range of parameters was selected to represent the most typical bar properties and manufacturing processes currently in production or development in the United States. All bars were fully strain-aged after bending and prior to re-bending, to represent typical conditions of bar bends in concrete structures. Strain aging tests were conducted to evaluate the effects of strain aging on all bar types considered, and to determine the required wait time after pre-straining or bending before re-bending could be performed.

CHAPTER 2: Background

2.1 Metallurgy

Three main production methods are currently used in the United States to produce HSRB. Each of these methods generates HSRB with differing mechanical and chemical properties. The three processes are quenching and tempering, micro-alloying, and manipulation of the microstructure using alloying and heat treatment. Steel bars produced through quenching and tempering typically exhibit relatively low tensile to yield strength (T/Y) ratios and relatively high strains at fracture. Steel bars produced by micro-alloying have a relatively high tensile to yield strength ratio and relatively high strains at fracture. HSRB produced using the third production method are the only ones with ASTM specifications (ASTM A1035 (2011)). These bars typically have large tensile to yield strength ratios but relatively low strains at fracture. The differences between the three production methods and the bar properties they produce are briefly discussed in this section.

2.1.1 Quenching and Tempering (QT)

The process of quenching and tempering (QT) consists of quenching the steel immediately after rolling and then allowing the bar to be tempered by the heat remaining in the core while gradually cooling. As a result, the QT process produces steel with mechanical properties that vary significantly between its inner core layer and its outer skin layer, with the inner core having a lower yield strength and more ductility than the outer layer. QT treated bars retain their yield plateau since they have not been strain hardened and, since the overall chemical composition has not been altered, they can be weldable if their chemistry satisfies ASTM A706 requirements. QT steel typically exhibits a low T/Y ratio on the order of 1.15 for grade 100 reinforcing bars. Slavin and Ghannoum (2015) provides more details about the QT process.

2.1.2 Micro-Alloying (MA)

Micro-alloying is a process that involves introducing small amounts of alloys in order to achieve the desired properties in steel bars. Vanadium is one of the alloys most commonly used to increase the strength of reinforcing bars. It increases strength and fracture toughness primarily due to inhibition of grain growth during heat-treatment and the precipitation of carbides and nitrides. The use of Vanadium can reduce the amount of carbon needed to achieve higher strengths and is therefore useful for achieving weldable HSRB. Micro-alloying can produce a marked yield point and a T/Y ratio larger than that from quenched and tempered steels (on the order of 1.25 for grade 100 reinforcing bars). Slavin and Ghannoum (2015) provides more details about the micro-alloying process.

2.1.3 Patented Microstructure Manipulation (MMFX)

The patented MMFX process involves manipulating the microstructure of steel to obtain the desired mechanical properties and strength. The process generates bars with stress-stain relations that do not have a well-defined yield point, exhibit a relatively high T/Y ratio, but have relatively low fracture elongations. The MMFX steel bars satisfy the ASTM A1035 specifications. The A1035 specifications maintain the same bend diameter for testing bar bends as in the ASTM A615 and A706 specifications used for the vast majority of bars currently in production in the United-States. ACI 318-14 (2014) allows the use of A1035 grade 100 bars in confinement applications and requires them to be bent at the same diameter as other steel grades including grade 60.

2.2 Strain Aging

Strain aging is defined as the process by which steel strained beyond its elastic limit undergoes time dependent changes in it mechanical properties. Typically, reinforcing bars strained beyond their elastic limit will, over time, see an increase in their tensile

strength and a decrease in their ductility as illustrated in Figure 1. Strain aging is also proven to affect the brittle transition temperature in steel (G.T. Van Rooyen, 1986). Factors affecting strain aging include the steel composition, temperature, and the time elapsed since large strains were incurred. Strain aging is mostly attributed to nitrogen reallocation within the steel matrix (G.T. Van Rooyen, 1986). Higher temperatures accelerate this process; hence strain aging occurs much faster in warmer regions. Typically, most of the effects of stain aging in steel reinforcing bars will occur within a few months after inelastic strains are incurred (G.T. Van Rooyen, 1986).

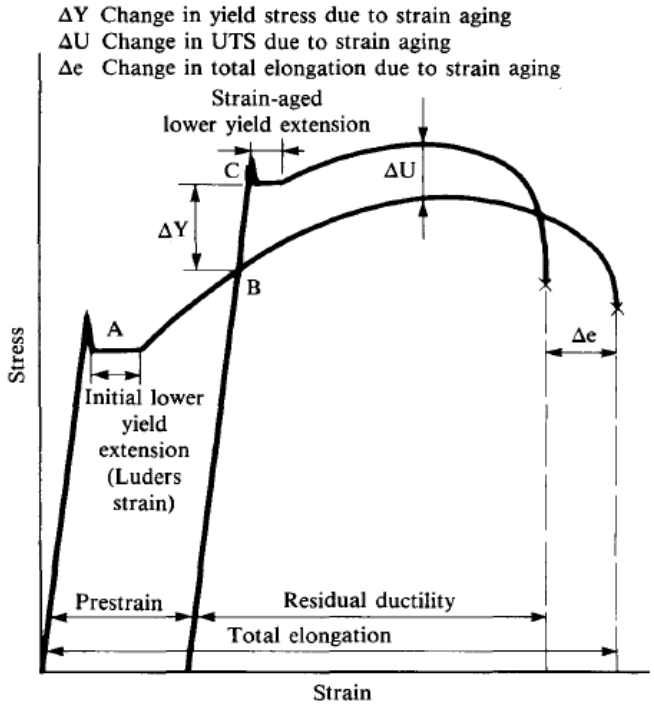

Figure 1: Typical stress-strain curves showing the effects of strain aging (G.T Van Rooyen, 1986)

As reinforcing bars are bent, they experience large inelastic strains. Bar bends are therefore prone to strain aging embrittlement, which may cause them to fracture prematurely and limit their ability to sustain inelastic deformations during structural loading.

Research done by G.T Van Rooyen (1986) and Rashid (1976) suggests that micro-alloyed steel including titanium and vanadium can lower the effects of strain aging on steel bars. Such alloys have properties that allow them to bond with the nitrogen in the composition to form nitrides. These reactions limit the amount of free nitrogen throughout the steel that is attributed to strain aging effects.

2.3 Bend Tests

Three main categories of experimental tests are useful for investigating the behavior of bends in reinforcing bars, with each category of tests geared to answer a particular set of questions:

1 - Visual inspections of bends (ASTM bend tests)

2 - Bend/re-bend tests

3 - Bend tests in concrete

1 - ASTM reinforcing bar specifications (such as A615, A706, and A1035) specify the following bending requirement “The bend test specimen shall withstand being bent around a pin without cracking on the outside of the bend portion.” The required bend test therefore involves bending bars to 180^{o} (or 90^{o} for #14 and larger bars) at a specified pin bend diameter. A visual inspection is then performed to identify cracking at the bend. If no cracking is visually observed, a specimen is deemed to pass the bend test. The pin diameters specified in ASTM bend tests are tighter than those used in construction, as specified by ACI 318-14 or the CRSI handbook, and therefore provide some degree of safety against observing cracking in bends during bar fabrication. However, while this test is simple to perform, it does not provide a measure of the reserve strength and ductility of bar bends, as a load-test can. It is possible that micro-cracking not visible to the eye may compromise the performance of bars in-situ.

2 - Bend and re-bend tests have been performed in New-Zealand (AS/NZS 4761:2001; Hopkins and Poole (2008) and the United-Kingdom (BS4449 (2005)). In these tests, bar coupons are bent to the required angle and bend diameter (Figure 2), and then straightened at either quasi-static or dynamic loading rates. For grade 60 bars, work hardening increases steel strength at the bends and typically causes the coupons to fracture away from the bends in a ductile manner. However, if bars have limited ductility such as HSRB, strain demands at the bends may cause cracks, which can make bends weaker than the unbent portions of the bars and more susceptible to brittle fracture. If a bar fails in a brittle manner at a bend, it is considered to have failed the bend/re-bend test. If, however, a bar fails in a ductile manner, then it is deemed to have passed the test. This type of test has the advantage of putting bar-bends under load and therefore provides a direct measure of the strength and ductility performance of bar-bends.

Hopkins and Poole (2008) conducted bend and re-bend tests on newly introduced grade 500E (~72 ksi) bars in New Zealand and Australia. The study accounted for strain aging and explored the effects of cold temperature on the performance of bends. The study tested bars produced using micro-alloying (MA), as well as quenching and tempering (QT). Test results confirmed that current bar bend diameters used in New Zealand were adequate for that grade of steel, regardless of the manufacturing process. A marked worsening of the performance of bar-bends was observed at temperatures below -10^{o} Celsius.

It should be noted that the bend/re-bend tests apply larger demands on the bar bends than they would normally see in a concrete structure. For this reason, it is best to compare the bend/re-bend performance of HSRB to that of grade 60 bars, which have been used for decades and have shown adequate performance in concrete members.

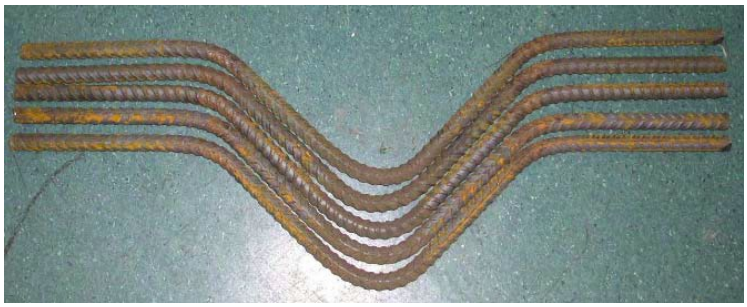

Figure 2: Picture of bend/re-bend test coupons (NIST GCR 13-917-30)

3 - Bends in reinforcing bars can also be tested in concrete. In such tests, the interaction between the concrete and bar-bends can be investigated. Simplified versions of the test include embedding a hooked bar into a concrete block and pulling on it until failure. Possible failure modes that can be expected in block tests include: bar fracture outside the block where demands on the bar are highest, bar failure inside the block closer to or at the bend, or splitting of the concrete block. Such tests, however, may not expose bends to the worst loading they could experience in a structure, as the surrounding concrete can relieve the bends of some load. In contrast, some of the worst loading on bar-bends can arise in confinement applications, where an expanding concrete core partially straightens hoop bends while applying high tensile loads to them. Another critical application for bar-bends is in damaged regions, where bond to concrete and its beneficial effects on bends are reduced (e.g., joints under severe seismic loading, or severely cracked regions).

Nevertheless, tests of bar bends in concrete members are essential for validating the adequate performance of bar bends in HSRB. However, such tests are expensive to conduct and do not easily lend themselves to the task of determining minimum bend diameters while exploring the numerous variables that affect the performance of bar-bends.

CHAPTER 3: Experimental Program

3.1 Overview of Program

The experimental program consisted of three types of tests.

1. Bend/re-bend Tests
2. Strain Aging Tests
3. Monotonic Tests

3.1.1 Bend/re-bend Tests

Objectives: Bend/re-bend tests were conducted to quantify residual strength and elongation capacities under load in bar bends and compare high-strength reinforcing bar bend performance with that of grade 60 bar bends.

3.1.1.1 Specimen Details and Preparation

The bend/re-bend specimens were similar to those used in New-Zealand by Hopkins and Poole (2008) and described in BS 4449:2005+A2:2009 (2005). Bar specimens were constructed by bending straight coupons into a "V" shape having two 45 degree bends and one 90 degree bend (Figure 2). Coupons were bent by a local fabricator according to typical bending practices using an RMS Arnold Bender (Figure 3). Bars were bent about their weak axis, with the longitudinal ribs facing vertically in the bender. Bending was conducted at a room temperature of about 20°C. Bars were then left to strain age prior to re-bending them in tension until fracture in a uniaxial testing machine. Tolerance templates were used to ensure that specimens were bent accurately (Figure 4). The internal bend diameters for the first batch of bar specimens were the smallest specified in ACI 318-14. The dimensions of bend/re-bend coupons with those bend diameters are presented in Figure 5. In subsequent bending, some #5 bar bend diameters were increased to $5d_b$ and $6d_b$ (with d_b = bar nominal diameter).

Figure 3: RMS Arnold Bender used to bend specimens

Figure 4: Verifying bend specimen tolerance

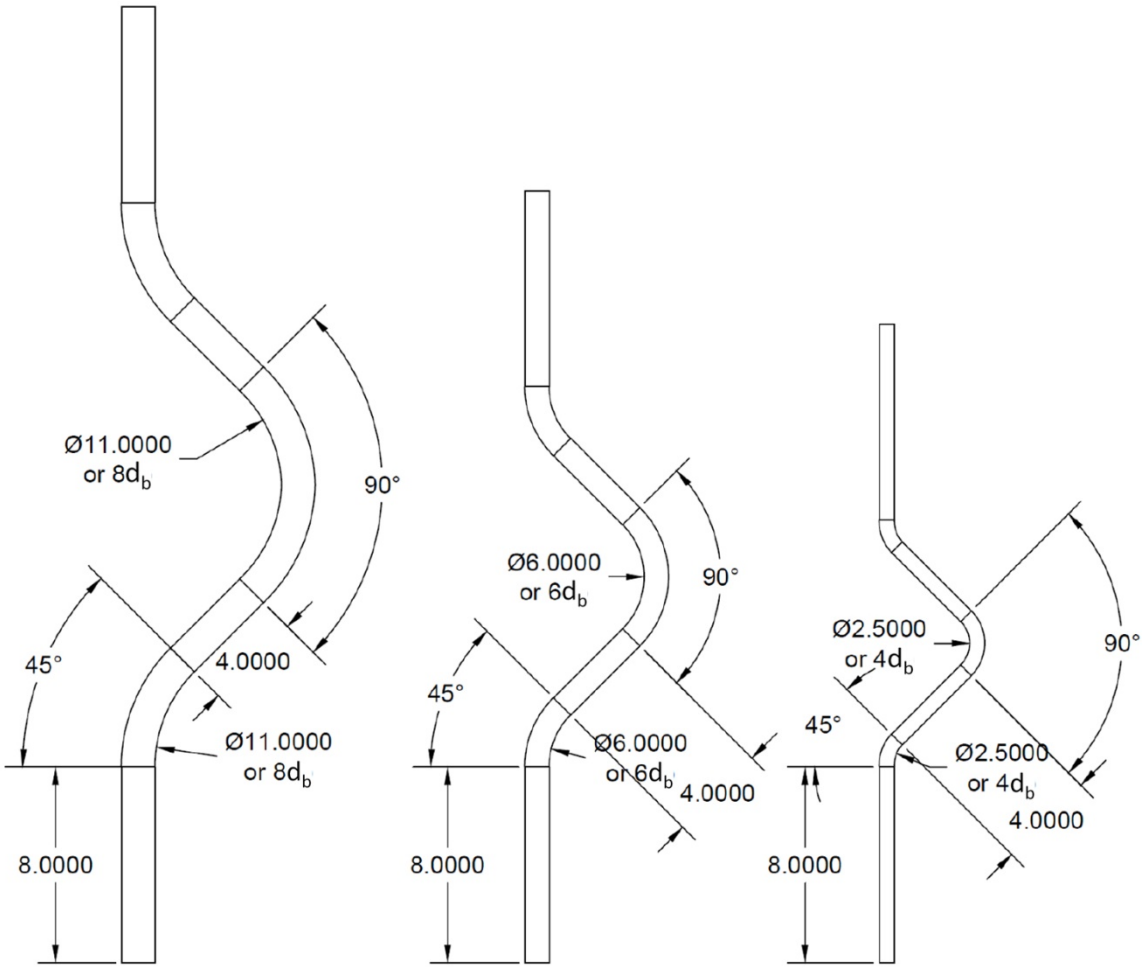

Figure 5: Specimen dimensions for #11, #8 and #5 bars with ACI 318-14 minimum bend diameter (d_b = bar nominal diameter)

3.1.1.2 Controlled Test Parameters

a- **<u>Steel Grade and Specifications:</u>** A706 (high ductility) and A615 (lower ductility) grade 60 bars were tested to provide benchmark performance. Grade 60 bars were obtained from three mills to obtain a representative sample of current production. HSRB produced using the main three production methods in the U.S. were also tested: MA (Micro-Alloying), QT (Quenching and Tempering), and

MMFX (ASTM A1035). The main focus in HSRB was on grade100 steel (having a yield strength equal to or higher than 100 ksi) but limited tests were conducted on grade 80 bars as well. In all, steel bars from four manufacturers were tested:

a. Manufacturer 1 (M1): Micro Alloyed Steel (MA)

b. Manufacturer 2 (M2): Patented Microstructure MMFX (ASTM A1035)

c. Manufacturer 3 (M3): Combination of Quench and Tempering and Micro Alloying (QT)

d. Manufacturer 4 (M4): Combination of Quench and Tempering and Micro Alloying (QT)

b- **Bar Size**: Three bar sizes were tested in this study covering a common range of sizes used in construction. The bars sizes used were #5, #8, and #11.

c- **Bend Diameters:** Bar specimens were first bent to the current ACI 318-14 minimum bend diameters. For #11 bars, the internal bend diameter was about 8 d_b. For #8 bars, the internal bend diameter was about $6d_b$. For #5 bars, the minimum bend diameter for transverse reinforcement was initially targeted, which is $4d_b$. However, after observing poorer performance in #5 HSRB at that bend diameter, #5 bars were bent and tested with $5d_b$ and $6d_b$ bend diameters. The latter bend diameter of $6d_b$ corresponds to the ACI 318-14 minimum bend diameters for #5 longitudinal or other bars in tension. It is noteworthy that the selected bar sizes (#5, #8, and #11) correspond to the largest size with a given bend diameter before the next bigger size requires a larger bend diameter in ACI 318-14.

Due to bending pin availability and spring-back in the bending process, final internal bend diameters were close to but not exactly equal to their target values. Table 1 lists the target ACI 318-14, as well as the mean achieved inside

bend diameter ratios for the 90 degree bends in the specimens (β_{ACI} = ACI 318-14 bend diameter / d_b and β_{Actual} = mean measured inside bend diameter / d_b). The table also lists the pin diameters used during bending and its associated bend ratio (β_{Pin} = pin diameter / d_b).

Table 1: Measured β for various bar sizes vs β from pin used for bending

	Target β_{ACI} (d_b)	Mean Measured β_{Actual} (d_b)	Pin Diameter (in.)	β_{Pin} (d_b)	Spring-back Difference = (β_{Actual} - β_{Pin}) / β_{Actual}	Error from Target = (β_{ACI} - β_{Actual}) / β_{ACI}
#11 ($8d_b$) 4 Samples	8	7.82	10.0	7.30	7.1%	2.3%
#8 ($6d_b$) 4 Samples	6	5.64	5.0	5.00	12.7%	6.1%
#5 ($6d_b$) 2 Samples	6	5.39	3.0	4.80	12.3%	10.1%
#5 ($5d_b$) 3 Samples	5	4.80	2.5	4.00	20.0%	4.0%
#5 ($4d_b$) 3 Samples	4	3.59	2.0	3.20	12.3%	10.2%

As can be seen in Table 1, the mean actual bend diameters were less than 10% lower than the target bend diameters. Bending pins were only offered in ½" increments, hence the pin diameters were chosen such that the final bend diameters were as close to target diameters as possible but not larger. The actual bend diameters were higher than the pin diameters by 7 to 20% due to spring-back after bending.

3.1.1.3 Fixed Parameters

a- **Bend Angle:** A primary bend angle of 90° was tested in this study. Other bend angles were not included in the scope of this project.

b- **Loading Rate** was applied quasi-statically to re-bend tests in this project.

c- **# of Specimens:** At least 3 bar specimens per type were tested.

d- **Strain Aging:** Bar types sensitive to strain aging (as determined in the strain aging tests) were bent and allowed to strain age prior to being subjected to the re-bend tests. This was done to account for the possible deleterious effects of aging on bar ductility, and to reproduce actual in-situ conditions of bends in concrete structures.

e- **Temperature:** The focus of this project was on assessing the bend performance of HSRB at relatively warm ambient temperatures (20 to 25 °C). This evaluation is a necessary first step prior to bending and testing bars in cold climate at or below their brittle transition temperatures. Cold temperature bending and testing should be evaluated in future work.

f- **Bending Equipment:** An RMS Arnold Bender with the capability to bend at 16 RPM and 14RPM (Revolutions Per Minute) was used for all specimens.

g- **Bending Rate:** All specimens were bent at 16 RPM.

3.1.1.4 Instrumentation

The load-cell in the universal testing machine provided readings of the applied load. Strains and deformations of the bars were obtained during testing using a high-resolution optical measurement system reported by Sokoli et al (2014). Targets were applied along the four straight portions of bent bar specimens (Figure 6). The locations of the targets were tracked using the optical system while the bars were being tested (Figure 6).

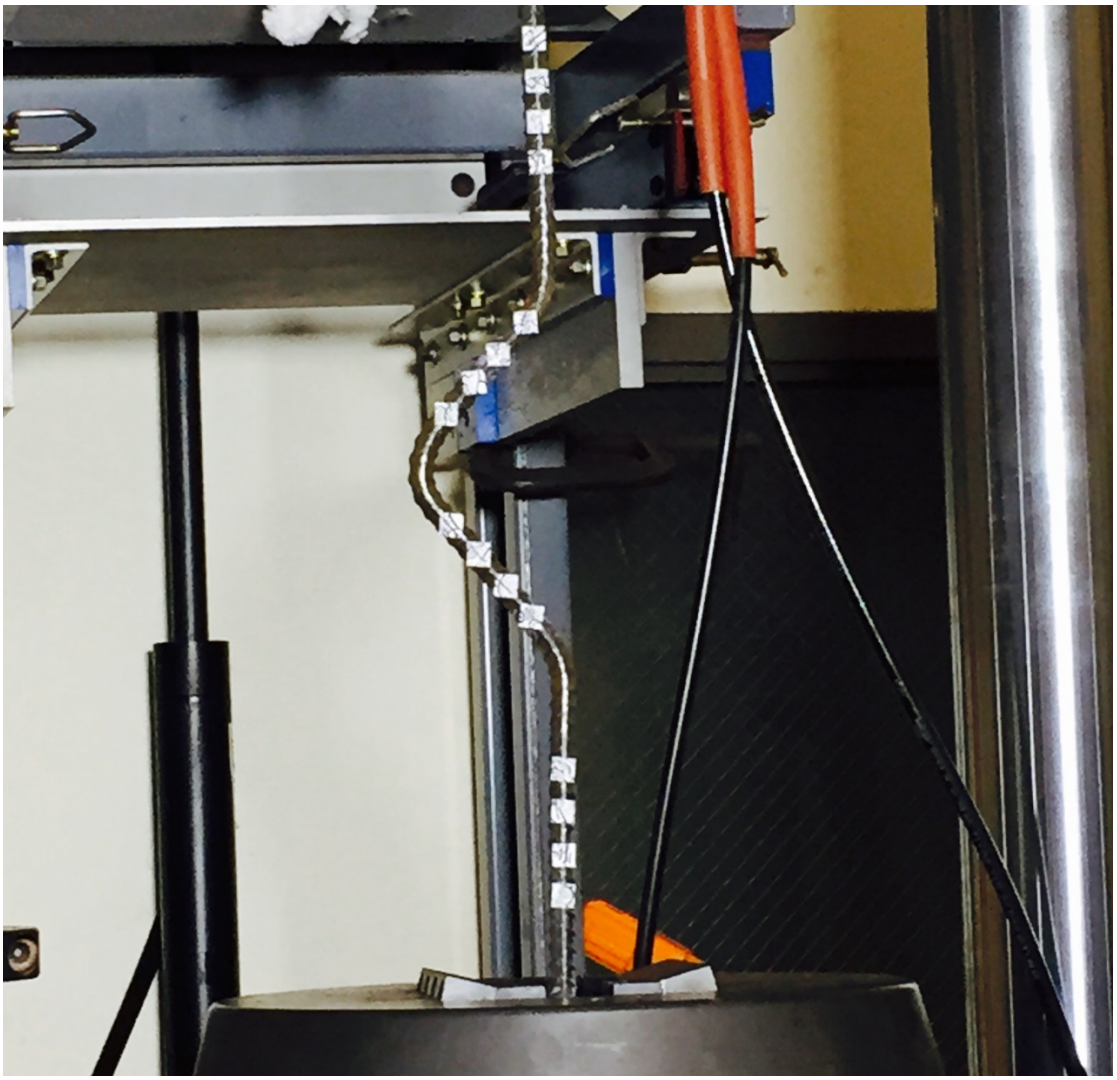

Figure 6: Example of bend/re-bend specimen under testing with targets

3.1.1.5 Test Protocol

Bar were gripped at each end using hydraulic grips that were 6 inches long. The loading during re-bend tests consisted of three loading rates. The loading protocol started with a low loading rate to pick up initial load in the specimens. This was done in order to obtain sufficient data in cases of bar fracture at low forces. Once specimens carried a larger force (~ 10% of yield) the loading rate was increased until the bars were almost straight. Then the rate was again lowered to observe fracture in more detail. All three bar sizes were loaded with the same rates presented in Table 2.

Table 2: Re-bend test loading rates

Loading Rates (in./s)	
Initial Loading	0.0050
Straightening	0.0150
Fracture	0.0075

3.1.2 Strain Aging Tests

Objectives: To quantify strain aging effects on all the bars tested in the bend/re-bend tests and identify the duration after which most strain aging effects level off.

Strain-aging tests were conducted on straight #5 bar coupons for all steel types. All bars, except those satisfying ASTM A1035, were strained in tension to a predetermined strain value of 0.04 in a universal test machine and then unloaded. A1035 bars were strained in tension only to a strain of 0.02 due to their relatively low uniform elongation values. Uniform elongation is defined as the bar elongation at peak stress. Tension tests were then performed on the pre-strained bars immediately after pre-straining, one month after pre-straining, and three months after pre-straining. Strain aging was allowed to occur at room temperature (~20°C). The bars were strained in the strain-aging tests at the strain rate used in the monotonic tension tests.

3.1.3 Monotonic Tests

Monotonic tension tests were performed on at least three straight specimens per bar type to identify the mechanical properties of the steel bars. The tests followed the procedures specified in ASTM A370 (ASTM Standard A370-15), with strains measured over a gauge length of 8 inches.

3.2 Specimen Nomenclature

For monotonic and re-bend tests, the following nomenclature is used to identify specimens:

Manufacturer#_Grade_Bar Type or Specification_Diameter (in eighth of an inch)_Test unique identifier

e.g.: (M1_Gr60_A706_5_01 or M1_Gr100_MA_5_01)

For strain aging tests the following nomenclature is used:

Manufacturer#_Grade_Bar Type or Specification_Diameter (in eighth of an inch)_MonthsAged_Test unique identifier

e.g.: (M1_Gr60_A706_5_3Mo_01)

CHAPTER 4: Test Results and General Observations

4.1 Monotonic Tests

Monotonic tests were conducted on three or more coupons for each bar type used in the bend/re-bend test matrix. The mean mechanical properties and typical stress-strain relations of each bar type are summarized in Table 3 and Figure 7 to Figure 11. Uniform elongation measures were obtained by following the ASTM E8 procedures (ASTM Standard E8/E8M-15a).

Table 3: Summary of mean material properties calculated from monotonic tension tests

Bar Size	Manf.	Grade	Yield Strength f_y (ksi)	Tensile Strength f_u (ksi)	T/Y Ratio	Uniform Elongation ε_{un} (%)	Fracture Elongation ε_f(%)
#11	1	A706 60	64.3	93.2	1.45	12.5%	21.9%
		A706 80	81.7	111.2	1.36	10.3%	18.2%
		MA 100	110.4	139.6	1.26	8.8%	12.7%
		A615 60	63.2	104.0	1.64	11.2%	17.9%
		A615 80	80.5	121.1	1.50	9.1%	14.4%
	2	A1035 100	125.0	162.1	1.30	4.9%	11.7%
	3	A706 60	77.4	102.8	1.33	9.1%	14.5%
		A706 80	83.1	109.7	1.32	9.1%	13.8%
	4	A615 60	63.6	90.7	1.43	12.1%	17.1%
		A706 60	67.5	95.8	1.42	11.5%	16.0%
#8	1	A706 60	60.5	90.0	1.49	11.5%	18.9%
		A706 80	84.4	114.1	1.35	9.8%	16.4%
		MA 100	99.0	125.2	1.27	8.9%	13.0%
		A615 60	63.7	101.3	1.59	10.7%	16.2%
		A615 80	84.4	123.5	1.46	9.2%	14.6%
	2	A1035 100	131.4	164.3	1.25	5.2%	10.8%
	3	A706 60	80.9	101.7	1.26	9.0%	14.9%
		A706 80	81.6	104.0	1.27	8.9%	14.6%
		QT 100	98.7	126.0	1.28	7.2%	9.9%
	4	A615 60	68.1	95.8	1.41	12.0%	18.3%
		A706 60	66.7	90.9	1.36	12.3%	18.5%
#5	1	A706 60	65.7	93.9	1.43	10.5%	14.7%
		A706 80	86.5	115.2	1.33	9.5%	13.8%
		MA 100	113.0	135.1	1.20	8.2%	11.9%
		A615 60	63.0	97.9	1.55	11.2%	16.5%
		A615 80	81.8	112.9	1.38	9.9%	13.9%
	2	A1035 100	125.6	163.6	1.30	5.4%	9.5%
	3	A706 60	81.6	99.7	1.22	8.8%	12.7%
		A706 80	83.3	102.7	1.23	8.8%	12.6%
		QT 100	90.0	129.7	1.44	6.9%	8.4%
	4	A615 60	80.2	102.9	1.28	10.3%	15.0%
		A706 60	66.0	90.8	1.38	12.1%	18.4%
		QT 100	106.1	125.6	1.18	7.6%	10.7%

A706 Grade 60

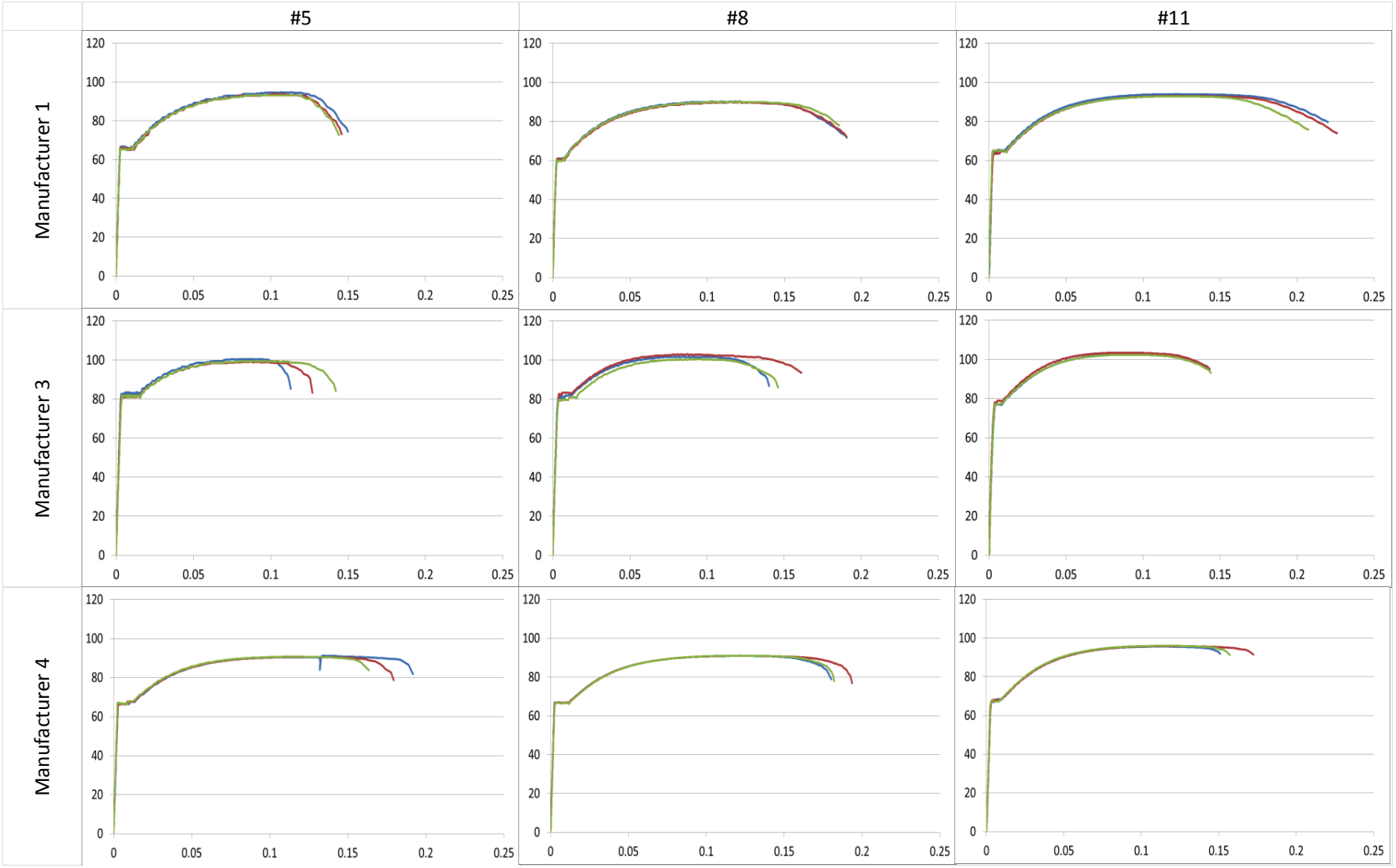

Figure 7: Stress-strain curves from monotonic tests of grade 60 A706 bars

A615 Grade 60

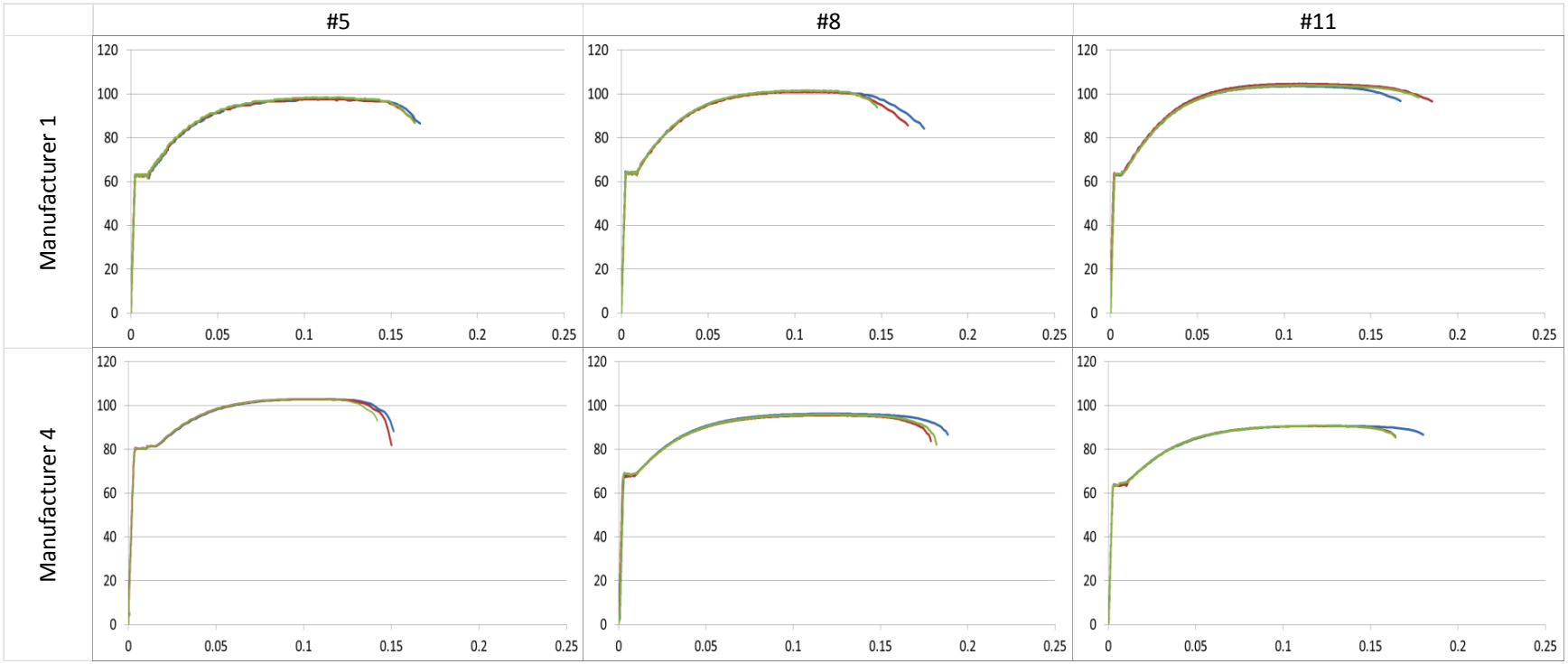

Figure 8: Stress-strain curves from monotonic tests of grade 60 A615 bars

A615 Grade 80

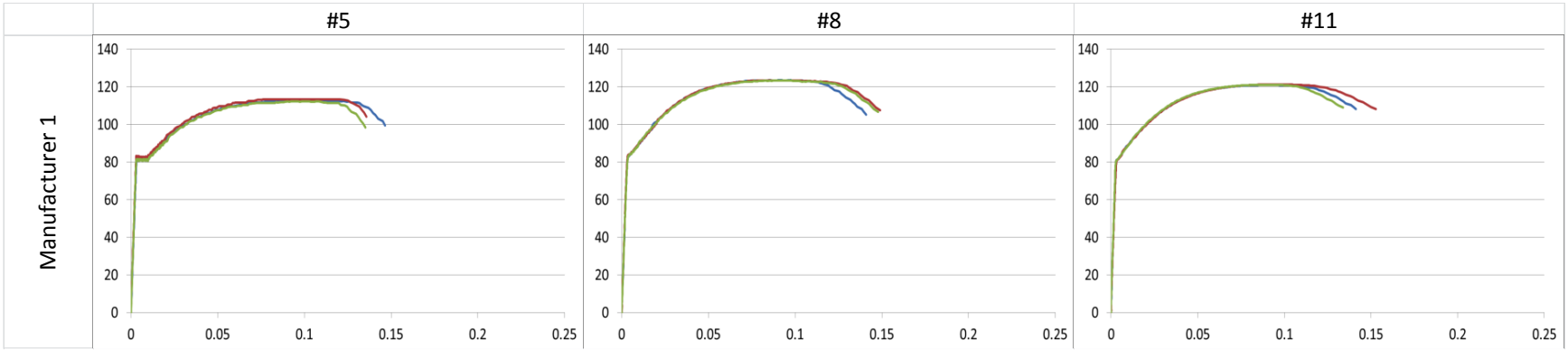

Figure 9: Stress-strain curves from monotonic tests of grade 80 A615 bars

A706 Grade 80

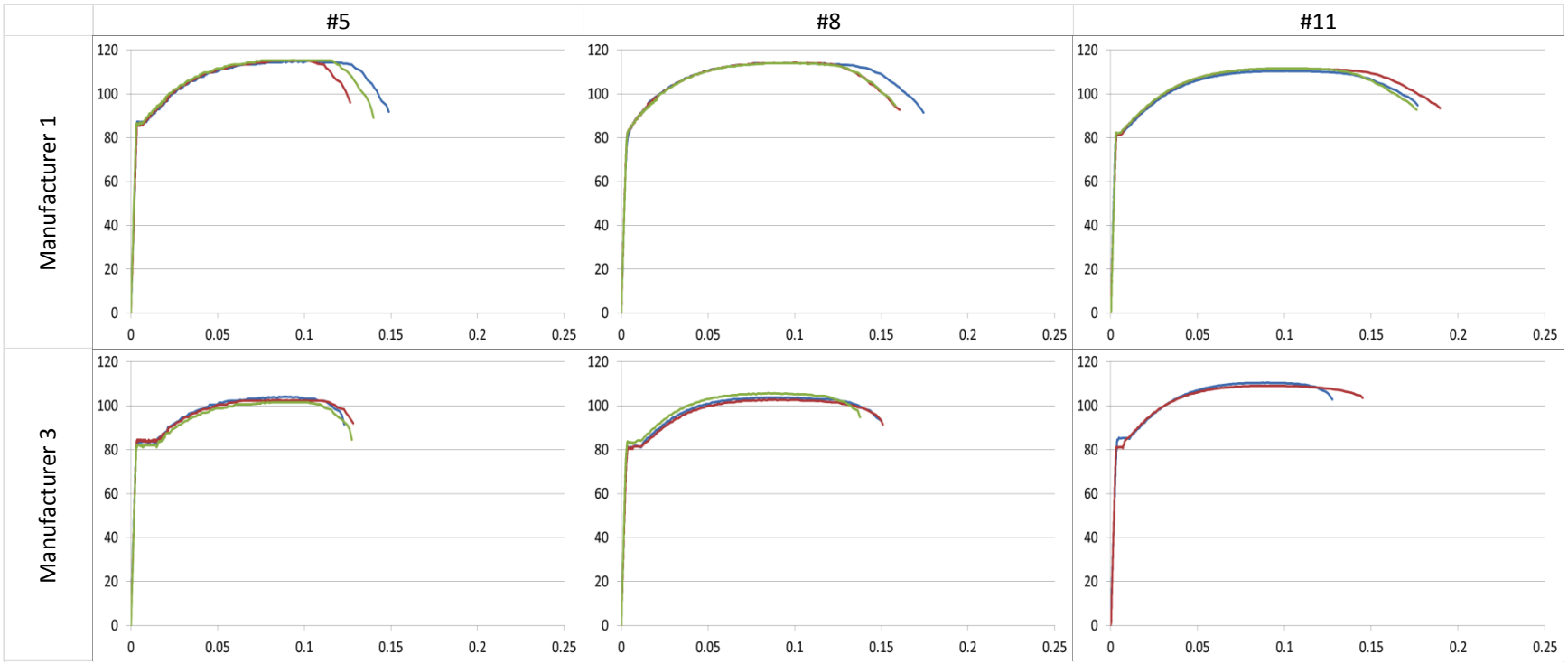

Figure 10: Stress-strain curves from monotonic tests of grade 80 A706 bars

Grade 100

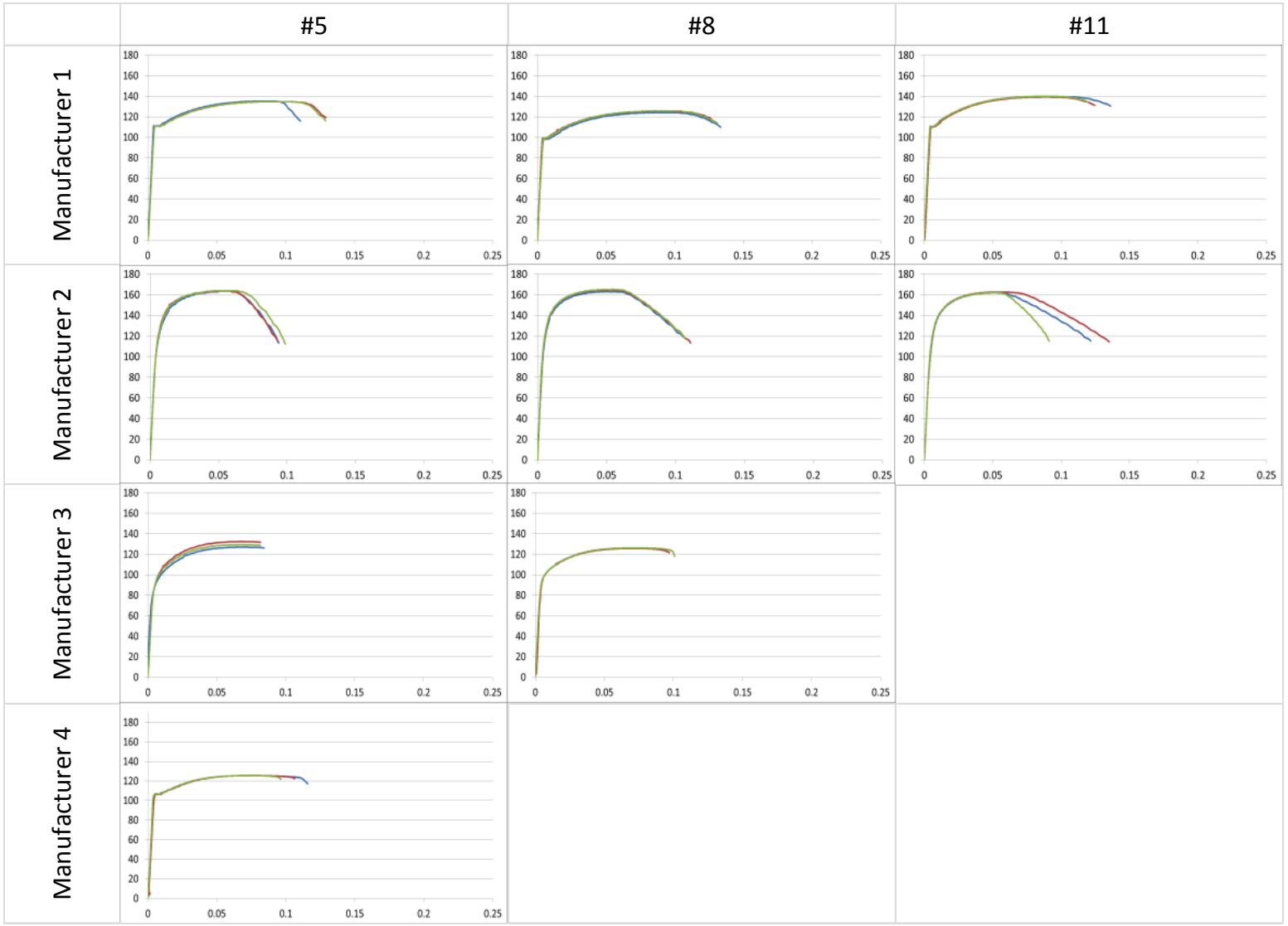

Figure 11: Stress-strain curves from monotonic tests of grade 100 bars

Table 4 summarizes the ratios of $\varepsilon_f / \varepsilon_{un}$ for various bars grades and sizes.

Table 4: Ratio of $\varepsilon_f / \varepsilon_{un}$

$\varepsilon_f / \varepsilon_{un}$		#5	#8	#11
A706	60	1.46	1.60	1.57
	80	1.45	1.66	1.64
A615	60	1.47	1.52	1.51
	80	1.40	1.59	1.57
A1035	100	1.77	2.09	2.37

4.1.1 Summary of Observations

The yield strengths of grade 60 A706 bars tested in this study ranged from 63-77 ksi. The fracture strains of those bars were in the range of 15% to 22%. The yield strengths of grade 60 A615 bas tested in this study were around 63 to 64 ksi with the exception of Manufacturer 4's #5 bars that came in at yield strength of 80.2 ksi. The fracture strains of grade 60 A615 bars were in the range of 15% to 19%.

Grade 80 A706 bars had yield strengths ranging from 81 to 87 ksi. The fracture strains of those bars were in the range of 13% to 19%. Grade 80 A615 bars were only obtained from Manufacturer 1 and had yield strengths ranging from 80 to 84 ksi for all sizes and fracture elongations ranging from 14% to 15%.

Grade 100 bar from Manufacturers 1 and 4 exhibited a yield plateau and had yield strengths in the range of 105 to 110 ksi, with fracture strains ranging from 11 to 13%. Bars from Manufacturers 2 and 3 showed no yield plateau. Yield strengths for those bars were obtained using a 0.2% strain offset method (ASTM A1035, 318-14). Yield strength values for Manufacturer 2 grade 100 bars ranged from 125 to 131 ksi while those for Manufacturer 3 ranged from 90 to 99 ksi. Manufacturer 2 grade 100 bars exhibited fracture strains from 10 to 12% whereas Manufacturer 3 grade 100 bars exhibited fracture strains from 9 to 10%. Manufacturer 2 grade 100 bars differ from other bars as they exhibited a relatively shallow descending relation between stress and strains past their uniform elongation.

4.2 Strain Aging Tests

4.2.1 Strain Aging Test Data

Strain aging tests were conducted on #5 bars of all types used in bend/re-bend tests. Figure 12 to Figure 14 present typical stress-strain relations obtained from the strain aging tests. The arrows in the figures are used to show the difference from non-strain aged to strain aged results. As expected based on past research (Rashid, 1976), grade 80 and 100 bars produced using micro-alloying with Vanadium (Manufacturer 1) exhibited limited strain aging compared with grade 60 bars from the same manufacturer (Figure 12). Bars from Manufacturer 4, which contained relatively small amounts of micro-alloys, exhibited more pronounced strain aging effects as indicated by apparent gains in tensile strength and decreased ductility (Figure 13). Figure 14 highlights how different manufacturing processes result in different strain aging results.

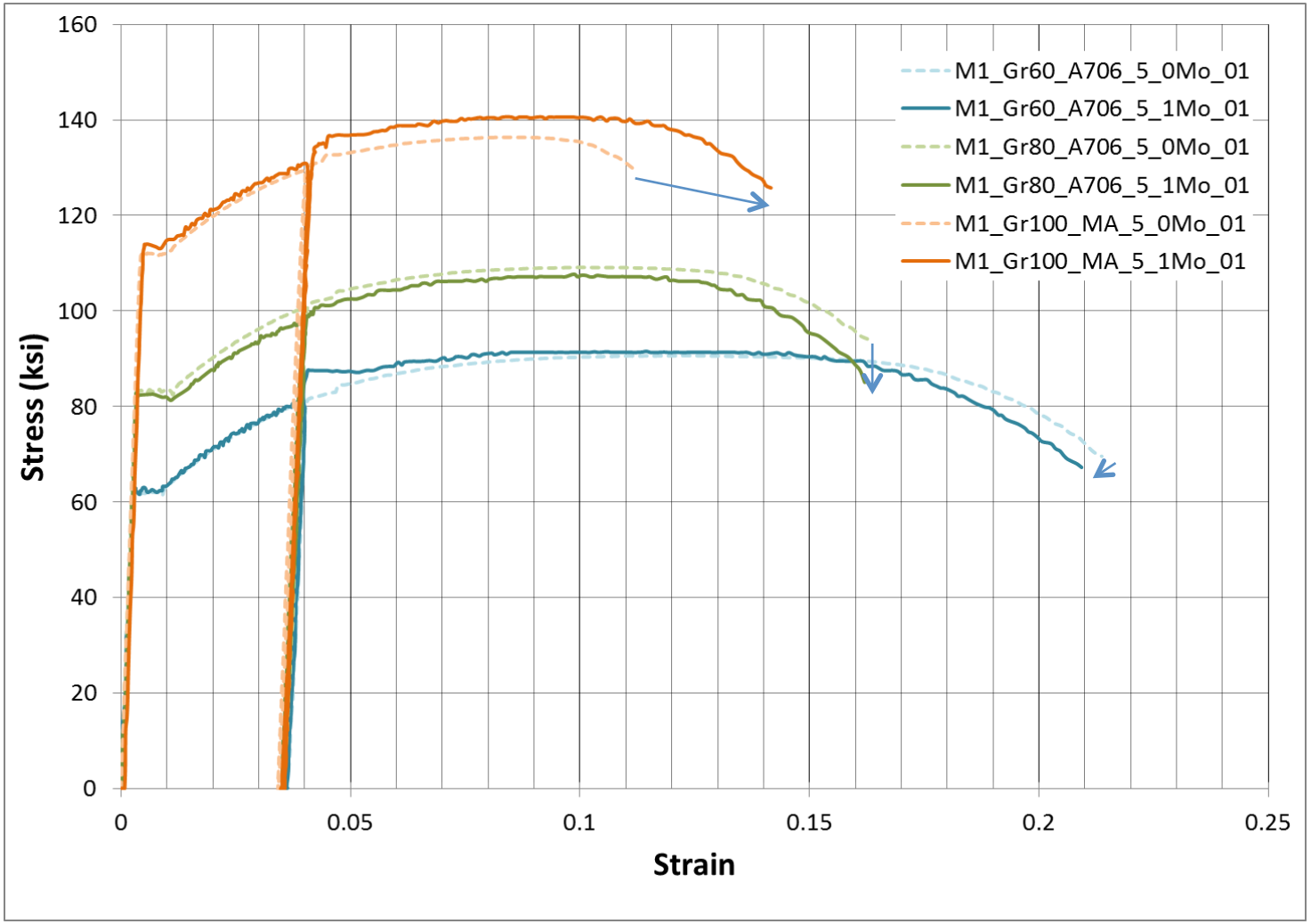

Figure 12: Stress-strain curves for grades 60 and 80 A706 and grade 100 MA bars from Manufacturer 1, not aged and strain aged 1 month

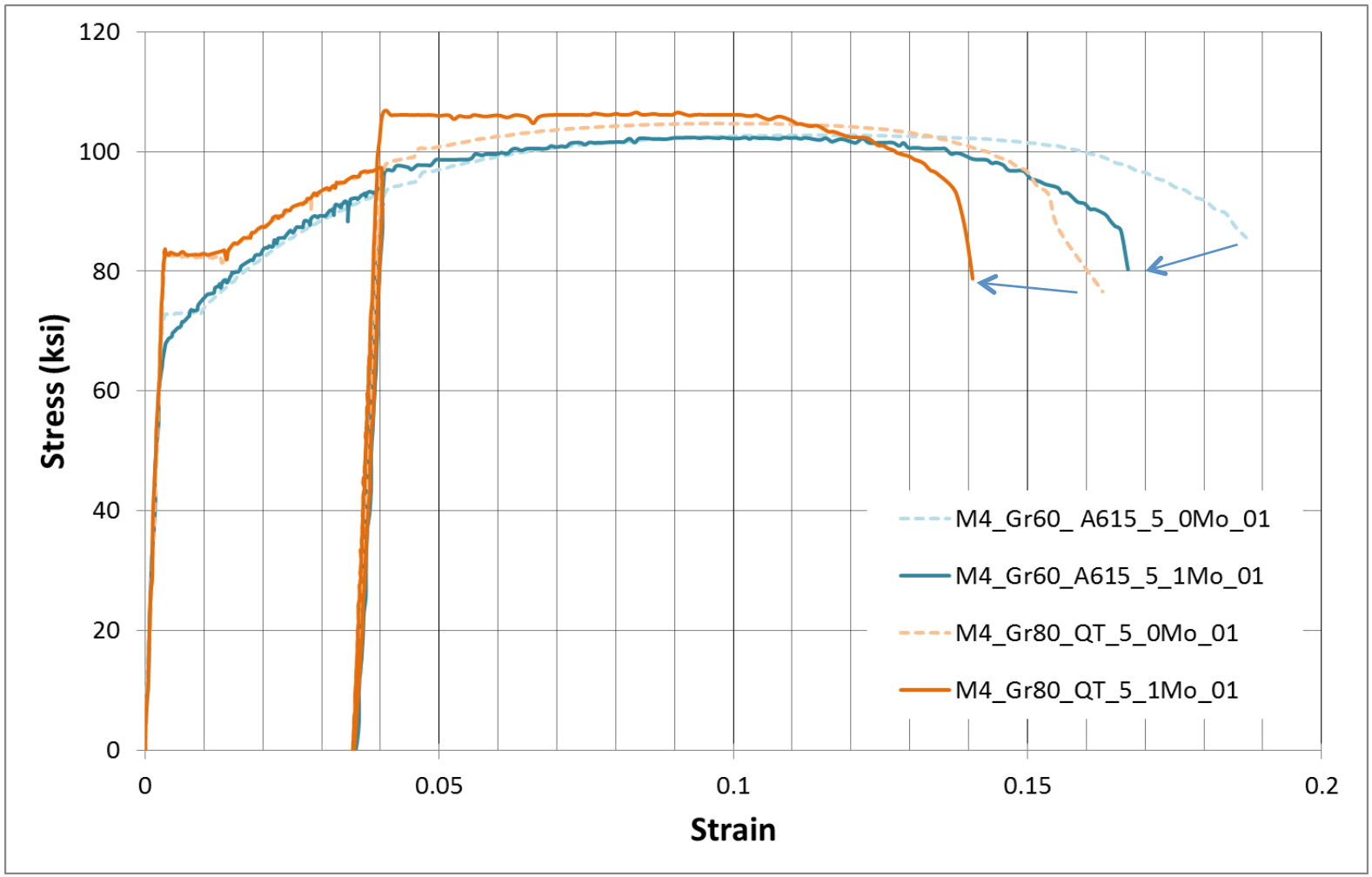

Figure 13: Stress-strain curves for grade 60 and 80 A706 bars from Manufacturer 4, not aged and strain aged 1 month

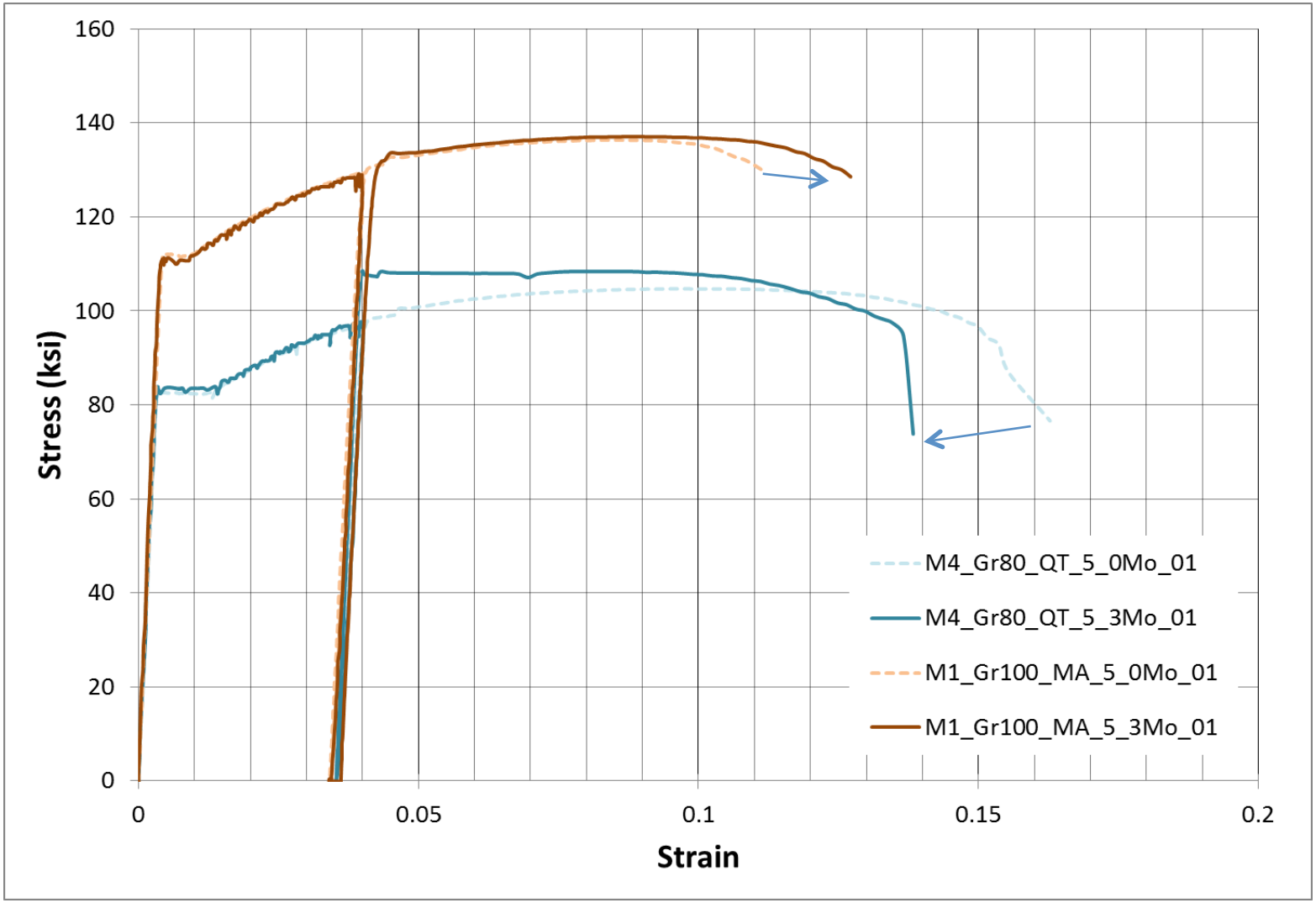

Figure 14: Stress-strain curve comparisons between grade 80 QT from Manufacturer 4 and grade 100 MA from Manufacturer 1, not aged and strain aged 3 months

4.2.2 Strain Aging Performance Measures

Two parameters were used to quantify the effects of strain aging, $(\Delta\sigma/f_y)$ and $(\varepsilon_{\text{fractureA}}/\varepsilon_{\text{fracture}})$. $\Delta\sigma$ is the difference between the apparent yield point upon reloading after specimen aging and the stress at unloading as seen in the Figure 15. $\Delta\sigma$ was normalized with respect to the measured yield strength of the bars, f_y, for comparison between different grades. The strain at bar fracture of aged bars normalized by the strain at fracture prior to aging $(\varepsilon_{\text{fractureA}} / \varepsilon_{\text{fracture}})$ was also used to assess the severity of strain aging. The strains were measured over an eight inch gauge length.

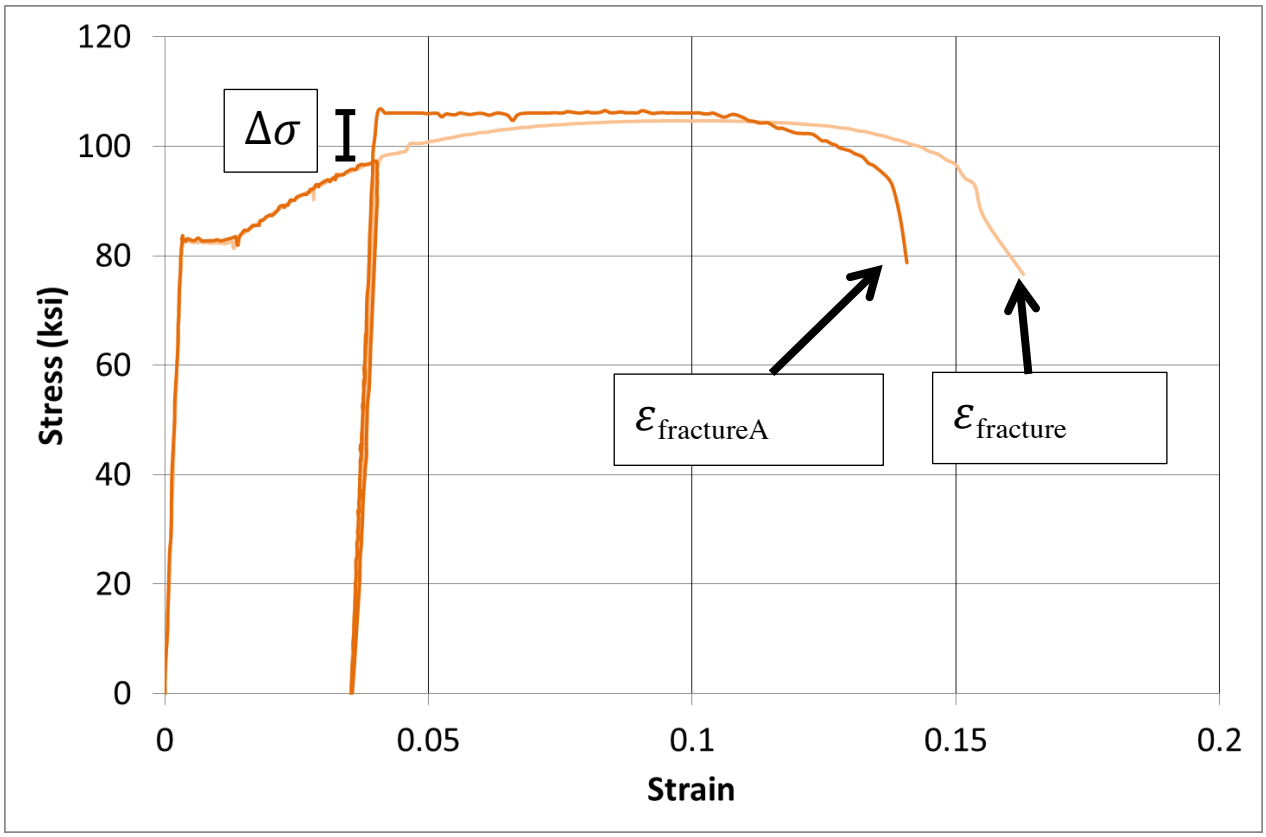

Figure 15: Apparent yield point and loss of elongation after strain aging

4.2.3 Strain Aging Results

Table 5 summarizes the strain aging results averaged over the coupons tested per bar type. At least three coupons were tested per bar type. The concentration of Vanadium was found to be highly correlated with strain aging effects, namely the increase in apparent yield strength and the reduction in facture elongation. Table 5 also summarizes the Vanadium concentrations for each bar type.

Table 5: Summary of strain aging test results

Bar Type	Measured Yield Stress f_y (ksi)	Percent concentration of Vanadium (V %)	$\Delta\sigma/f_y$ after 1Mo of Strain Aging	$\Delta\sigma/f_y$ after 3Mo of Strain Aging	$(\varepsilon_{\text{fractureA}}/\varepsilon_{\text{fracture}})$ after 1Mo of Strain Aging	$(\varepsilon_{\text{fractureA}}/\varepsilon_{\text{fracture}})$ after 3Mo of Strain Aging
M4_Gr60_A706_5	73.2	0.038	0.05	0.08	0.89	0.90
M4_Gr80_A615_5	82.8	0.002	0.11	0.13	0.85	0.85
M1_Gr60_A706_5	63	0.024	0.10	0.10	0.87	0.82
M1_Gr80_A706_5	82.4	0.098	0.03	0.03	0.95	0.91
M1_Gr100_MA_5	112	0.355	0.02	0.04	1.17	1.08
M1_Gr60_A615_5	63.34	0.012	0.13	0.13	0.96	0.99
M1_Gr80_A615_5	83.5	0.063	0.02	0.02	0.98	1.07

4.2.3.1 Effects of Strain Aging Duration

Figure 16 and Figure 17 illustrate the variation of $(\Delta\sigma/f_y)$ and $(\varepsilon_{\text{fractureA}}/\varepsilon_{\text{fracture}})$ with strain aging duration. Dashed lines represent grade 60 bars, shaded lines represent grade 80 bars and solid lines represent grade 100 bars. As can be seen in the figures, the majority of strain aging effects occur within the first month with limited changes observed thereafter for all bar types. Based on these findings, bend/re-bend tests were conducted on bars starting at least one month after the initial bending was conducted.

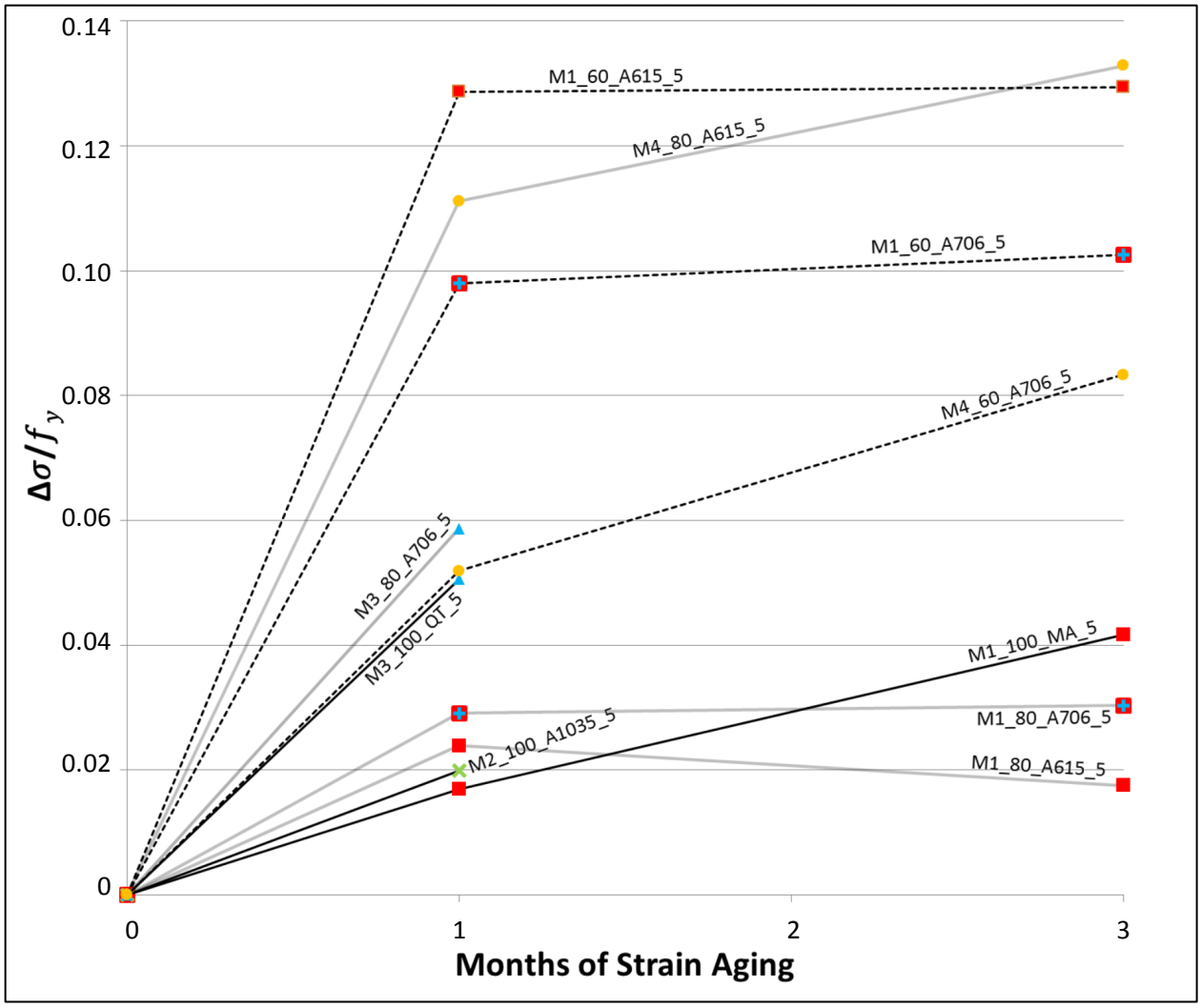

Figure 16: Normalized $\Delta\sigma$ vs strain aging duration

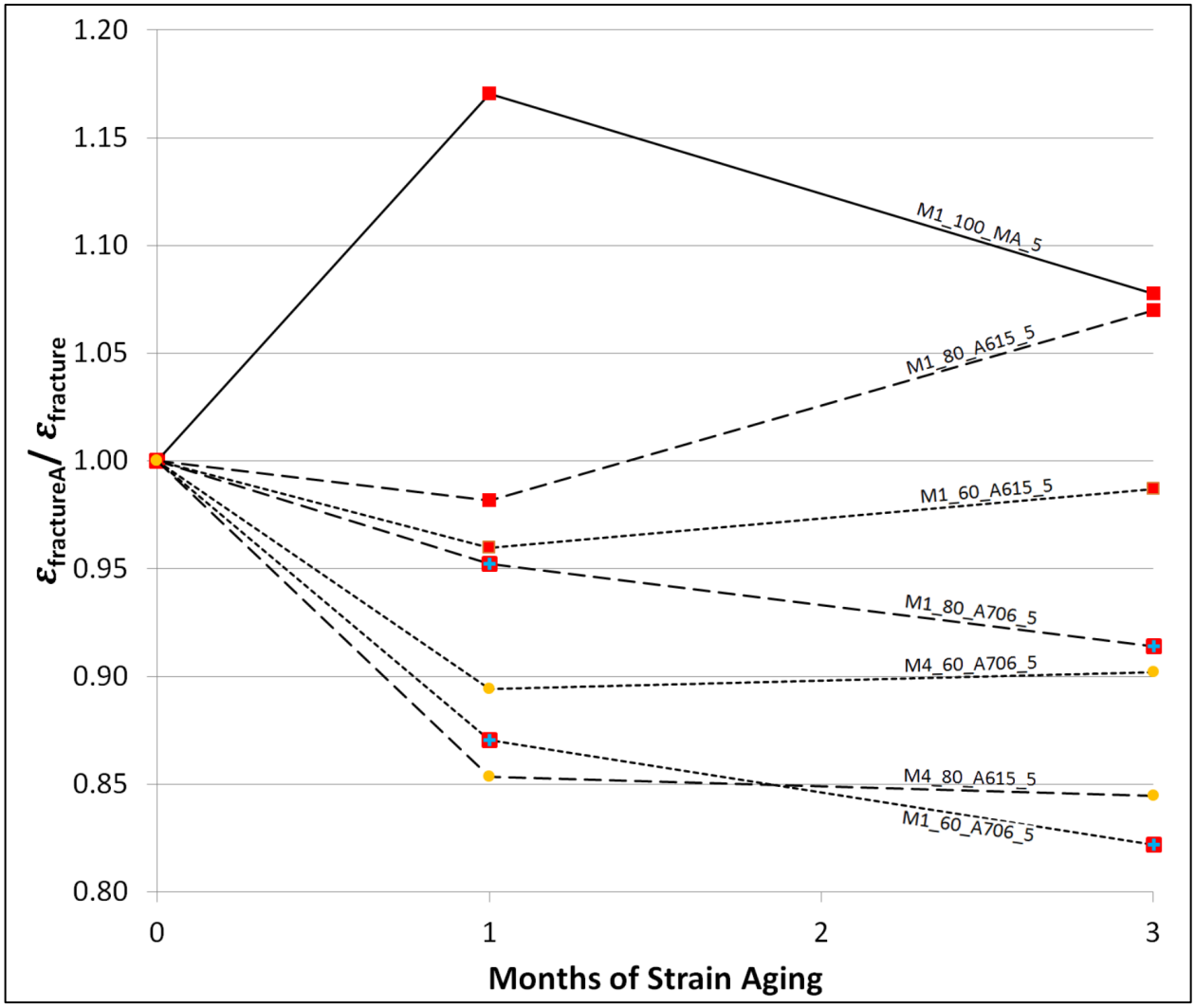

Figure 17: Normalized $\varepsilon_{fractureA.}$ vs strain aging duration

4.2.4.2 Effects of Vanadium on Strain Aging

In Figure 18 and Figure 19, clear relationships can be seen between Vanadium concentrations and the effects of strain aging. The apparent yield strength of strain-aged bars decreases with increasing concentrations of Vanadium, up to a concentration of about 0.08% (Figure 18). Beyond that concentration, $(\Delta\sigma/f_y)$ appears to level off at 0.03 regardless of the concentration of Vanadium. Changes in fracture elongation also appear to vary with the concentration of Vanadium with strain-aged bars becoming more ductile with higher Vanadium concentrations. An increase in ductility post-aging was observed at relatively high concentrations of Vanadium (in excess of 0.35%). Only two data points are available however with those high concentrations.

Based on these observations, the following relations were developed between Vanadium concentrations in percentages (%V) and $(\Delta\sigma/f_y)$ or $(\varepsilon_{\text{fractureA}}/\ \varepsilon_{\text{fracture}})$.

$\Delta\sigma/f_y = -1.26 * (\%V) + 0.13$ 0.00 ≤ %V ≤ 0.08 (Equation 4.2.1)

$\Delta\sigma/f_y = 0.03$ 0.08 < %V (Equation 4.2.2)

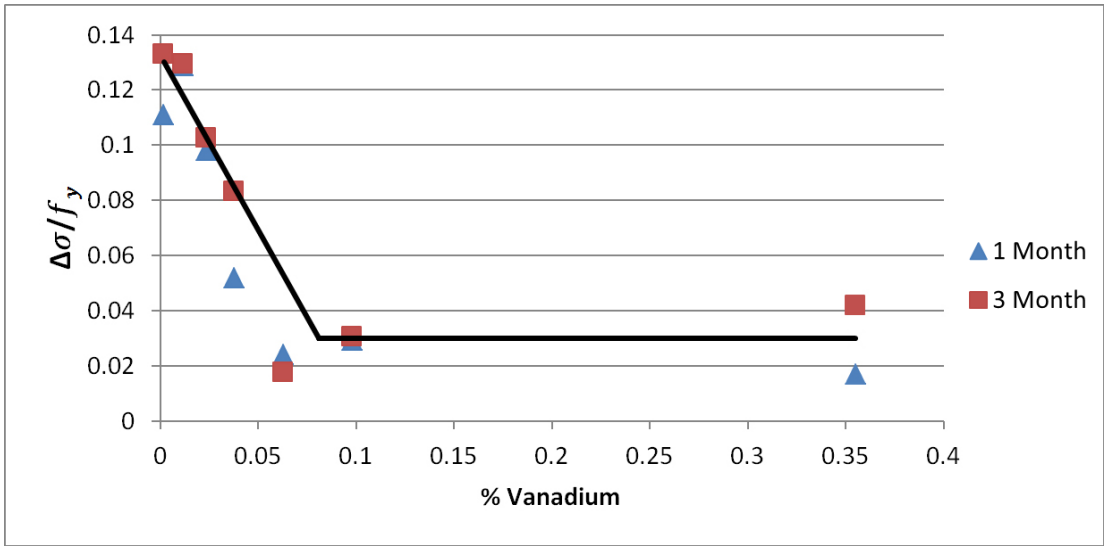

Figure 18: $\Delta\sigma/f_y$ vs %Vanadium

$$\varepsilon_{fractureA}/\varepsilon_{fracture} = 0.9 * (\%V) + 0.9 \qquad 0.00 \leq \%V \leq 0.26 \qquad \text{(Equation 4.2.3)}$$

$$\varepsilon_{fractureA}/\varepsilon_{fracture} = 1.12 \qquad 0.26 < \%V \qquad \text{(Equation 4.2.4)}$$

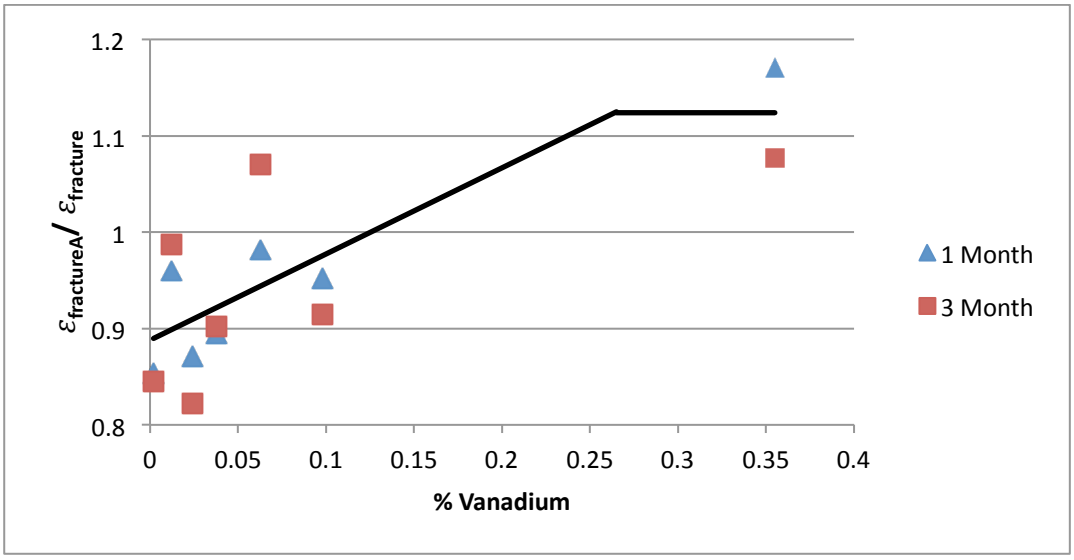

Figure 19: Normalized $\varepsilon_{fractureA}$ vs % Vanadium

4.3 Bend/re-bend Tests

A total of 60 bend/re-bend tests were performed. The following performance measures were used to compare the performance between the various bar types and grades:

a) Fracture location (in 90^o bend, 45^o bend or in straight regions)
b) Remaining bend angle at fracture during re-bending (θ_b)
c) Axial strain in bar at fracture normalized by its uniform elongation strain (ε_b / ε_{un})
d) Axial stress in bar at fracture normalized by its yield strength (f_{ub} / f_y)
e) Axial stress in bar at fracture normalized by its tensile strength (f_{ub} / f_t)

Figure 20 shows a fracture in the 90 degree bend. The remaining bend angle during re-bending was measured using the targets bracketing the 90 degree bend. Two slopes were calculated from the two straight regions adjacent to the 90 degree bend. Using the relationship between the two slopes, the remaining bend angle was calculated, which starts around 90 degrees and goes to almost zero when a bar is fully straightened. Axial strain in bars was obtained by averaging the strains between the targets furthest away from each other in the top and bottom straight regions as indicated by the arrows in Figure 20. Axial stress in bars was obtained by dividing the load reading of the test machine by the nominal area of the bars.

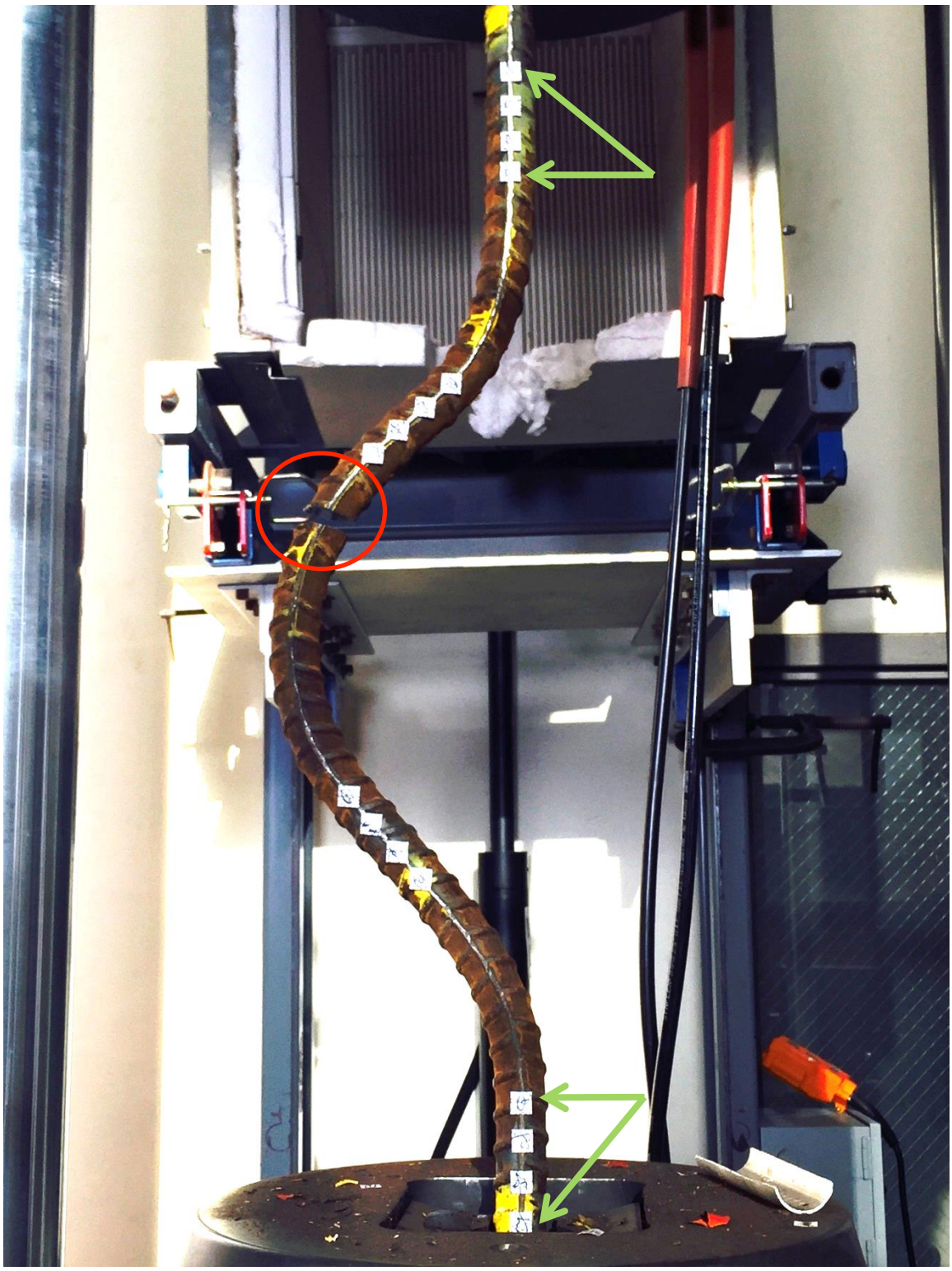

Figure 20: Photograph of a bar that fractured in the 90^{o} bend after limited straightening

4.3.1 Typical Stress vs. Strain Relations in Bend/re-bend Tests

The axial stress-strain relations for three re-bend tests in which fracture occurred prior to full bend straightening are shown in Figure 21. The axial stress-strain relations for bars in which fracture occurred after straightening and after significant inelastic straining occurred in the straight regions are shown in Figure 22. As can be seen in Figures 21 and 22, the initial portion of the stress strain relations measured are not linear. This is attributed to the bending moments that develop during re-bending in the top and bottom straight portions of the specimens where the strains were measured (Figure 20). These moments die out once the bars straigthen.

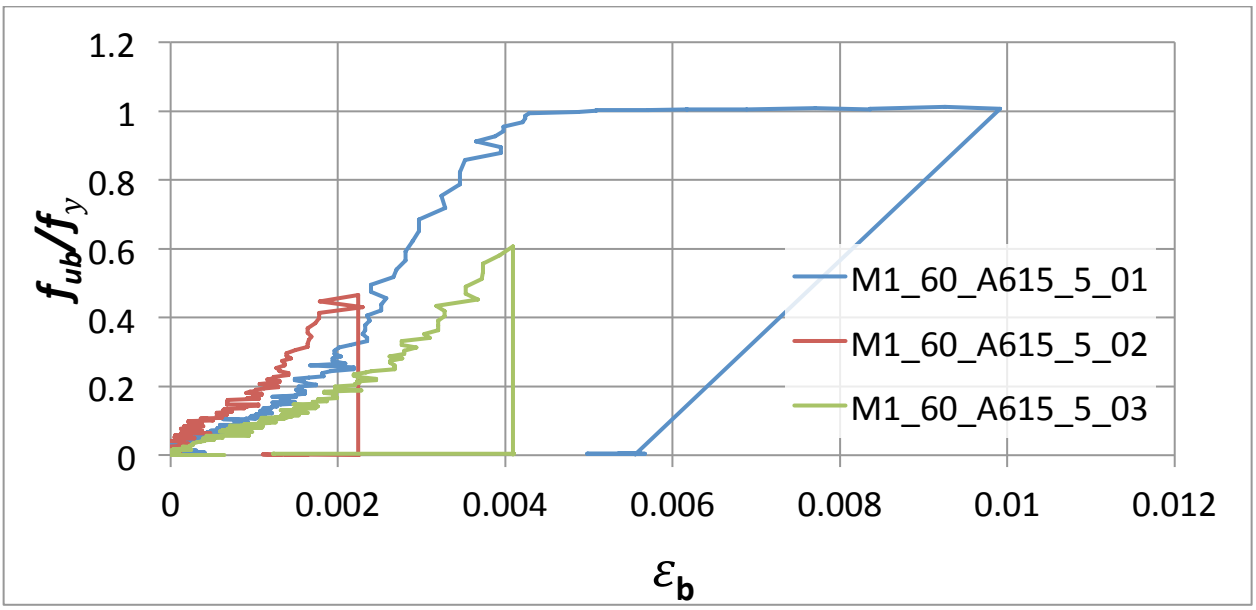

Figure 21: Typical stress vs strain relations for non-straightened bars

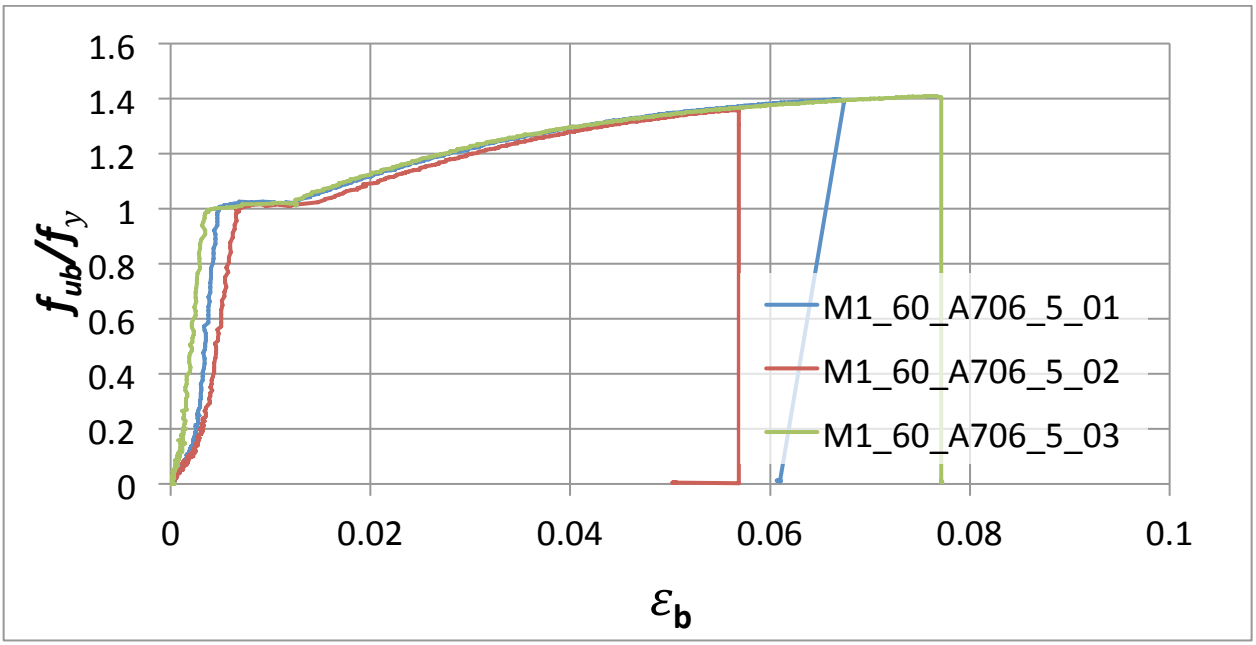

Figure 22: Typical stress vs strain relations for straightened bars exhibiting high ductility during re-bending

4.3.1 Typical Stress vs. Remaining Bend Angle Relations in Bend/re-bend Tests

Typical bar stress versus remaining bend angle relations are plotted in Figure 23 for bars that fractured prior to full straightening. Typical bar stress versus remaining bend angle relations are plotted in Figure 24 for bars that fractured after full straightening. In the figures, 90 degrees denotes the initial bend angle and 0 degrees denotes that a bar-bend has been fully straightened. Tests highlighted in Figure 23 and Figure 24 are those highlighted in Figure 21 and Figure 22, respectively.

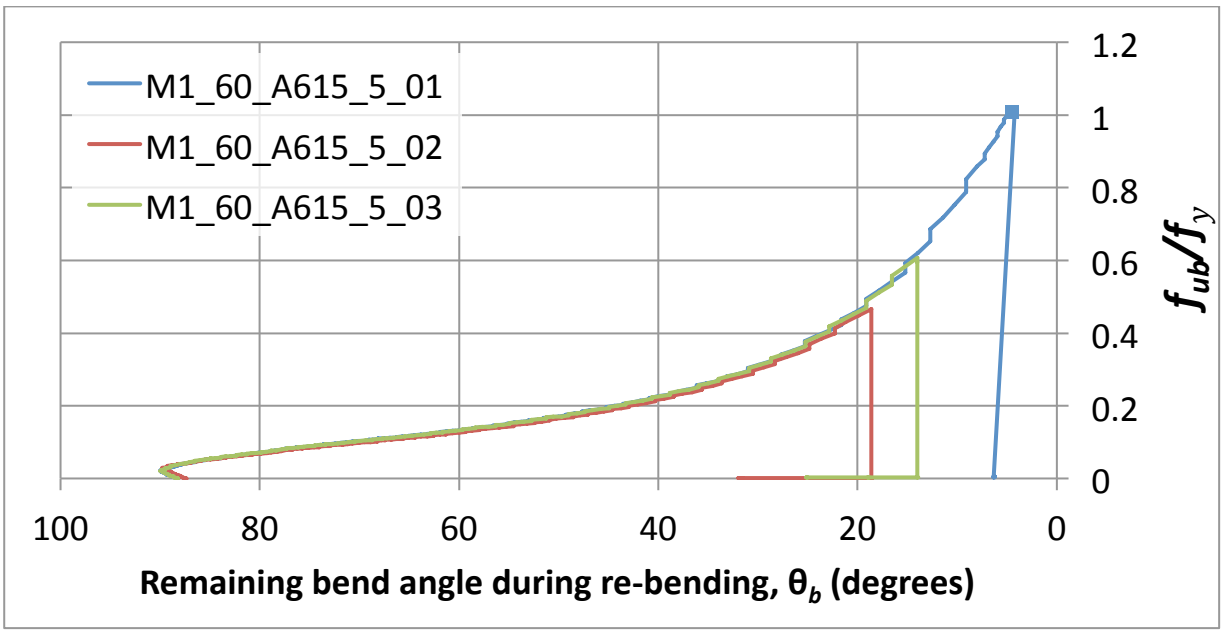

Figure 23: Typical stress vs. remaining bend angle relations for non-straightened bars

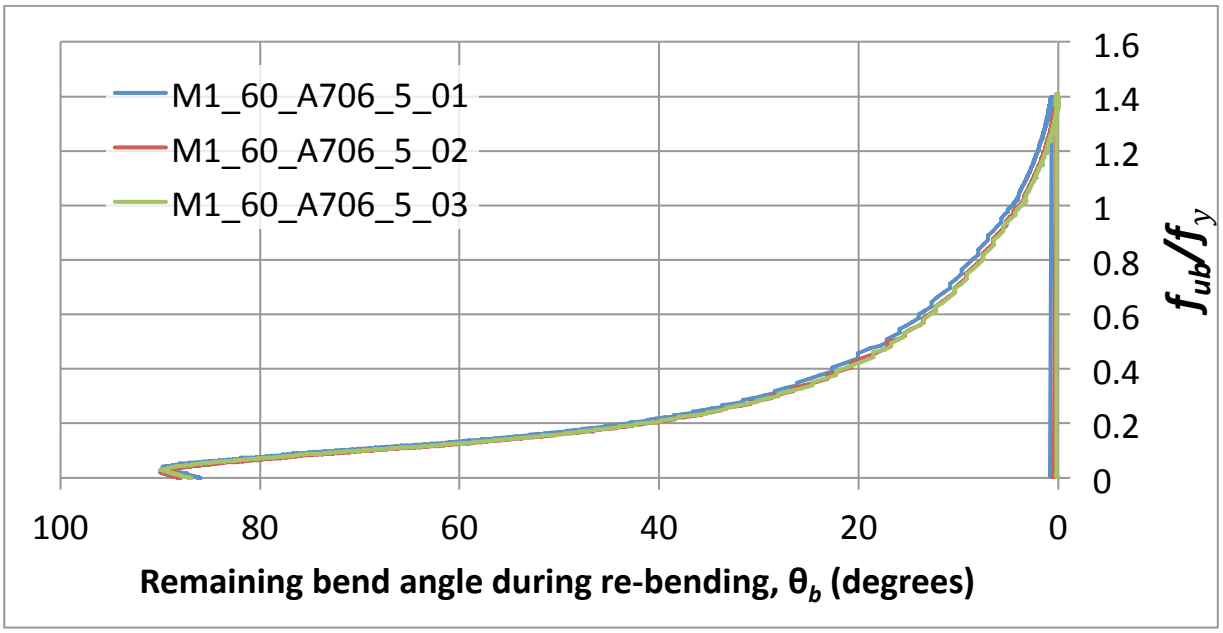

Figure 24: Typical stress vs. remaining bend angle relations for straightened bars

4.3.2 Summary of Results for Bend/re-bend Tests

Table 6 and Table 7 summarize values of the bend/re-bend test performance measures, averaged over at least three tests per bar type. Table 6 contains results from #8 and #11 bars, and Table 7 contains results from #5 bars.

The bend/re-bend tests subjected bar bends to harsher stress and strain histories than they typically encounter in concrete structures. As such, defining acceptance criteria values that delineate deficient in-situ bend performance is not straightforward. However, selecting values of performance measures above which bend performance can be deemed adequate in concrete can be done conservatively. In this study, bars with values of the normalized stress at fracture (f_{ub}/f_y) exceeding 1.0 are deemed to have adequate bend performance, as these bars have reached their design strength prior to fracture. Likewise, bars with values of the normalized fracture strain (ε_{sb} / ε_{un}) exceeding 0.2 are deemed to have adequate bend performance, as these bars typically straighten fully, reach stresses in excess of yield, and strain to at least 20% of their uniform elongation prior to fracture.

Table 6: Bend/re-bend Results for #8 and #11 Bars

Bar Size (Bend Diameter)	Manf.	Grade	Specimen Name	Yield Stress f_y (ksi)	Tensile Stress f_t (ksi)	Uniform Strain ε_{un} (%)	Normalized Strain at Fracture ($\varepsilon_b/\varepsilon_{un}$)	Normalized Stress at Fracture (f_{ub}/f_y)	Angle at Fracture θ_b (degrees)	Fracture Location			$\theta_b < 5$ degrees
										Straight Regions	45	90	
#11 ($8d_b$)	M1	A706 60	M1_60_A706_11	64.3	93.2	12.5%	1.05	1.47	0	1/3	1/3	1/3	3/3
		A706 80	M1_80_A706_11	81.7	111.2	10.3%	0.96	1.38	0	3/3			3/3
		MA 100	M1_100_MA_11	110.4	139.6	8.8%	0.52	0.83	28	2/3		1/3	2/3
		A615 60	M1_60_A615_11	63.2	104.0	11.2%	1.05	1.64	0	3/3			3/3
		A615 80	M1_80_A615_11	80.5	121.1	9.1%	0.77	1.46	1	2/3	1/3		3/3
	M2	A1035 100	M2_100_A1035_11	125.0	162.1	4.9%	0.47	1.23	1		3/3		3/3
	M3	A706 80	M3_80_A706_11	83.1	109.7	9.1%	0.86	1.32	0			3/3	3/3
	M4	A615 60	M4_60_A615_11	63.6	90.7	12.1%	1.11	1.42	0	3/3			3/3
		A706 60	M4_60_A706_11	67.5	95.8	11.5%	1.36	1.42	0	3/3			3/3
#8 ($6d_b$)	M1	A706 60	M1_60_A706_8	60.5	90.0	11.5%	1.01	1.50	0	3/3			3/3
		A706 80	M1_80_A706_8	84.4	114.1	9.8%	0.92	1.35	0	3/3			3/3
		A706 100	M1_100_MA_8	99.0	125.2	8.9%	1.11	1.28	0	3/3			3/3
		A615 60	M1_60_A615_8	63.7	101.3	10.7%	1.12	1.61	0	3/3			3/3
		A615 80	M1_80_A615_8	84.4	123.5	9.2%	0.73	1.45	0			3/3	3/3
	M2	A1035 100	M2_100_A1035_8	131.4	164.3	5.2%	0.43	1.17	1		3/3		3/3
	M3	A706 80	M3_80_A706_8	81.6	104.0	8.9%	0.99	1.28	0			3/3	3/3
		QT 100	M3_100_QT_8	98.7	126.0	7.2%	0.38	1.16	1		1/3	2/3	3/3
	M4	A615 60	M4_60_A615_8	68.1	95.8	12.0%	1.06	1.41	0	2/3		1/3	3/3
		A706 60	M4_60_A706_8	66.7	90.9	12.3%	1.18	1.36	0	1/3		2/3	3/3

Table 7: Bend/re-bend Results for #5 Bars

Bar Size (Bend Diameter)	Manf.	Grade	Specimen Name	Yield Stress f_y (ksi)	Tensile Stress f_t (ksi)	Uniform Strain ε_{un} (%)	Normalized Strain at Fracture ($\varepsilon_b/\varepsilon_{un}$)	Normalized Stress at Fracture (f_{ub}/f_y)	Angle at Fracture θ_b (degrees)	Fracture Location			$\theta_b < 5$ degrees
										Straight Regions	45	90	
#5 ($4d_b$)	M1	A706 60	M1_60_A706_5	65.7	93.9	10.5%	0.64	1.39	0			3/3	3/3
		A706 80	M1_80_A706_5	86.5	115.2	9.5%	0.03	0.28	26			3/3	0/3
		A706 100	M1_100_MA_5	113.0	135.1	8.2%	0.01	0.15	52			3/3	0/3
		A615 60	M1_60_A615_5	63.0	97.9	11.2%	0.05	0.70	12			3/3	1/3
		A615 80	M1_80_A615_5	81.8	112.9	9.9%	0.03	0.25	31			3/3	0/3
	M2	A1035 100	M2_100_A1035_5	125.6	163.6	5.4%	0.11	0.51	26			3/3	1/3
	M3	A706 80	M3_80_A706_5	83.3	102.7	8.8%	0.24	1.06	1			3/3	3/3
		QT 100	M3_80_QT_5	90.0	129.7	6.9%	0.02	0.12	61			3/3	0/3
	M4	A706 60	M4_60_A706_5	66.0	90.8	10.3%	0.51	1.28	0			3/3	3/3
		A615 60	M4_60_A615_5	80.2	102.9	12.1%	0.44	1.22	0			3/3	3/3
		MA 100	M4_100_MA_5	106.1	125.6	7.6%	0.04	0.71	7			3/3	2/3
#5 ($5d_b$)	M1	A706 60	M1_60_A706_5	65.7	93.9	10.5%	1.01	1.41	0	1/3	1/3	1/3	3/3
		A706 80	M1_80_A706_5	86.5	115.2	9.5%	0.53	1.28	17			3/3	1/3
		A706 100	M1_100_MA_5	113.0	135.1	8.2%	0.36	0.70	12	1/3		2/3	1/3
		A615 60	M1_60_A615_5	63.0	97.9	11.2%	0.62	1.49	0	1/3		2/3	3/3
		A615 80	M1_80_A615_5	81.8	112.9	9.9%	0.02	0.52	0			3/3	3/3
	M2	A1035 100	M2_100_A1035_5	125.6	163.6	5.4%	0.24	0.86	17		1/3	2/3	2/3
	M3	A706 80	M3_80_A706_5	83.3	102.7	8.8%	0.62	1.21	0			3/3	3/3
		QT 100	M3_80_QT_5	90.0	129.7	6.9%	0.02	0.23	36			3/3	0/3
	M4	A706 60	M4_60_A706_5	66.0	90.8	10.3%	1.10	1.35	0			3/3	3/3
		A615 60	M4_60_A615_5	80.2	102.9	12.1%	0.67	1.27	0			3/3	3/3
		MA 100	M4_100_MA_5	106.1	125.6	7.6%	0.19	1.00	2			3/3	3/3
#5 ($6d_b$)	M1	A706 100	M1_100_MA_5	113.0	135.1	8.2%	1.01	1.18	0	2/3		1/3	3/3
	M2	A1035 100	M2_100_A1035_5	125.6	163.6	5.4%	0.47	1.25	0			3/3	3/3
	M3	A706 80	M3_80_A706_5	83.3	102.7	8.8%	0.73	1.21	0			3/3	3/3
		QT 100	M3_80_QT_5	90.0	129.7	6.9%	0.04	0.44	21			3/3	0/3
	M4	MA 100	M4_100_MA_5	106.1	125.6	7.6%	0.32	1.08	0		2/3	1/3	3/3

4.3.3 Effects of Bar Yield Strength on Re-bend Performance

As can be seen in Figure 25 to 28 the performance of bar bends generally decreased as the measured yield strength of the bars increased. This trend holds across all bar sizes.

A negative correlation can be observed between (f_{ub}/f_y) during re-bending and the measured bar yield strength (Figure 25). For #8 bar specimens with a target inside bend diameter of $6d_b$ (or #8 ($6d_b$)) and for #11 ($8d_b$) specimens, test data exhibited relatively low variability about the observed trends highlighted by the linear regression lines in Figure 25. However, for #5 ($4d_b$) specimens, test data exhibited relatively large variability about the observed trend. The #8 ($6d_b$) and #11 ($8d_b$) specimens consistently failed at stresses well above the yield strength and closer to the tensile strengths of the bars at all bar strength levels; with the exception of the M1_Gr100_MA_11 specimen. To decouple the trend of lower tensile-to-yield-strength ratios with increasing yield strength from bend performance, the stresses at fracture normalized by the tensile strength of the bars (f_{ub}/f_t) are plotted versus the measured yield strength of the bars in Figure 26. As can be seen in the figure, the negative correlation can be observed for #5 bars as yield strength increases. #8 and #11 bars seem to reach more than 95% of f_t with the exception of M3_Gr100_QT_8 and M1_Gr100_MA_11.

A negative correlation between the yield strength and the normalized strain at fracture can also be observed in Figure 27. Most #8 bars ($6d_b$) and #11 ($8d_b$) bars, regardless of yield strength, straightened almost fully during re-bending (Figure 28). For #5 ($4d_b$) bars, however, there is a clear increase in the remaining bend angle at fracture as the bar yield strength increased.

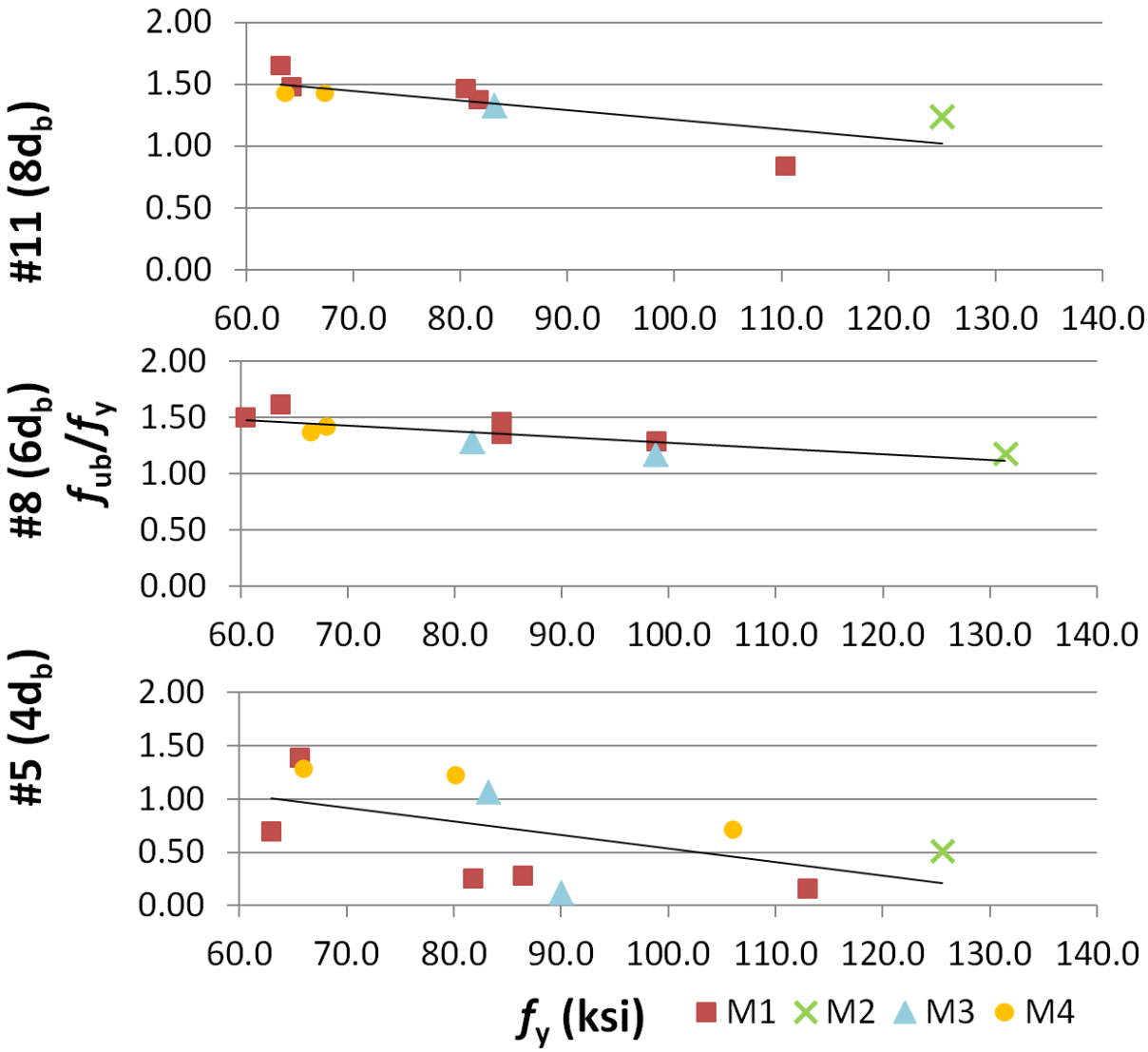

Figure 25: Normalized re-bend stress at fracture vs measured bar yield strength

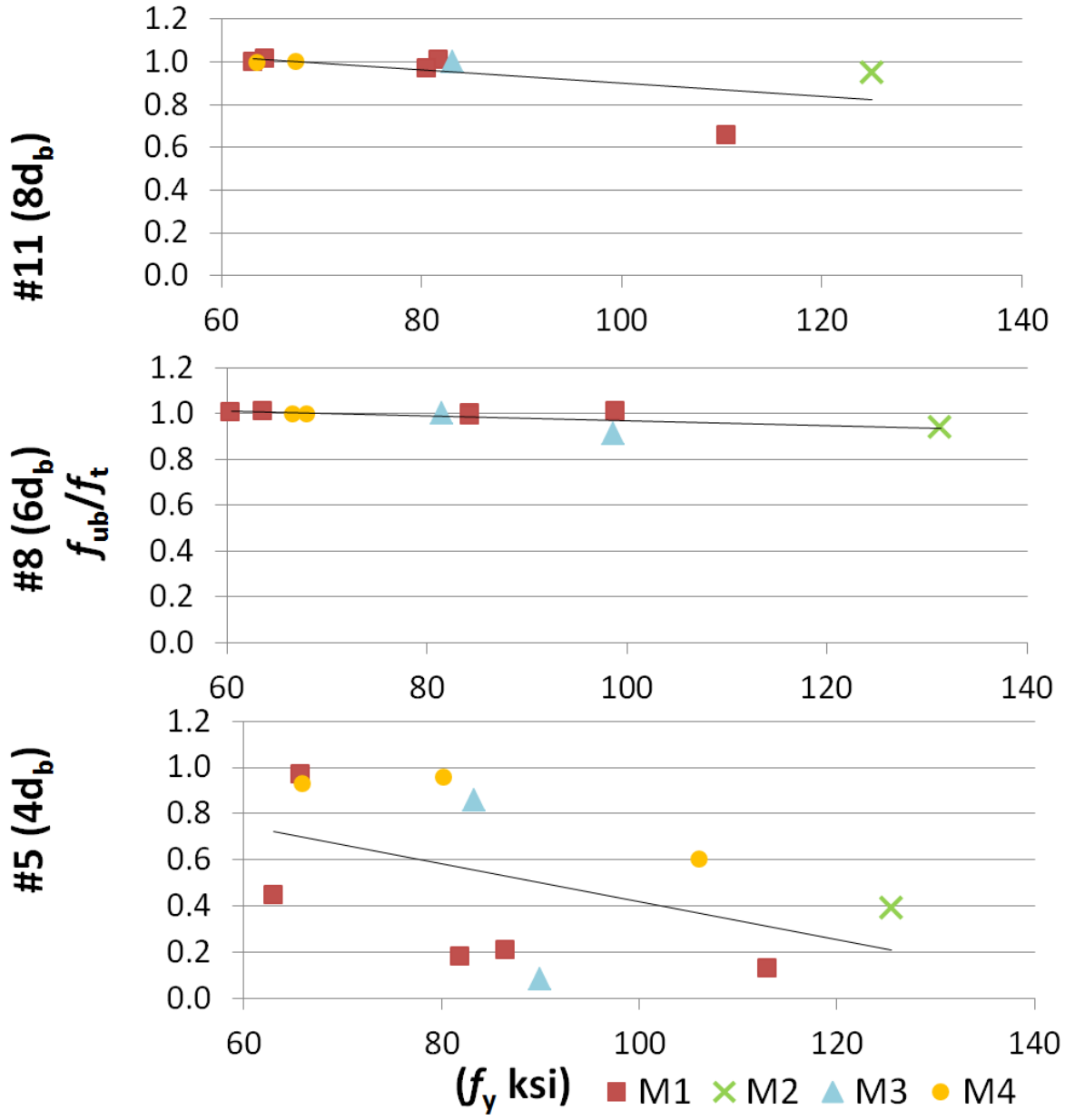

Figure 26: Normalized re-bend stress at fracture vs measured bar yield strength

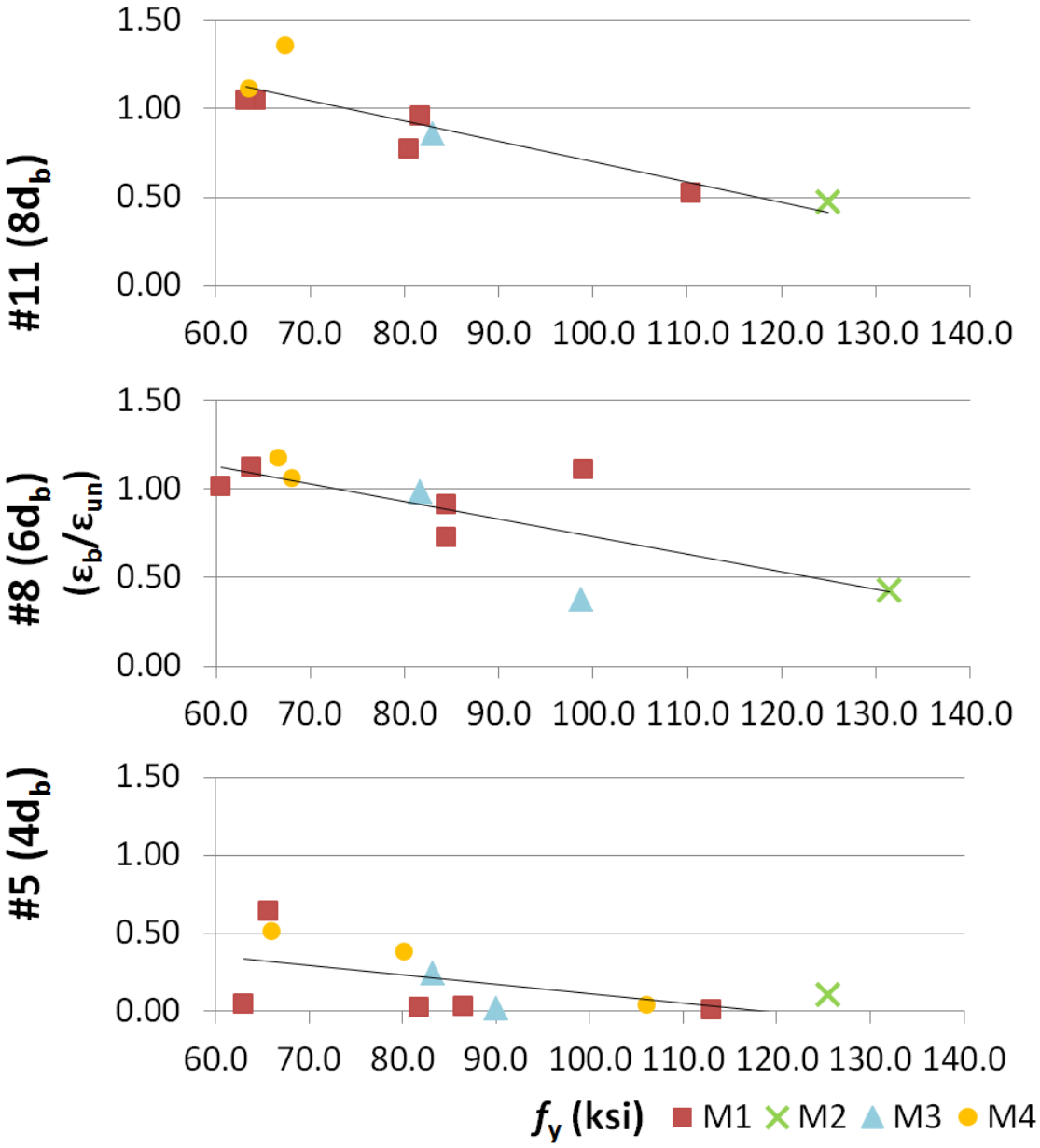

Figure 27: Normalized re-bend strain at fracture vs measured bar yield strength

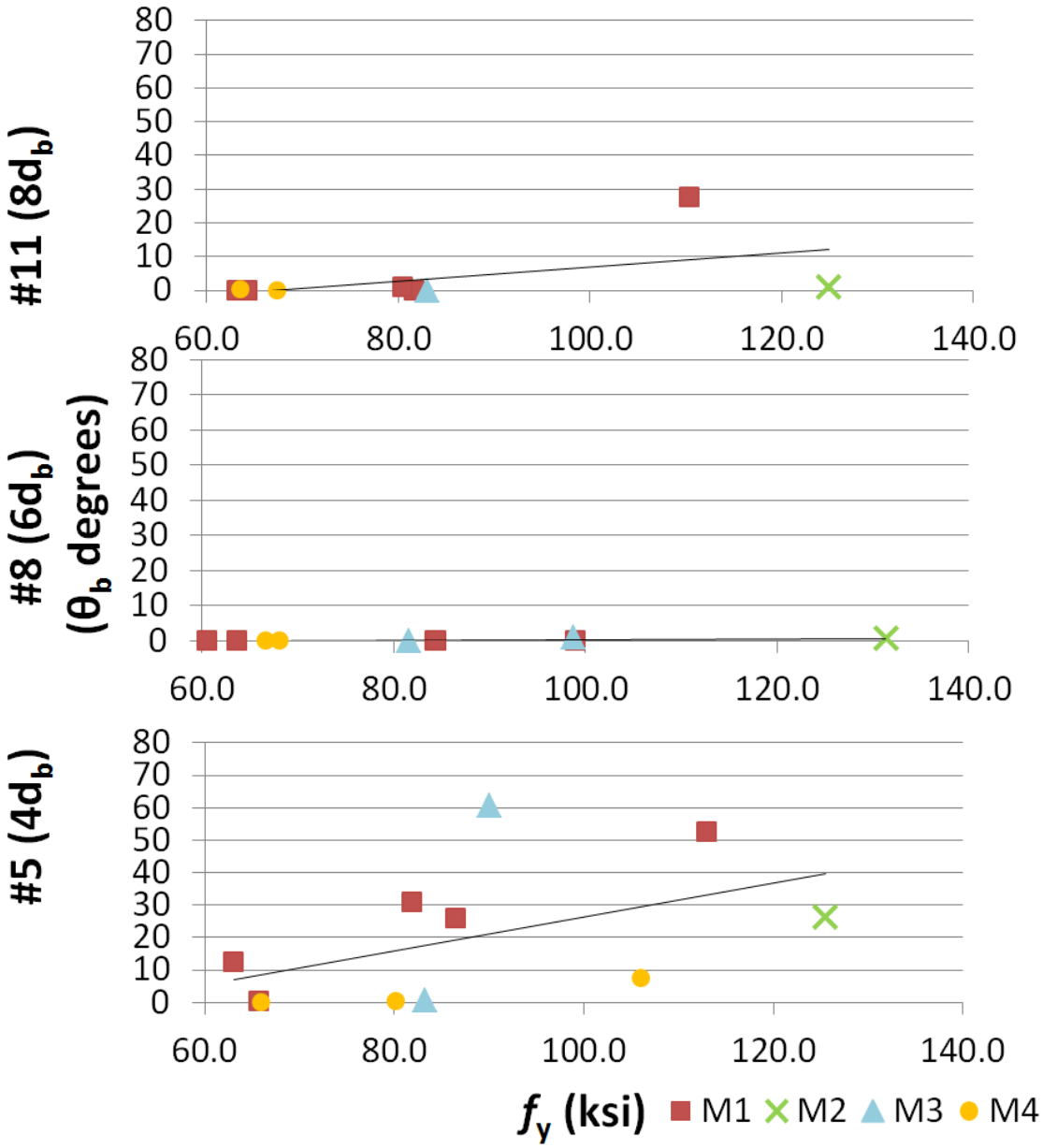

Figure 28: Remaining bend angle at fracture vs measured bar yield strength

4.3.4 Effects of Bar Size on Re-bend Performance

The relationship between (f_{ub}/f_y) and bar yield strength is compared for different bar sizes in Figure 29. As can be seen in the figure, #11 ($8d_b$) and #8 ($6d_b$) bars reached significantly larger stresses at fracture than #5 ($4d_b$) bars. In fact, except for one bar type, all #11 and #8 bars reached stresses in excess of their yield strength during re-bending. However, as the bend diameter of #5 bars was increased from $4d_b$, the bend performance of #5 bars improved and became comparable to that of the larger bars when the target inside bend dimeter of the #5 bars was $6d_b$ (same as that of #8 bars). Test data therefore suggest a limited influence of bar size on the bar stress at fracture during re-bending, but a significant influence of bend inside diameter on stress at fracture. Similar trends can be observed between bar size and the normalized strain at fracture Figure 30.

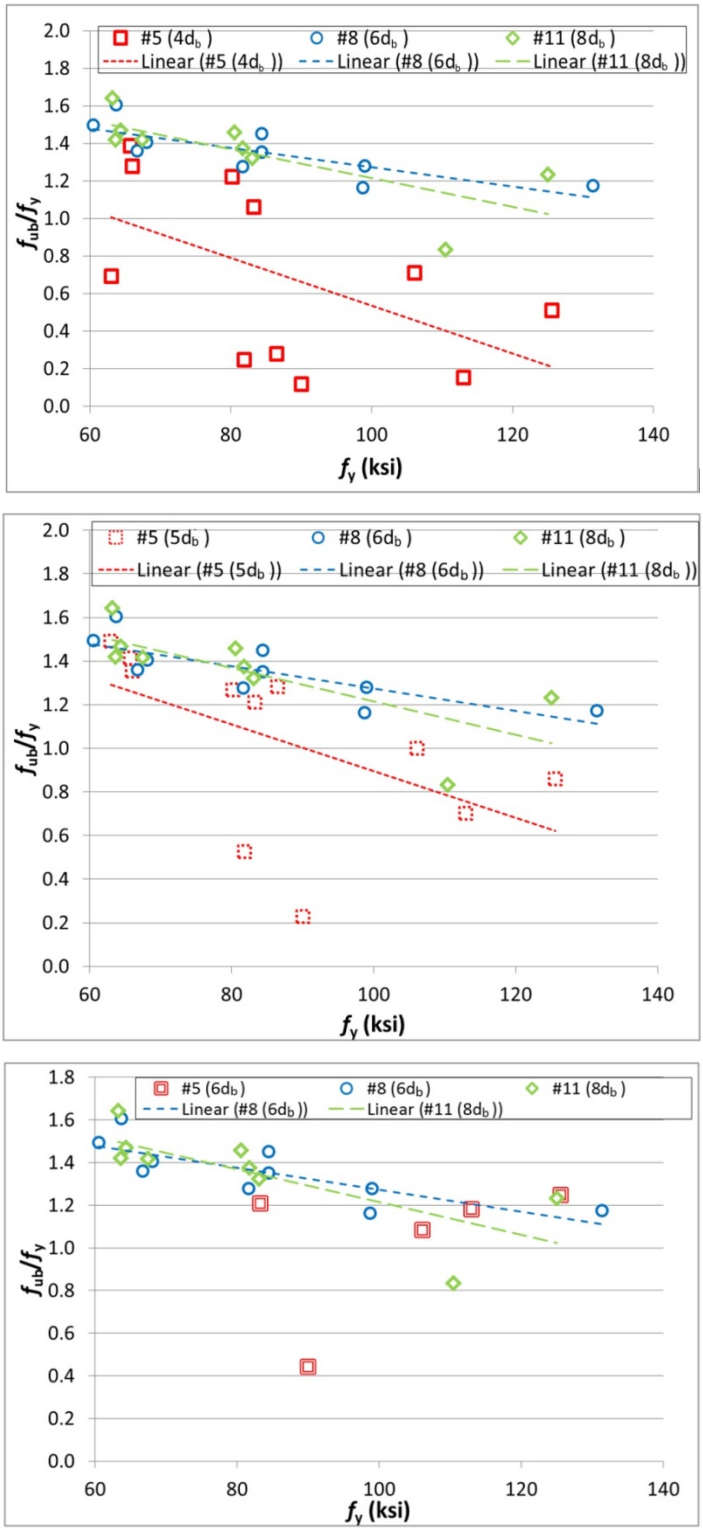

Figure 29: Comparison of normalized stress at fracture vs measured yield strength for various bar sizes

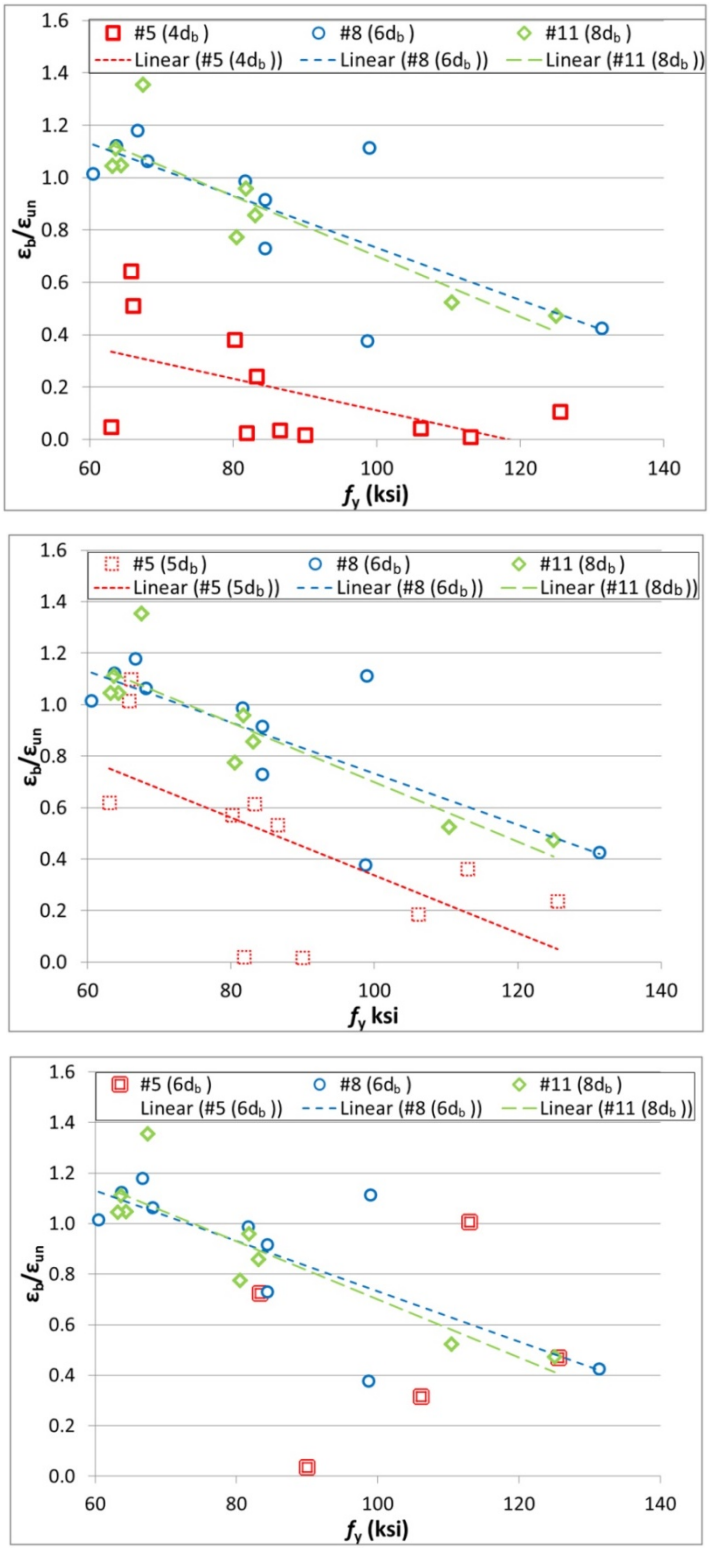

Figure 30: Comparison of normalized strain at fracture vs measured yield strength for various bar sizes

Given the relatively large scatter in the performance of #5 bars compared with that of the larger bars, the possible effects of the manufacturing processes on the performance of #5 bars are explored in Figure 31. The #5 bars from Manufacturer 1 bent at $4d_b$, with the exception of M1_Gr60_A706 bars, fractured at stresses below the linear regression trend line for all #5 ($4d_b$) bars. However, the fractures stresses of bars from Manufacturer 1 bent at $5d_b$ were distributed above and below the trend line, but exhibited high variability. Bars produced by Manufacturer 3 showed the high variability as well, with some bars failing at significantly higher stresses than the trend lines and others at significantly lower stresses. Bars from Manufacturers 2 and 4 were consistently above the trend lines.

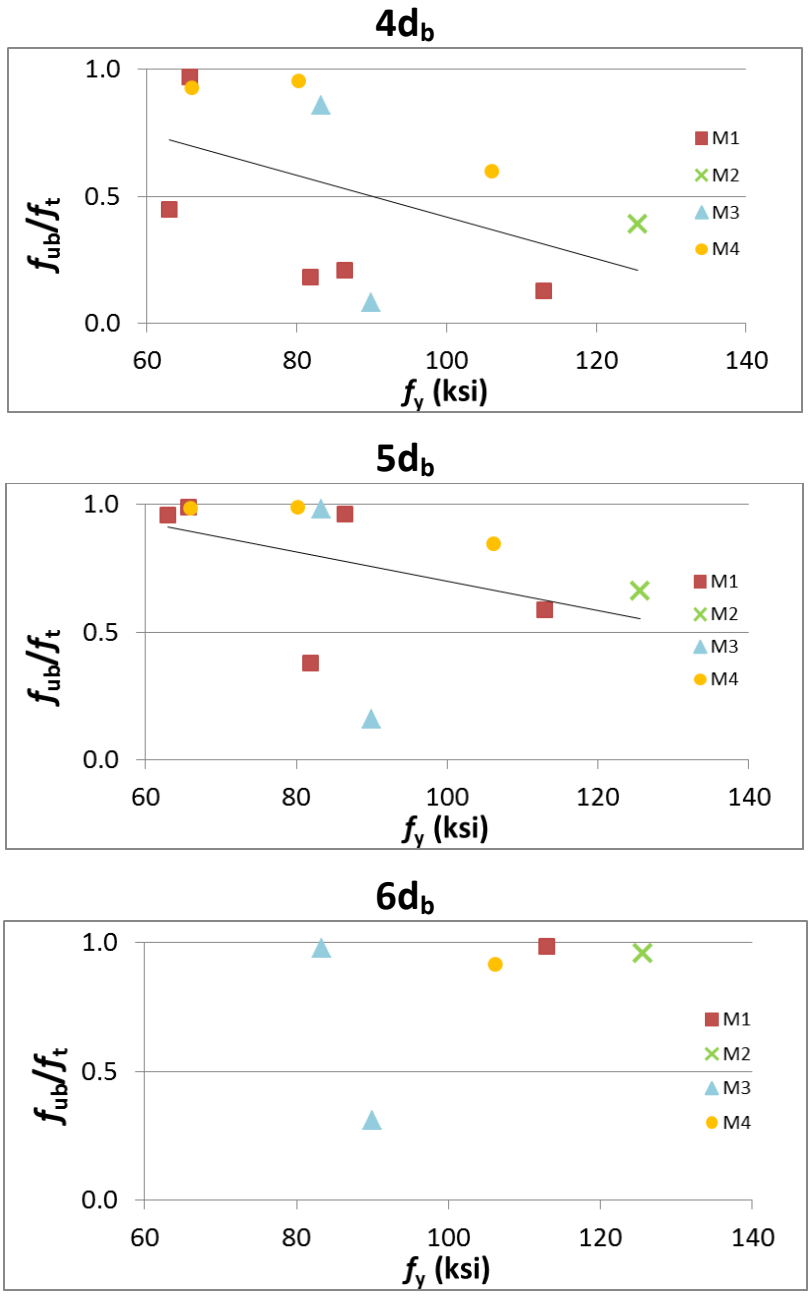

Figure 31: Re-bend stress at fracture normalized by tensile strength vs measured yield strength for #5 bars

4.3.6 Effects of Bend Diameter on Re-bend Performance

The #11 ($8d_b$) and #8 ($6d_b$) bar specimens performed reasonably well across all grades. However, the #5 ($4d_b$) bars did not. For this reason, additional #5 bars were bent at inside bend diameters of $5d_b$ and $6d_b$.

The effects of increasing bend diameters on (f_{ub}/f_y) can be seen in Figure 32. In the figure, lines with short dashes denote bars with yield strengths around 60 ksi (grade 60), lines with longer dashes denote bars with yield strengths around 80 ksi (grade 80), and solid lines denote bars with yield strengths around or exceeding 100 ksi (grade 100). As can be seen in

Figure 32, the stress at fracture of grade 60 bars is not affected significantly when increasing bend diameters from $4d_b$ to $5d_b$; with the exception of M1_60_A615 specimens. This is because these bars are failing at stresses close to their tensile strength at both bend diameters (Figure 31). On the other hand, the higher grades 80 and 100, fractured at stresses significantly below their tensile strength at a bend diameter of $4d_b$. This may be the reason why bars of these grades experienced significantly higher stresses at fracture with larger bend diameters.

While most grade 60 bars fractured at stresses above yield with bend diameters of $4d_b$, the majority of grade 80 and 100 bars did not. Even with a bend diameter of $5d_b$, the majority of grade 80 and 100 bars still did not reach their yield strengths prior to fracture during re-bending. It is only when the bend diameter is increased to $6d_b$ that the majority of grade 80 and 100 bars reached their yield strengths at fracture.

Considering the strain performance measure (ε_b / ε_{un}), all grades saw increases in strains at fracture with increasing bend diameters, with only a few reaching their uniform elongations during re-bending (Figure 33). Interestingly, even though grade 60 bars did not see significant increases in their stresses at fracture, they did see marked increases in their strain at fracture during re-bending with increasing bend diameters.

Considering the remaining bend angle at fracture (Figure 34), all grade 60 and 80 specimens bent at $5d_b$ essentially straightened during re-bending and most did so with $4d_b$

bends. Most grade 100 bars, on the other hand, fully straightened only when they were bent at $6d_b$ and most did not straighten when bent to tighter diameters.

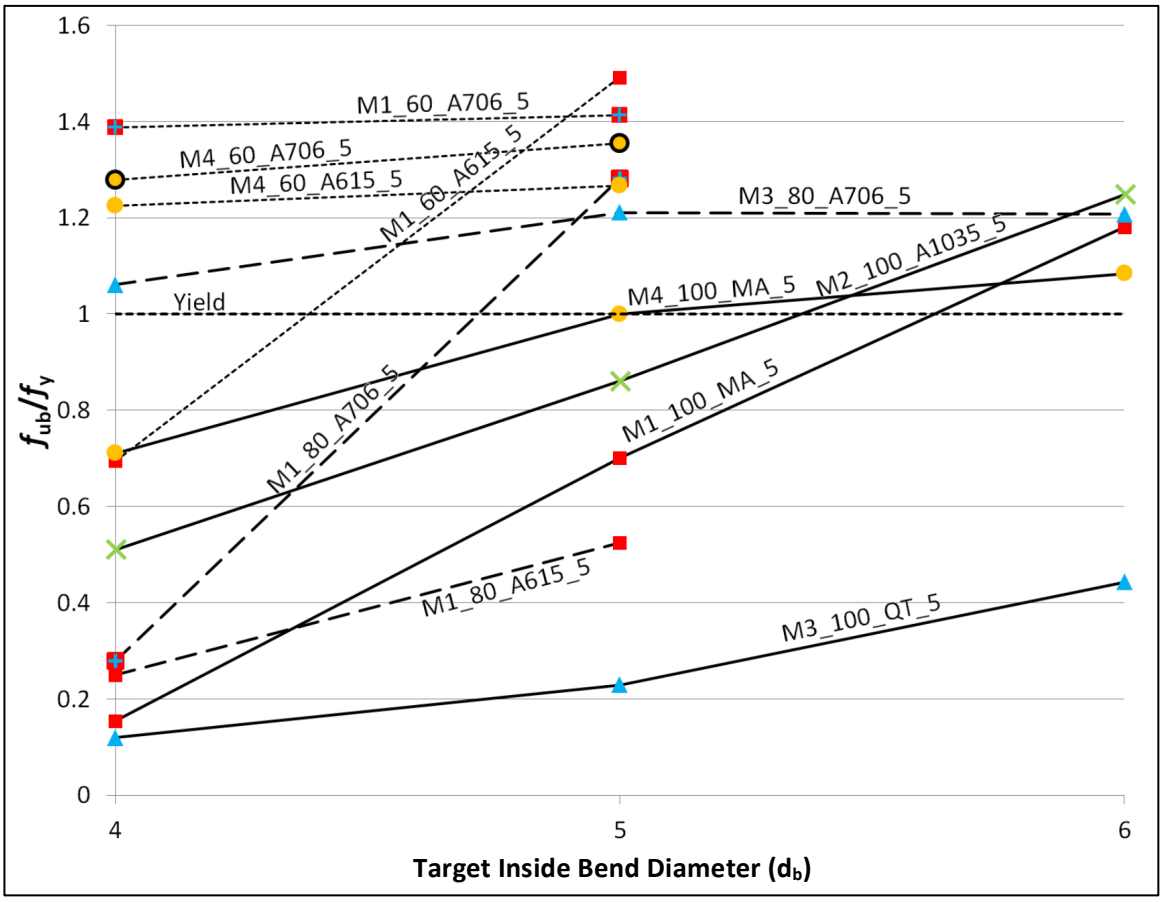

Figure 32: Normalized Re-bend Fracture Stress vs Target Bend Diameter

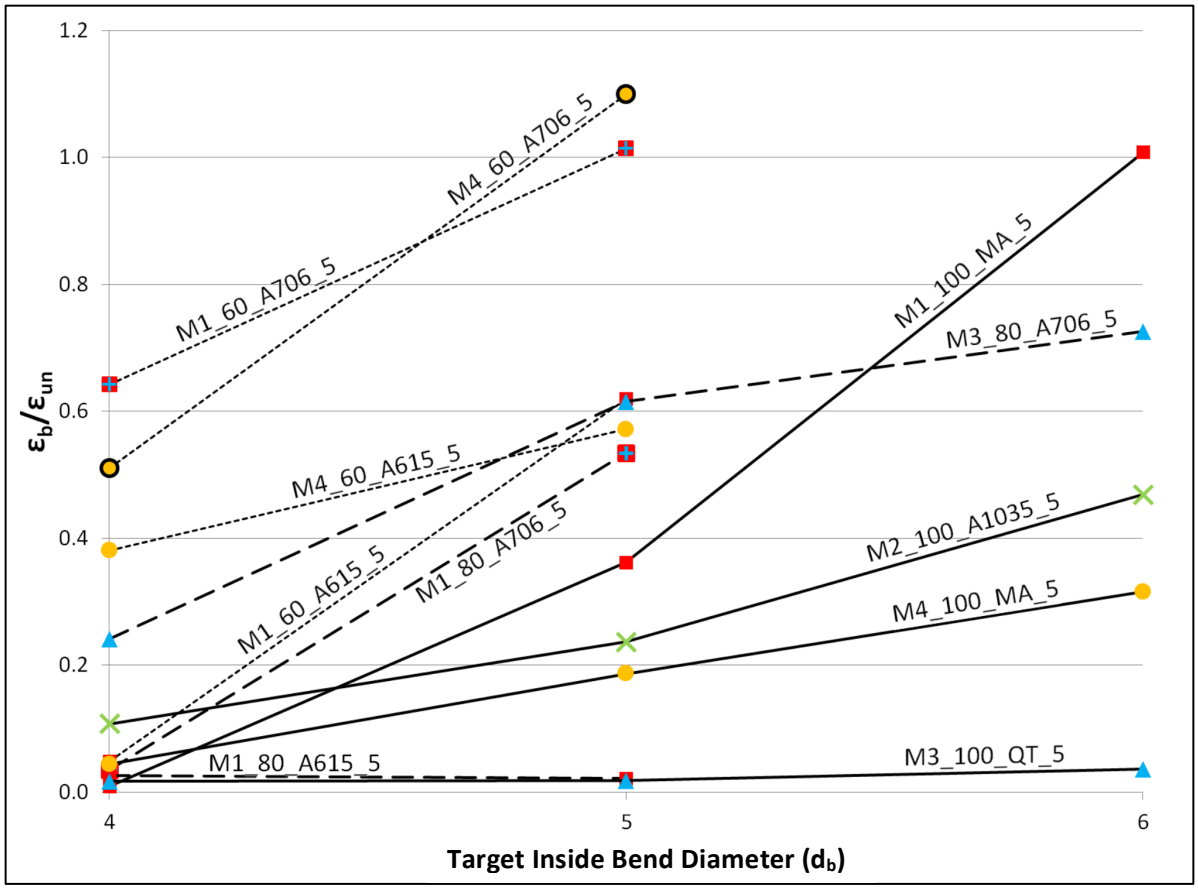

Figure 33: Normalized Re-bend Fracture Strain vs Target Bend Diameter

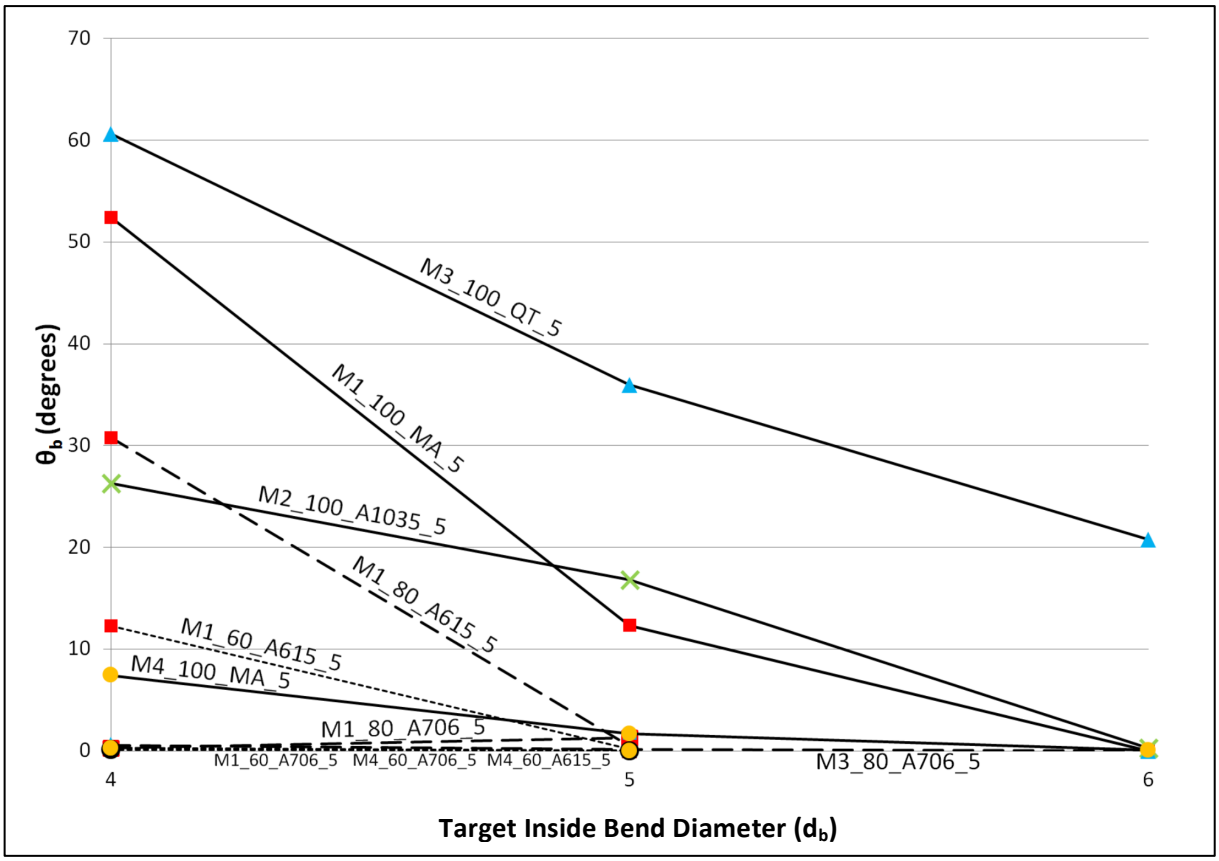

Figure 34: Normalized Re-bend Fracture Angle vs Target Bend Diameter

In summary for all performance measures considered, increasing the bend diameter from $4d_b$ to $6d_b$ was found to generally have a positive effect. Overall, #5 bars of all grades saw increased ductility at the bends with increasing bend diameters. Grade 80 and 100 #5 bars saw increases in stress at fracture during re-bending with increasing bend diameters. Grade 60 #5 bars, however did not as they reached stresses close to their tensile strength even with a bend diameter of $4d_b$.

4.3.7 Theoretical Strain in Bent Specimens

The impact of the lower ductility of HSRB on bend performance is investigated by comparing the strains induced by bending with the strain capacity of bars, namely their uniform elongation (ε_{un}). Uniform elongating is used here as it is less dependent on bar size and measurement gauge length than fracture elongation. Since bending strains are difficult to measure, the maximum theoretical tension strain at the outer surface of the bars was estimated as follows, assuming zero elongation at the neutral axis ($\varepsilon_{theoretical}$) .

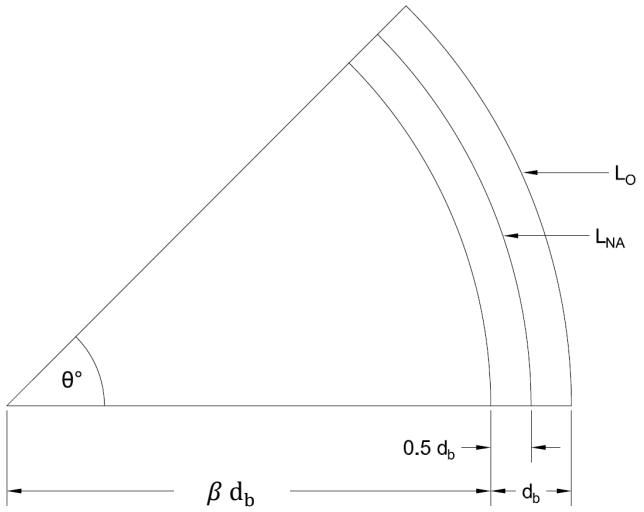

Figure 35: Max Theoretical Strain Derivation

$$\varepsilon_{theoretical} = \frac{L_O}{L_{NA}} \qquad \text{(Equation 4.3.1)}$$

$$L_O = 2 * \pi * (\beta * d_b + d_b) * \frac{\theta}{360} \qquad \text{(Equation 4.3.2)}$$

$$L_{NA} = 2 * \pi * \left(\beta * d_b + \frac{1}{2} d_b\right) * \frac{\theta}{360} \qquad \text{(Equation 4.3.3)}$$

$$\varepsilon_{theoretical} = \frac{\beta * d_b + d_b}{\beta * d_b + \frac{1}{2} d_b} - 1 = \frac{\beta + 1}{\beta + \frac{1}{2}} - 1 \qquad \text{(Equation 4.3.4)}$$

As can be seen in Equation 4.3.4, the theoretical strain is independent of bar size and is only a function of β, the ratio of bend inside diameter to bar diameter.

Using Equation 4.3.4, the maximum theoretical strain, ε_{mt}, experienced at the edge of the specimens using the targeted ACI 318-14 minimum bend diameters was calculated. Similarly, the maximum theoretical bend stain corresponding to the actual pin sizes used during bending, ε_{ma}, was calculated using Equation 4.3.4. The strains based on pin diameter rather than those based on the final bend diameter after spring back (Table 1) were considered as they were deemed to be more representative of the maximum strains experienced during bending. The calculated strain values are presented in Table 8.

Table 8: Theoretical Strains at Bends

	Bar Specimens				
	#5 ($4d_b$)	**#5 ($5d_b$)**	**#5 ($6d_b$)**	**#8 ($6d_b$)**	**#11 ($8d_b$)**
Pin Diameters Used (in.)	2.0	2.5	3.0	5.0	10.0
β_{ACI} = Target Bend Diameter / d_b	4	5	6	6	8
β_{Pin} = Pin Diameter / d_b	3.20	4.00	4.80	5.00	7.27
Target Maximum Theoretical Strain, ε_{mt}	0.110	0.091	0.077	0.077	0.059
Max Theoretical Strain Based on Pin Size, ε_{ma}	0.135	0.111	0.094	0.091	0.064

Figure 36 compares the maximum theoretical strains associated with the bending pin diameters (ε_{ma}) with the uniform strain values of the bars tested. A point below the theoretical strain line suggests that the bar specimen was bent past its uniform strain. As can be seen in the figure, all but one of the #11 bars were bent to a maximum estimated strain that is considerably lower than the uniform strains of the bars. This is owing to the large ratio of bend to bar diameter used for #11 bars (β_{Pin}). Most #8 bars were also strained significantly less than uniform strains (Figure 36). All #5 bars, including grade 60 bars, were strained past their uniform strain with β_{Pin} = 3.2 (for a $4d_b$ target bend diameter). In addition, most #5 bars, especially higher grade bars, were strained past their uniform strain with β_{Pin} = 4.0 (for a $5d_b$ target bend diameter). It is only when #5 bars are bend to a β_{Pin} = 4.8 (for a $6d_b$ target bend diameter), that grade 60 and 80 bars experience an estimated bend strain at or below their

uniform strains. Grade 100 # 5 bars, however, still appeared to have been strained higher than their uniform strain values at β_{Pin} = 4.8.

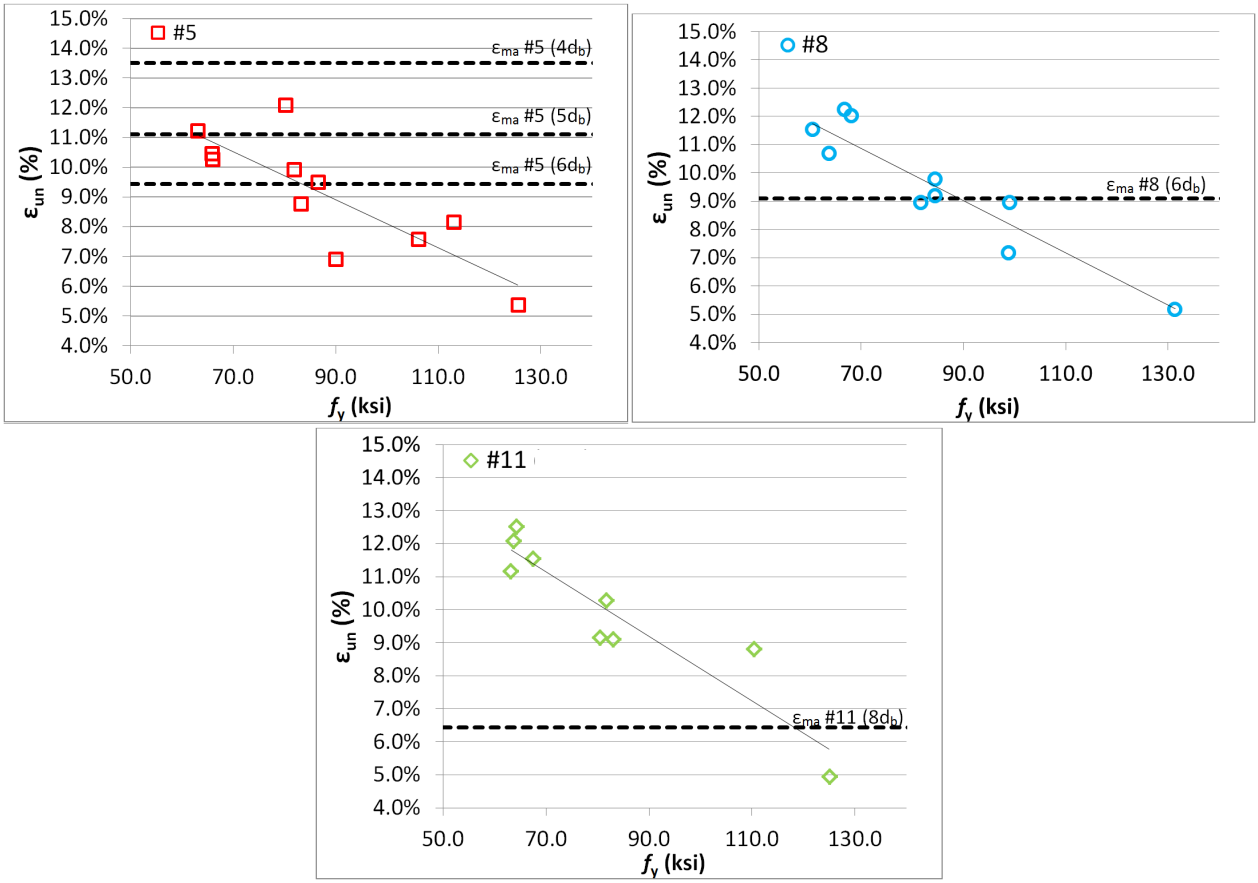

Figure 36: Bar uniform strain vs measured yield strength overlaid with the estimated maximum bend strains (ε_{ma})

These observed trends between strains experienced and bar uniform strains may help explain the poorer performance of #5 bars compared with the larger bars, and the poorer performance of higher grade bars that typically have lower uniform elongations than their lower grade counterparts. To explore these relations further, ($\varepsilon_{ma}/\varepsilon_{un}$) values were plotted versus (f_{ub}/f_y) for all bars in Figure 37, versus (f_{ub}/f_t) in Figure 38 and versus ($\varepsilon_b/\varepsilon_{un}$) in Figure 39. These figures indicate a clear negative correlation between the ratio of theoretical maximum strains incurred during bending and bar uniform strains ($\varepsilon_{ma}/\varepsilon_{un}$) for all performance measures considered. The figures therefore corroborate the hypothesis that bends in #5 and higher grade bars showed poorer performance because they were strained higher with respect to their uniform elongations.

Relations can be drawn between performance measures and the demand parameter ($\varepsilon_{ma}/\varepsilon_{un}$) as seen in Figure 37 to Figure 39. Given a target performance measure, these figures allow the selection of the maximum permissible bending strain to uniform strain ($\varepsilon_{ma}/\varepsilon_{un}$) allowable in bending. For a performance objective defined as $f_{ub}/f_y \geq 1.0$ during re-bending, Figure 37 indicates that $\varepsilon_{ma}/\varepsilon_{un}$ should not exceed about 1.2 during bending. With the exception of an outlying #11 data point and one #5 bar data point, we can see that all bar specimens with $\varepsilon_{ma}/\varepsilon_{un} \leq 1.2$ were able to develop their yield strength during re-bending (Figure 37). Moreover, with the exception of a limited number of specimens, those with an $\varepsilon_{ma}/\varepsilon_{un} \leq 1.2$ were also able to achieve stresses during re-bending that exceed 80% of their tensile strength (Figure 38), and strains that exceed 50% of their uniform strain capacities (Figure 39).

According to an $\varepsilon_{ma}/\varepsilon_{un} \leq 1.2$ criteria, the bend pin diameters used for #11 ($8d_b$), #8 ($6d_b$) and #5 ($6d_b$) bars (Table 8) result in adequate bend performance for all bars and grades tested in this study (Figure 36). A tighter pin diameter of four times the bar diameter, $\beta_{Pin} = 4.0$, used for #5 ($5d_b$) specimens, can be permitted for grade 60 and 80 bars but not grade 100 bars. Finally a $\beta_{Pin} = 3.2$ value should only be used for grade 60 bars.

Other limits on $\varepsilon_{ma}/\varepsilon_{un}$ can also be selected based on other performance objectives using Figure 37 to Figure 39.

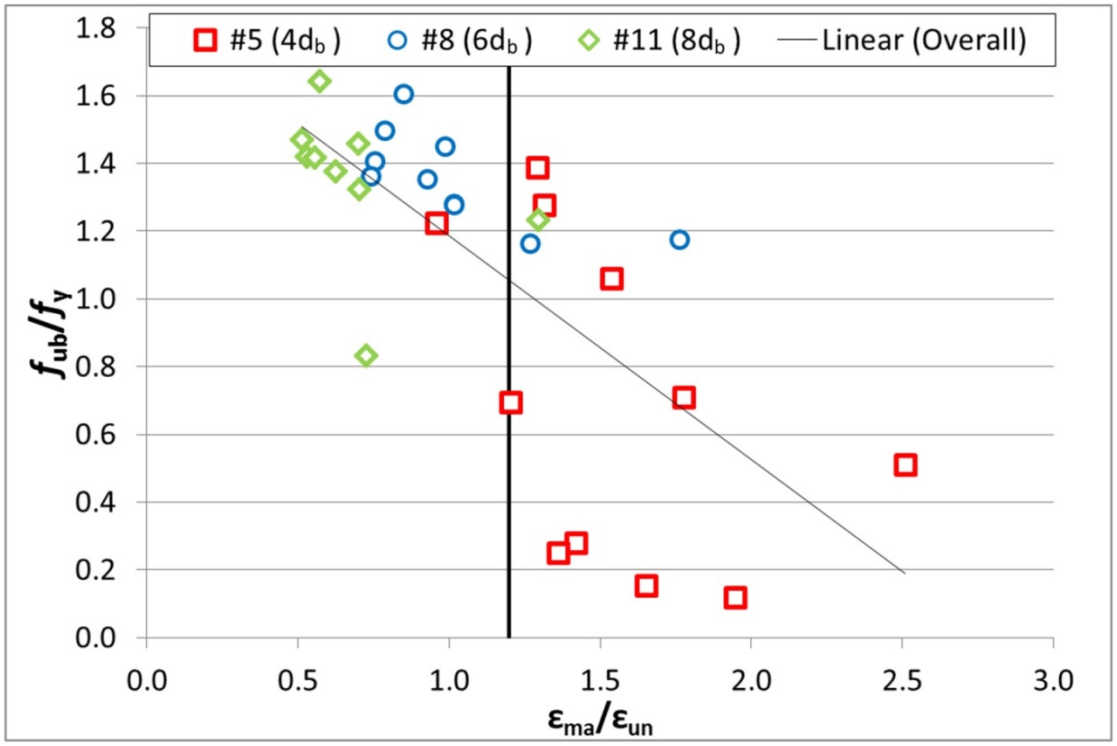

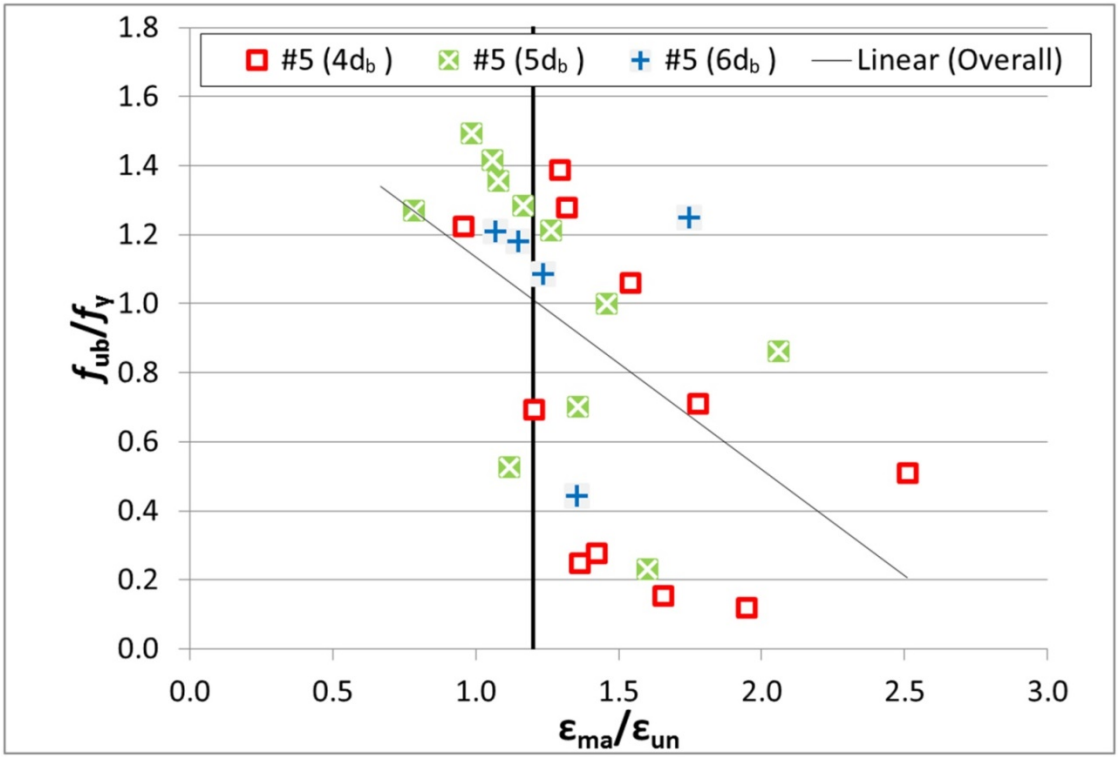

Figure 37: Normalized fracture stress vs normalized theoretical bend strain

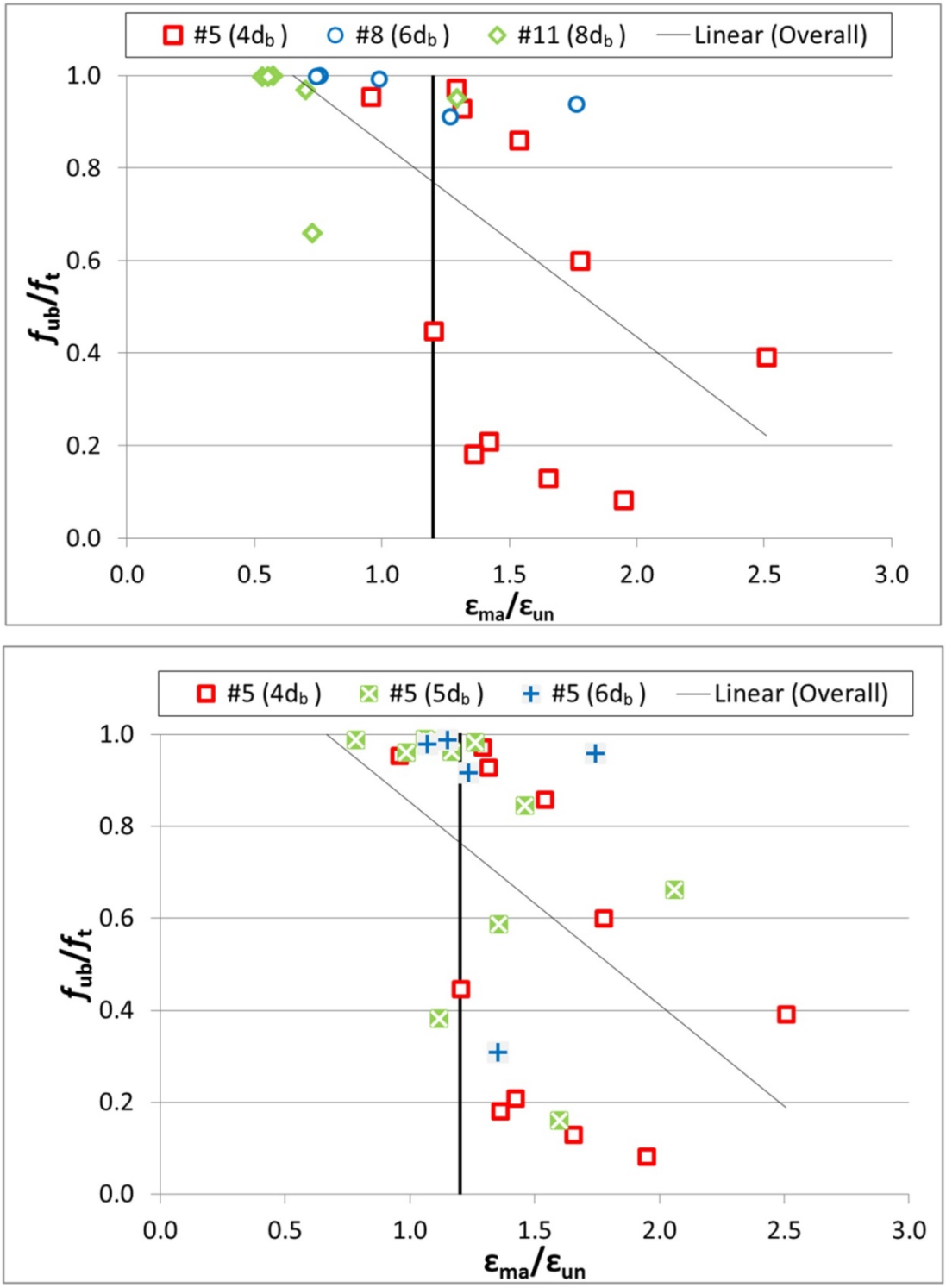

Figure 38: Normalized fracture stress (f_{ub}/f_t) vs normalized theoretical bend strain

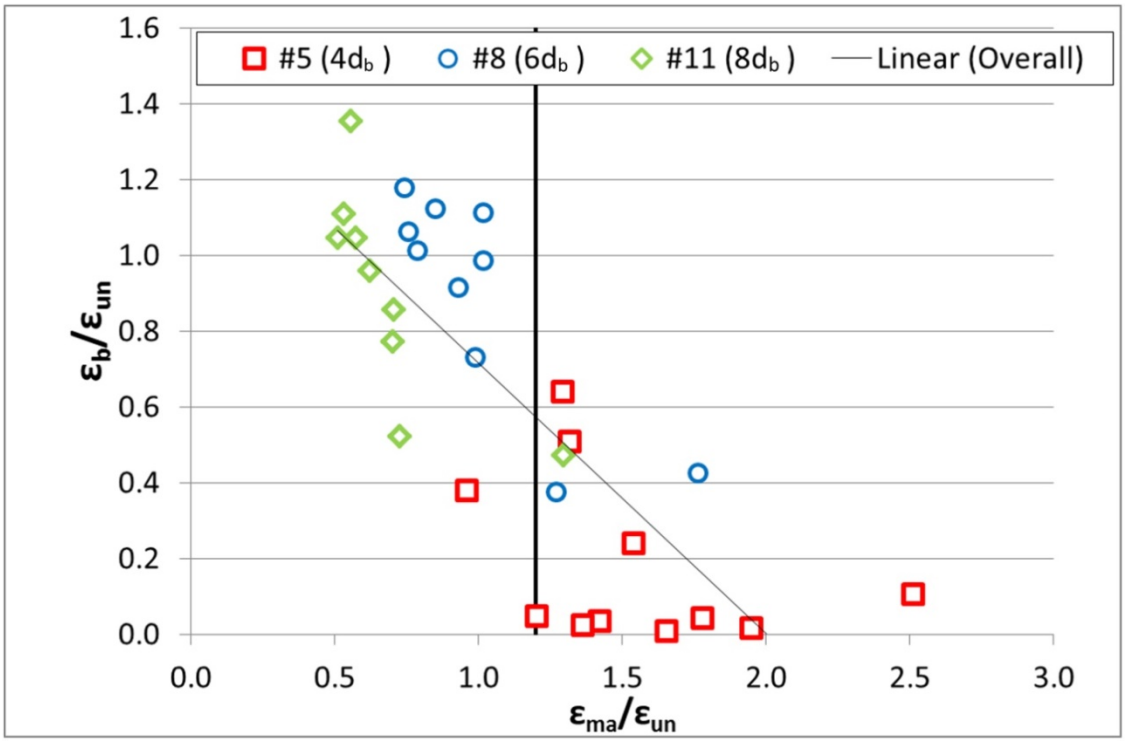

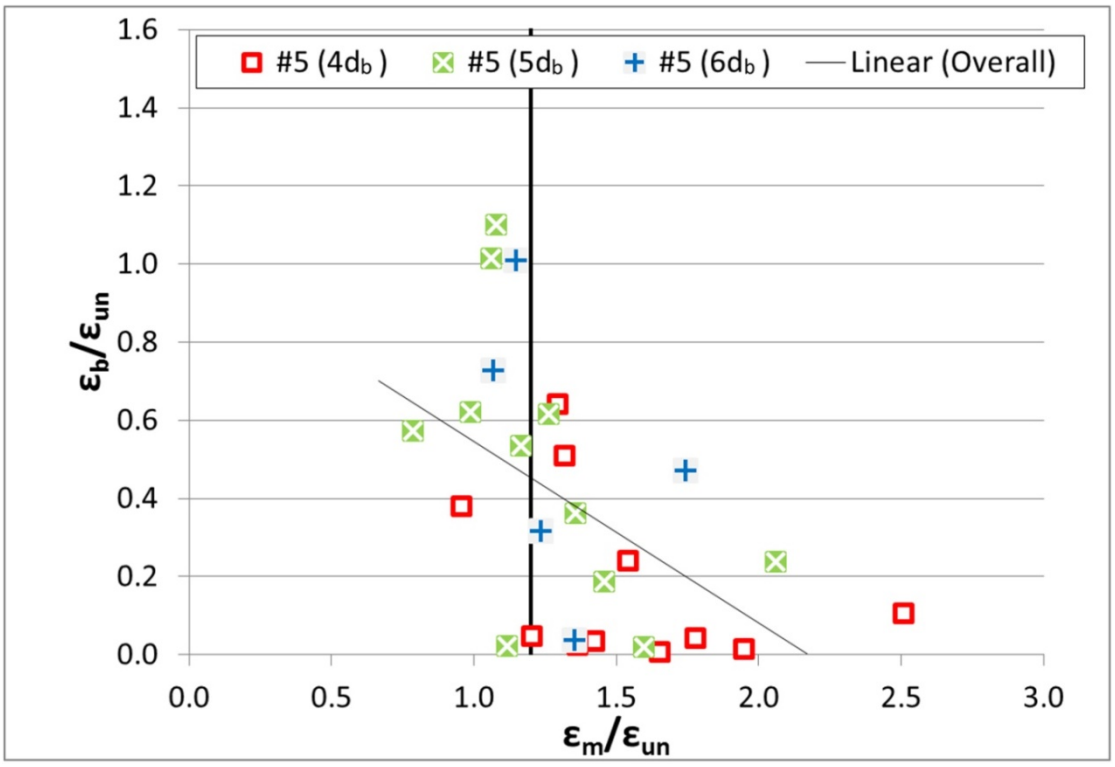

Figure 39: Normalized fracture strain vs normalized theoretical bend strain

CHAPTER 5: Recommendations for Minimum Bend Diameters

In this chapter, recommendations for minimum inside bend diameters for reinforcing bars are given for various bar sizes and ASTM steel grades. The recommendations are given as a function of the minimum required fracture elongation of the bars, as given in the ASTM standards A615, A706, and A1035. Minimum bend diameter recommendations are also provided as a function of the historic elongation data obtained from the CRSI Mill Database (CRSI). The minimum bend diameters provided are intended to deliver bends that are capable, at a minimum, of sustaining their yield strength prior to fracture in a re-bend test. Fracture elongation, ε_f, is used here as it is the strain given in ASTM standards for reinforcing bars and in the CRSI Mill Database; even though this measure is dependent on the ratio between the standard 8" measurement gauge length and bar diameter.

5.1 Performance Objective

As demonstrated in Chapter 4, the ratio of theoretical maximum tensile strain at a bend based on pin diameters (ε_{ma}) to bar uniform elongation (ε_{un}) governs bend performance under load. A similar relation can be observed with respect to the fracture elongation of bars (ε_f) (Figure 40). As can be seen in Figure 40, all bars bent to pin diameters that did not generate a theoretical peak strain exceeding $0.8\varepsilon_f$ ($\varepsilon_{ma} \leq 0.8\varepsilon_f$) were able to reach the yield performance objective; except for one outlying #11 bar test. For a threshold strain ratio $\alpha_f = \varepsilon_{ma} / \varepsilon_f$ between 0.8 and 1.0, 8 bar types exceed the yield stress performance objective while 5 do not (Figure 40). For $\alpha_f = \varepsilon_{ma} / \varepsilon_f > 1.0$, all but one bar types fail the performance objective. Bar bends that do not exceed the threshold value of $\varepsilon_{ma} = 0.8\varepsilon_f$ are therefore deemed to satisfy the minimum performance objective and should have adequate performance under loading.

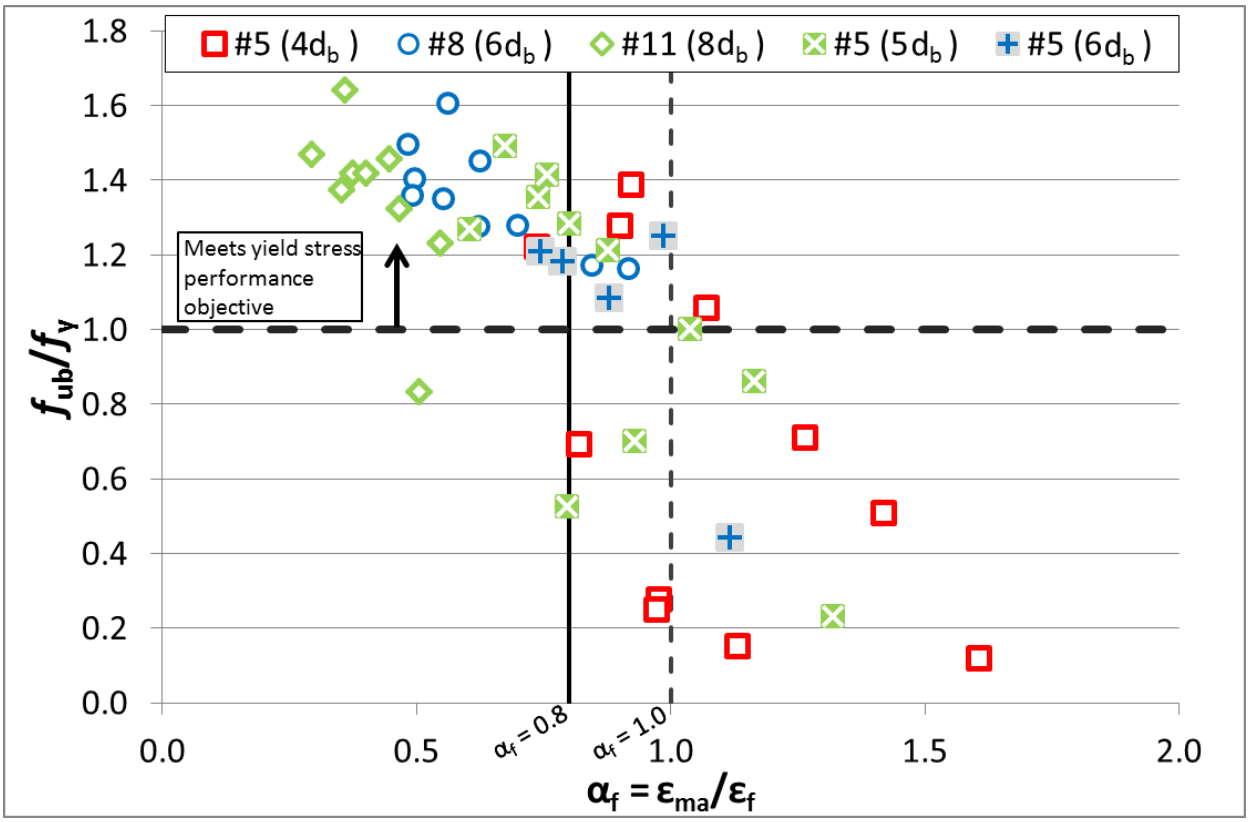

Figure 40: Normalized fracture stress vs normalized theoretical bend strain

5.2 Relation between Inside Bend Diameter and Threshold Strain Ratio (α_f)

Recall Equation 4.3.4 relating the theoretical peak tensile strain in a bend ($\varepsilon_{theoretical}$) to the bend diameter ratio ($\beta = bend\ diamter/d_b$).

$$\varepsilon_{theoretical} = \frac{\beta + 1}{\beta + 1/2} - 1$$

Substituting $\varepsilon_{theoretical}$ with $\alpha_f \varepsilon_f$, the threshold peak strain, we get the theoretical minimum bend diameter ratio to be:

$$\beta_{TH} = \frac{\frac{1}{2} - \frac{\alpha_f \varepsilon_f}{2}}{\alpha_f \varepsilon_f} \qquad \text{(Equation 5.1.1)}$$

Figure 41 illustrates the geometric relationship between β_{TH} and a bar's fracture strain (ε_f) for various threshold strain ratios (α_f) based on Equation 5.1.1. This graph indicates the minimum bend pin diameter to use to generate a peak bend strain within a prescribed fraction (α_f) of the bar fracture elongation. For example, for a bar with a fracture elongation $\varepsilon_f = 0.1$, a pin diameter $\beta_{TH} = 5.75$ should be used to achieve a theoretical peak strain of 80% of ε_f (or $\alpha_f = 0.8$).

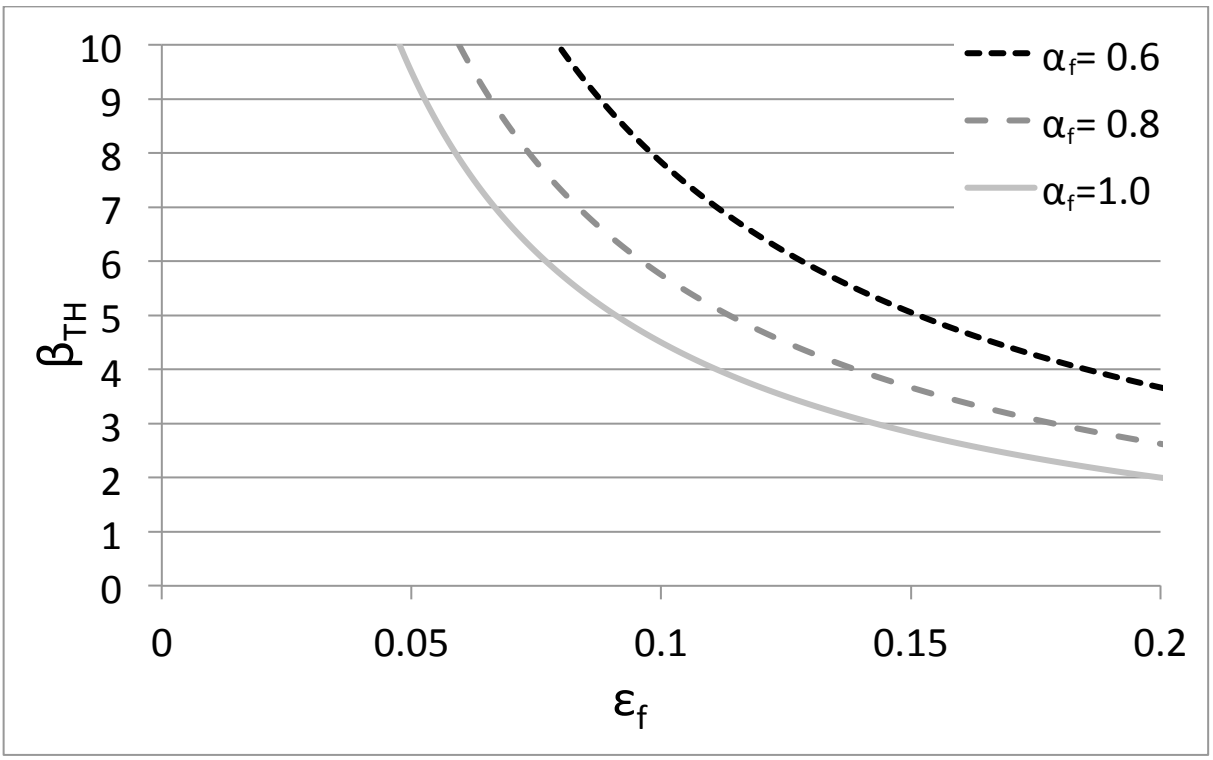

Figure 41: Relation between β_{TH} and bar fracture strain (ε_f) for various threshold strain ratios (α_f)

5.3 Minimum Bend Diameters based on Minimum ASTM Elongations

The minimum bend pin diameter (β_{ASTM}) based on ASTM minimum elongation values that achieves the desired yield strength performance objective can be obtained by setting the bar fracture elongation $\varepsilon_{f,ASTM}$ = minimum ASTM specified fracture elongation, and α_f = 0.8 in Equation 5.1.1. This estimate of the pin diameter is conservative because all bars with an α_f = 0.8 are expected to achieve the performance objective while all bars satisfying the ASTM specification have fracture elongations exceeding $\varepsilon_{f,ASTM}$ (Table 9,

Table 10, and Table 11). A less conservative estimate on pin diameter can be obtained by using $\varepsilon_{f,ASTM}$ but α_f = 1.0. Table 12 presents the bend pin diameters (β_{ASTM}) based on ASTM elongations for various steel specifications, grades, and α_f values. A spring-back resulting in a 15% increase in bend diameter from the pin diameter to the final at-rest inside bend diameter can be conservatively assumed based on measured spring-back values in this study (Table 1). This assumption results in the adjusted values $\beta_{ASTM,ADI}$ = β_{ASTM} * 1.15 that can be compared with current ACI 318-14 minimum inside bend diameters (β_{ACI}). Figure 42 illustrates this comparison for A615, #5 bars of various steel grades. In Table 12, bolded ratios of $\beta_{ASTM,ADJ}$ / β_{ACI} indicate that ACI bend diameters achieve the desired performance objective.

Table 9: ASTM A615 Fracture Elongation Requirements

ASTM A615 Fracture Elongation Requirements $\varepsilon_{f,ASTM}$ = Min. elongation in 8in. %				
Bar Designation No.	Grade 40	Grade 60	Grade 80	Grade 100
3	11	9	7	7
4, 5	12	9	7	7
6	12	9	7	7
7, 8	…	8	7	7
9, 10, 11	…	7	6	6
14, 18, 20	…	7	6	6

Table 10: ASTM A706 Fracture Elongation Requirements

ASTM A706 Fracture Elongation Requirements $\varepsilon_{f,ASTM}$ = Min. elongation in 8in. %		
Bar Designation No.	Grade 60	Grade 80
3, 4, 5, 6	14	12
7, 8, 9, 10, 11	12	12
14, 18	10	10

Table 11: ASTM A1035 Fracture Elongation Requirements

ASTM A1035 Fracture Elongation Requirements $\varepsilon_{f,ASTM}$ = Min. elongation in 8in. %		
Bar Designation No.	Grade 100	Grade 120
3, 4, 5, 6, 7, 8, 9, 10, 11	7	7
14, 8	6	6

Table 12: Comparison between minimum bend diameters to achieve the yield strength performance objective and ACI 318-14 minimum bend diameters (assuming the same ACI 318-14 bend diameters apply to high-strength bars)

ASTM A615	Grade	β_{ACI}	$\alpha_f = 0.8$		$\alpha_f = 1.0$	
			$\beta_{ASTM,ADJ}$	$\beta_{ASTM,ADJ}/\beta_{ACI}$	$\beta_{ASTM,ADJ}$	$\beta_{ASTM,ADJ}/\beta_{ACI}$
#5 transverse	40	4.0	5.4	1.35	4.3	1.06
	60	4.0	7.4	1.84	5.9	1.47
	80	4.0	9.7	2.42	7.6	1.90
	100	4.0	9.7	2.42	7.6	1.90
#5 longitudinal	40	6.0	5.4	**0.90**	4.3	**0.71**
	60	6.0	7.4	1.23	5.9	**0.98**
	80	6.0	9.7	1.61	7.6	1.27
	100	6.0	9.7	1.61	7.6	1.27
#8	60	6.0	8.4	1.40	6.7	1.11
	80	6.0	9.7	1.61	7.6	1.27
	100	6.0	9.7	1.61	7.6	1.27
#11	60	8.0	9.7	1.21	7.6	**0.95**
	80	8.0	11.4	1.42	9.0	1.12
	100	8.0	11.4	1.42	9.0	1.12
ASTM A706	Grade	β_{ACI}	$\alpha_f = 0.8$		$\alpha_f = 1.0$	
			$\beta_{ASTM,ADJ}$	$\beta_{ASTM,ADJ}/\beta_{ACI}$	$\beta_{ASTM,ADJ}$	$\beta_{ASTM,ADJ}/\beta_{ACI}$
#5 tran.	60	4.0	4.6	1.15	3.6	**0.89**
	80	4.0	5.4	1.35	4.3	1.06
#5 long.	60	6.0	4.6	**0.77**	3.6	**0.59**
	80	6.0	5.4	**0.90**	4.3	**0.71**
#8	60	6.0	5.4	**0.90**	4.3	**0.71**
	80	6.0	5.4	**0.90**	4.3	**0.71**
#11	60	8.0	5.4	**0.68**	4.3	**0.53**
	80	8.0	5.4	**0.68**	4.3	**0.53**
ASTM A1035	Grade	β_{ACI}	$\alpha_f = 0.8$		$\alpha_f = 1.0$	
			$\beta_{ASTM,ADJ}$	$\beta_{ASTM,ADJ}/\beta_{ACI}$	$\beta_{ASTM,ADJ}$	$\beta_{ASTM,ADJ}/\beta_{ACI}$
#5 tran.	100	4.0	9.7	2.42	7.6	1.90
	120	4.0	9.7	2.42	7.6	1.90
#5 long.	100	6.0	9.7	1.61	7.6	1.27
	120	6.0	9.7	1.61	7.6	1.27
#8	100	6.0	9.7	1.61	7.6	1.27
	120	6.0	9.7	1.61	7.6	1.27
#11	100	8.0	9.7	1.21	7.6	**0.95**
	120	8.0	9.7	1.21	7.6	**0.95**

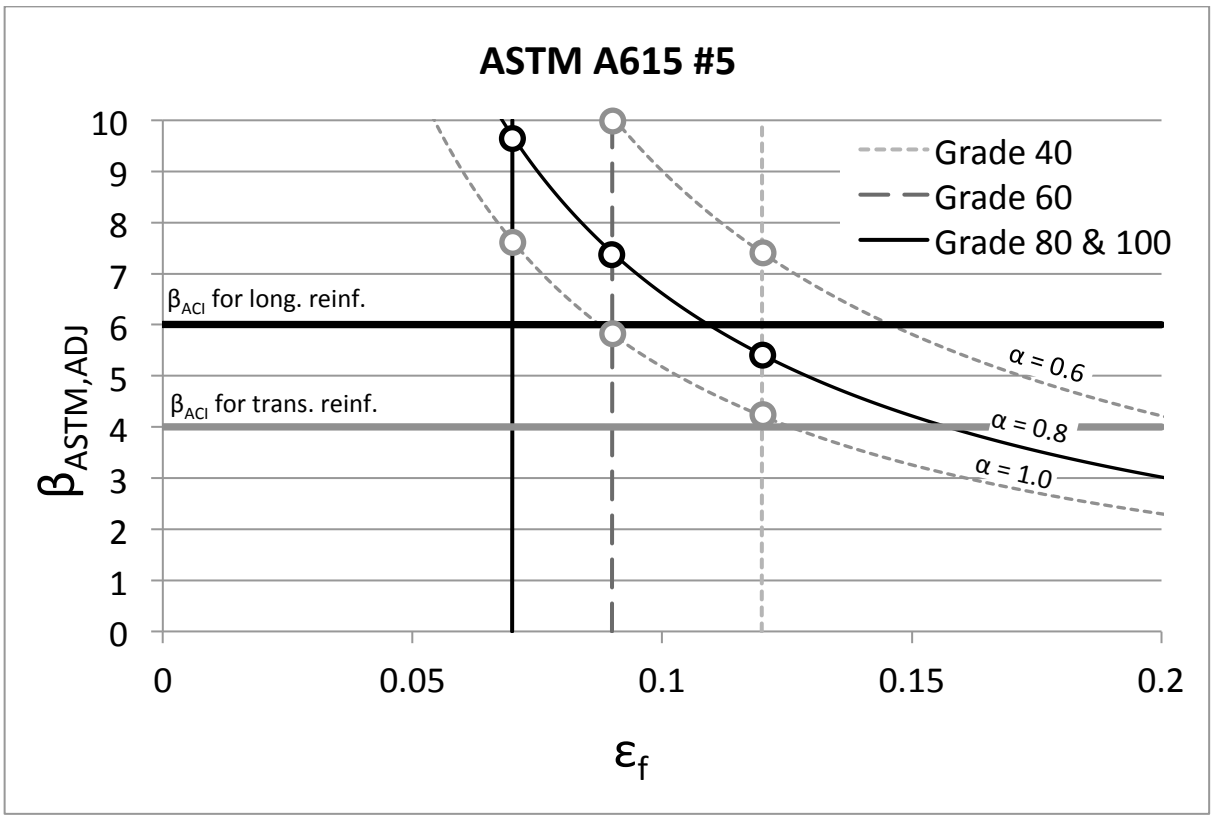

Figure 42: $\beta_{ASTM,ADJ}$ and bar fracture strain (ε_f) for various threshold strain ratios (α_f) for ASTM A615 #5 bars

As can be seen in Table 12, all ASTM A615 bar types, except one, bent to ACI 318-14 diameters are deemed not to achieve the yield strength performance objective with α_f = 0.8, with only a few more achieving it with an α_f of 1.0. On the other hand, Table 12 indicates that all longitudinal bars satisfying the ASTM A706 specifications can achieve the desired performance with an α_f of 0.8. Transverse bars satisfying ASTM A706 specifications having tighter ACI 318 bend diameters than longitudinal bars do not meet this objective but only by a small margin. Similarly to A615 bars, all A1035 bars bent to ACI 318-14 diameters are deemed not to achieve the yield strength performance objective with α_f = 0.8, with only the # 11 bars achieving it with an α_f of 1.0.

These results therefore indicate that most A615 and A1035 bar bends satisfying ACI 318-14 should exhibit poor performance while A706 bars bends should exhibit adequate performance.

However, that is not the case in concrete structures where A615 grade 60 bars and A1035 bars have been shown to have adequate performance. The disconnect may be attributed to the conservative nature of the acceptance criteria selected. Of particular concern is the overly conservative use of the minimum specified ASTM values for fracture strains ($\varepsilon_{f,ASTM}$) in the evaluation. The following section investigates this point further.

5.4 Minimum Bend Diameters based on CRSI Mill Database Elongations

Because the ASTM values for ε_f are minimum values and are typically exceeded by a significant margin in production (especially for the lower grade bars), it is useful to compare the β_{TH} obtained by using the statistical values of fracture elongations (ε_f) and the current ACI 318-14 bend diameter ratios (β_{ACI}).

This comparison is first made using statistical elongations for grade 60 bars obtained from the Concrete Reinforcing Institute's (CRSI) Mill Database (CRSI, 2015), presented in Section 5.4.1. The probabilities of failing the yield stress performance objective for grade 60 bars bent to ACI 318-14 diameters were evaluated using statistical elongation data, and used to demonstrate that the yield stress objective is in line with actual bend performance in concrete structures (Section 5.4.2).

In Section 5.4.3, the target bend diameter ratios required to achieve a given probability of failing the yield performance objective (β_{Pf}) are evaluated for all bar types and grades, for which sufficient elongation data was available in the CRSI database. Particularly, the fracture elongation values for ASTM A615 grade 60, 80 and 100 and A706 grade 60 and 80 bars were used. Bend diameter recommendations are given for those bar types and grades based on this analysis.

5.4.1 CRSI Mill Database

The CRSI Mill Database (2015) summarizes the various monotonic-test properties of bars produced in the United-States in 2015. The mean (μ) and standard deviation values (σ) for fracture elongations obtained from the database are summarized for grade 60 bars in Table 13 to Table 15 for the various bar sizes used in this study.

Table 13: Summary of fracture elongation values from CRSI Mill Database for ASTM A615 bars

A615 GR60	ε_f		
	μ	σ	μ - 2×σ
#5	0.132	0.018	0.096
#8	0.137	0.021	0.095
#11	0.131	0.026	0.079

Table 14: Summary of fracture elongation values from CRSI Mill Database for ASTM A706 bars

A706 GR60	ε_f		
	μ	σ	μ - 2×σ
#5	0.16	0.017	0.126
#8	0.162	0.026	0.110
#11	0.149	0.027	0.095

Table 15: Summary of fracture elongation values from CRSI Mill Database for dual grade ASTM A615/A706 bars

DUAL A615/A706	ε_f		
	μ	σ	μ - 2×σ
#5	0.154	0.017	0.120
#8	0.165	0.017	0.131
#11	0.172	0.021	0.130

The mean (μ) and standard deviation values (σ) for fracture elongations obtained from the database are summarized for grade 80 and 100 bars in Table 13 to Table 15 for the various bar sizes used in this study.

5.4.1 Probabilities of Failure of Bends Based on Grade 60 Production Data

In this section, the percentages of grade 60 bars in production that would fail the yield strength performance objective if bent to ACI 318-14 minimum bend diameters are evaluated based on bar properties summarized in Table 13-Table 15.

To achieve this, the following probabilities of failing the yield strength performance objective are assumed based on test data illustrated in Figure 40:

$$P_{f1} = P[f_{ub}/f_y \leq 1.0 \mid \alpha_f \leq 0.8] = 0.0 \qquad \text{Equation 5.4.1}$$

$$P_{f2} = P[f_{ub}/f_y \leq 1.0 \mid 0.8 < \alpha_f \leq 1.0] = 0.5 \qquad \text{Equation 5.4.2}$$

$$P_{f3} = P[f_{ub}/f_y \leq 1.0 \mid 1.0 < \alpha_f] = 1.0 \qquad \text{Equation 5.4.3}$$

Then the probability of failure of bends for a given bar type, size, and target bend diameter ratio (β_{ACI}) can be estimated as:

$$P_{fTotal} = P[\varepsilon_f < \varepsilon_{f,1.0}]*P_{f3} + P[\varepsilon_{f,1.0} < \varepsilon_f \leq \varepsilon_{f,0.8}]*P_{f2} + P[\varepsilon_f \geq \varepsilon_{f,0.8}]*P_{f1} \qquad \text{Equation 5.4.4}$$

With:

$P[\varepsilon_f < \varepsilon_{f,1.0}]$, $P[\varepsilon_{f,1.0} < \varepsilon_f \leq \varepsilon_{f,0.8}]$, and $P[\varepsilon_f \geq \varepsilon_{f,0.8}]$ being the probabilities that bars in a bar type have a measured fracture elongation within the ranges specified by the minimum required fracture strains for bars bent to current ACI 318-14 bend diameters and for a given α_f. In these calculations, the fracture elongation (ε_f) is assumed to follow a normal distribution with mean (μ) and standard deviation values (σ) given in Tables 13 to 15.

$$\varepsilon_{f,0.8} = \frac{\left[\frac{\beta_{ACI}/1.15+1}{\beta_{ACI}/1.15+1/2} - 1\right]}{0.8} \qquad \text{Equation 5.4.5}$$

$$\varepsilon_{f,1.0} = \frac{\left[\frac{\beta_{ACI}/1.15+1}{\beta_{ACI}/1.15+1/2}-1\right]}{1.0}$$ Equation 5.4.6

Table 16 summarizes the minimum required fracture strains for bars bent to current ACI 318-14 bend diameters based on Eqs. 5.4.5 and 5.4.6.

Table 16: Minimum required fracture strains for bars bent to current ACI 318-14 bend diameters

β_{ACI}	$\varepsilon_{f,0.8}$	$\varepsilon_{f,1.0}$
4.0	0.157	0.126
5.0	0.129	0.103
6.0	0.109	0.087
8.0	0.084	0.067

Table 17 summarizes the probabilities of failing the performance objective of bends for ASTM A615 and A706 grade 60 bars produced in 2015 in the U.S. As can be seen in the table, all bars bent to achieve a final bend diameter ratio of 6.0 or more, regardless of size, have very low probabilities of failure and should exhibit adequate performance under load. At a target bend diameter ratio of 5.0, grade 60 A706 and dual grade bars still have relatively low probabilities of failure. However, at a target ratio of 4.0, Table 17 indicates that A615 bars have a 64% probability of not reaching the performance objective, while those probabilities remain relatively high but drop to 23% and 31% for A706 and dual grade bars, respectively.

Given that this failure analysis, which utilizes actual production data, determines that the vast majority of bars bent to ACI 318-14 specifications achieve the yield strength performance objective, which in line with observed bend performance in concrete structure, this performance objective is deemed to be a reasonable measure of performance for bar bends in concrete structures.

Based on these findings and results in Table 17, it may therefore be warranted to increase the minimum bend diameter requirement in ACI 318-14 form $4d_b$ to $5d_b$ for #5 and smaller grade 60 transverse bars.

Table 17: Probabilities of failing the performance objective for bars in production today bent to ACI 318-14 inside diameters

A615 Grade 60		
Bar Size	Target Bend Diameter Ratio	$P_{f,Total}$
#5	$\beta_{target}=4d_b$	64.1%
	$\beta_{target}=5d_b$	24.3%
	$\beta_{target}=6d_b$	5.5%
#8	$\beta_{target}=6d_b$	5.1%
#11	$\beta_{target}=8d_b$	2.1%

A706 Grade 60		
Bar Size	Target Bend Diameter Ratio	$P_{f,Total}$
#5	$\beta_{target}=4d_b$	22.7%
	$\beta_{target}=5d_b$	1.7%
	$\beta_{target}=6d_b$	0.1%
#8	$\beta_{target}=6d_b$	1.2%
#11	$\beta_{target}=8d_b$	0.0%

DUAL A615/A706 Grade 60		
Bar Size	Target Bend Diameter Ratio	$P_{f,Total}$
#5	$\beta_{target}=4d_b$	31.0%
	$\beta_{target}=5d_b$	3.6%
	$\beta_{target}=6d_b$	0.2%
#8	$\beta_{target}=6d_b$	0.0%
#11	$\beta_{target}=8d_b$	0.0%

5.4.2 Required Bend Diameters to Achieve Target Probabilities of Failure Based on Production Data

The target bend diameter ratios required to achieve a given probability of failing the yield performance objective (β_{Pf}) are presented in Table 18 for all bar types and grades, for which sufficient elongation data was available in the CRSI database. The ratios were calculated for the probabilities of failure of 2%, 5%, 10%, and 20%.

As can be seen in Table 17 a bend diameter ratio of 4.0, which is specified in ACI 318-14 for #5 and smaller transverse bars, should not be used for any of the grades and types of #5 bars considered, even if probabilities of failure of 20% are accepted. However, grade 60 ASTM A706 and dual grade #5 bars do come close to being able to be bent to a ratio of 4.0.

Table 19 presents recommended target bar bend inside diameters through bend ratios that achieve probabilities of failure within 5% for most bar types and grades. In cases where results support reducing the bend diameters prescribed in ACI 318-14, the recommended bend diameters were not reduced as that may have unintended consequences on the performance of concrete around the bends. Departures from currently prescribed bend diameter ratios in ACI 318-14 are highlighted in the table. Notably, A615 and A706 #5 and smaller transverse bars are recommended to be bent to at least a bend diameter ratio of 5.0 for grade 60 and 80 and 6.0 for grade 100. Grade 100 A615 longitudinal bars are recommended to be bent to a ratio of 9.0 for #9 to #11 bars and 8.0 for #6 to #8 bars. It is noteworthy the latter recommendation for #6 to #8 grade 100 bars is made without the support of elongation data.

Table 18: Target bend diameter ratios required to achieve a given probability of failing the yield performance objective

		Bar Size	ε_f		$\beta_{Pf=2\%}$	$\beta_{Pf=5\%}$	$\beta_{Pf=10\%}$	$\beta_{Pf=20\%}$
			μ	σ				
ASTM A615	Grade 60	5	0.132	0.018	6.6	6.1	5.6	5.2
		8	0.137	0.021	6.6	6.0	5.5	5.0
		11	0.131	0.026	8.0	7.0	6.2	5.5
	Grade 80	5	0.123	0.016	7.0	6.5	6.0	5.5
		8	0.132	0.013	6.0	5.7	5.4	5.0
		11	0.123	0.02	7.7	6.9	6.3	5.7
	Grade 100	5	N/A	N/A	N/A	N/A	N/A	N/A
		8	N/A	N/A	N/A	N/A	N/A	N/A
		11	0.096	0.017	10.4	9.3	8.4	7.5
ASTM A706	Grade 60	5	0.16	0.017	4.9	4.6	4.4	4.1
		8	0.162	0.026	5.6	5.1	4.6	4.2
		11	0.149	0.027	6.6	5.8	5.3	4.7
	Grade 80	5	0.129	0.011	6.0	5.7	5.4	5.1
		8	0.134	0.014	6.0	5.6	5.3	5.0
		11	0.139	0.018	6.1	5.6	5.3	4.8
DUAL ASTM A615/A706	Grade 60	5	0.154	0.017	5.2	4.9	4.6	4.3
		8	0.165	0.017	4.7	4.4	4.2	3.9
		11	0.172	0.021	4.7	4.4	4.1	3.8
	Grade 80	5	N/A	N/A	N/A	N/A	N/A	N/A
		8	N/A	N/A	N/A	N/A	N/A	N/A
		11	N/A	N/A	N/A	N/A	N/A	N/A

Table 19: Recommended target bar bend diameter ratios

		Bar Size	β_{ACI}	β_{Recom}
ASTM A615	Grade 60	3 to 5 Transverse	4.0	5.0*
		3 to 5 Longitudinal	6.0	6.0
		6 to 8	6.0	6.0
		11	8.0	8.0
	Grade 80	3 to 5 Transverse	4.0	5.0*
		3 to 5 Longitudinal	6.0	6.0
		6 to 8	6.0	6.0
		11	8.0	8.0
	Grade 100	3 to 5 Transverse	Not Specified	6.0
		3 to 5 Longitudinal	Not Specified	6.0
		6 to 8	Not Specified	8.0
		9 to 11	Not Specified	9.0
ASTM A706	Grade 60	3 to 5 Transverse	4.0	5.0
		3 to 5 Longitudinal	6.0	6.0
		6 to 8	6.0	6.0
		9 to 11	8.0	8.0
	Grade 80	3 to 5 Transverse	4.0	5.0
		3 to 5 Longitudinal	6.0	6.0
		6 to 8	6.0	6.0
		9 to 11	8.0	8.0

* these bend ratios result in higher than 5% probabilities of failure, which is deemed acceptable since the A615 bars are used in non-seismic applications

Chapter 6: Summary and Conclusions

Summary

Bend/re-bend tests were conducted on reinforcing bars with yield strengths ranging from 60 ksi to approximately 120 ksi. Strain aging tests were also conducted on the bars to ensure that the bar bends were re-bent after most of the strain aging embrittlement effects had occurred. The bend/re-bend test variables were: bar grade, bar manufacturing process, bar diameter (d_b), and bend inside diameter. High-strength reinforcing bars (grade 80 and above) produced using the most prevalent methods in the U.S. were obtained from four of the main manufacturers in the U.S. Bar sizes were #5, #8, and #11 and the bars were bent to meet the minimum specified ACI 318-14 bend diameters for each of the sizes. #5 bars were bent with inside bend diameters of 4 bar diameters (transverse steel requirement) to 6 bar diameters (longitudinal steel requirements). The bar specimens were bent into a V-shape and pulled in tension until fracture. All bars were bent and tested at a temperature of about 20°C. An optical measurement system was used to record bars strains and changes in the bend angle during re-bending. Performance measures used to quantify the performance of bends included:

a) The remaining bend angle at fracture during re-bending (θ_b)
b) The axial strain at fracture normalized by the bar uniform elongation strain (ε_b / ε_{un})
c) The axial stress at fracture normalized by the bar yield strength (f_{ub} / f_y)
d) The axial stress in bar at fracture normalized by the bar tensile strength (f_{ub} / f_t)

Conclusions

The chemistry of the bars was found to affect the extent of strain aging significantly. The higher the concentration of Vanadium in the steel, which was used by some manufacturers to increase strength, the lower the embrittlement due to strain aging was found. Overall, however, strain aging embrittlement never resulted in more than a 20% reduction in bar fracture strains.

Overall, for all bar sizes and types, as bar strength (or grade) increased, bend performance decreased as demonstrated by lower stresses, strains, and changes in the bend angle at fracture during re-bending. Moreover, for all bar types, as the bend inside diameter increased, bend performance was seen to improve.

Overall, bends in #8 and #11 bars were found to perform adequately at the current ACI 318-14 minimum bend diameters for all grades. Most #8 and #11 bar bends strengthened fully, prior to fracturing at stresses above yield and at relatively large inelastic strains.

Bends in #5 bars showed significantly varied performance. Grade 60 #5 bars, bent to achieve a target inside diameter of $4d_b$, were able to reach stresses close to yield prior to fracture during re-bending. Bends in grade 80 and 100 bars, however, only reached fractions of their yield strength during re-bending when bent to achieve a $4d_b$ inside diameter. The performance of bends in higher grade #5 bars reached larger stresses and strains as the bend diameter was increased, with grade 80 bars reaching stresses close to their yield with $5d_b$ bends and grade 100 bars reaching yield strengths with bend diameters of $6d_b$.

A relationship was derived between the bend inside diameter and the theoretical peak tensile strain at the bend. This relationship indicates that the ratio of bend diameter to bar diameter (β) governs the level of strain applied during bending; i.e., given the same bend ratio, the theoretical peak strains incurred at bar bends will be the same regardless of bar size. The relation derived assumes zero net strain at the bar centerline and therefore only applies to bending processes where bars are free to move longitudinally during bending. The relation does not apply to simultaneous double bending applications that can introduce additional tensile strains due to longitudinal restraint during bending. Strain parameters were obtained by

normalizing the theoretical peak strains incurred during bending by the bar uniform or fracture strain capacities ($\varepsilon_{ma}/\varepsilon_{un}$ or $\varepsilon_{ma}/\varepsilon_{f}$). The parameters were found to be negatively correlated with all performance measures. As bending strains increased with respect strain capacities, bent specimens were found to sustain lower stress and strain at fracture during re-bending. To achieve specimens that reached at least their yield stress at fracture, it was found that the $\varepsilon_{ma}/\varepsilon_{un}$ should not exceed 1.2, or $\varepsilon_{ma}/\varepsilon_{f}$ should not exceed 0.8, which corresponds approximately to target inside bend diameters of no less than $4d_b$ for the grade 60, $5d_b$ for the grade 80, and $6d_b$ for the grade 100 bars tested in this study.

To generalize recommendations for bar bend diameters, relations between ASTM minimum fracture elongation values as well as actual production elongation values obtain from the CRSI Mill Database were studied. In this study, bar bends that are able to sustain their yield strength during re-bending were deemed to have acceptable performance.

When setting bar fracture elongations equal to the minimum ASTM fracture elongation limits, most bar bends of grade 60 and 80 ASTM A706 were found to have acceptable performance. On the other hand, the vast majority of grade 60 A615 and A1035 bar bends, regardless of grade, were found to have unacceptable performance, which is contrary to observed bend performance in concrete members. This was attributed to the fact that bars generally exceed the minimum ASTM specified elongation by a substantial margin.

A statistical analysis was conducted to determine the probability of failure, or not achieving the performance objective, for bar bends using the statistical distribution of fracture elongations obtained from the CRSI Mill Database for 2015. The analysis showed that grade 60 bars in production today should have acceptable performance based on their measured fracture elongation down to a bend diameter of $5d_b$. This finding corroborated that the selected performance objective is a reasonable measure of performance for bar bends in concrete structures. At a bend diameter of $4d_b$, however, a large portion of grade 60 bars did not achieve acceptable performance. Increasing the minimum bend diameter for 4 d_b to $5d_b$ for # 5 and smaller bars is therefore recommended for grade 60 bars.

The statistical analysis was extended using elongation values for grade 80 and 100 bars obtained from the CRSI Mill Database. Recommendations for bar bend diameters for various A615 and A706 grades and bar sizes were provided to achieve a probability of failing the yield stress performance objective around 5%, for most cases. Departures from currently prescribed bend diameter ration in ACI 318-14 were highlighted. Notably, A615 and A706 #5 and smaller transverse bars were recommended to be bent to a bend diameter ratio of at least 5.0 for grade 60 and 80 and 6.0 for grade 100. Grade 100 A615 longitudinal bars are recommended to be bent to a ratio of at least 9.0 for #9 to #11 bars and 8.0 for #6 to #8 bars.

Since the performance evaluations of bends based on ASTM minimum elongations estimate poor bend performance for a majority of bar types while those based on actual elongation values did not, results imply that the ACI 318-14 bend diameter specifications are relying on the inherent additional strain capacity of bars beyond the ASTM minimum values to achieve acceptable bend performance. The same is true for the recommended bend diameters.

Currently, ACI 318-14 provides minimum bar-bend diameters as a function of bar size mainly and bar application (transverse or longitudinal bars). However, as production methods evolve or higher and less ductile grades of bars are introduced, it may become necessary to set minimum bend diameters as a function of uniform or fracture elongations and possibly as a function of loading (i.e., seismic or non-seismic), such that bends achieve performance objectives that may be different.

The recommendations for minimum bar bend diameters provided in this study are based on current production elongation statistics. These recommendations will need to be adjusted if actual bar elongation values change significantly over time. Moreover, since all bending and testing was conducted at relatively warm ambient temperatures, cold weather bend performance may result in different bend performance at the recommended bend diameters. Low temperature bend performance should be assessed for cold weather regions.

References

[1] AS/NZS 4671:2001 (2001). "Steel Reinforcing Materials." Standards Australia/Standards New Zealand, Wellington, New Zealand.

[2] ASTM Standard A615/A615M-13 (2013). "Standard Specification for Deformed and Plain Carbon-Steel Bars for Concrete Reinforcement." ASTM International, West Conshohocken, PA.

[3] ASTM Standard A706/A706M-13 (2013). "Standard Specification for Low-Alloy Steel Deformed and Plain Bars for Concrete Reinforcement." ASTM International, West Conshohocken, PA.

[4] ASTM Standard A1035/A1035M-11 (2011). "Standard Specification for Deformed and Plain, Low-carbon, Chromium, Steel Bars for Concrete Reinforcement." ASTM International, West Conshohocken, PA.

[5] ASTM Standard E8/E8M-15a (2015). "Standard Test Methods for Tension Testing of Metallic Materials." ASTM International, West Conshohocken, PA.

[6] CRSI Material Properties and Bar Producers Committee and Mill Database Sub-Committee (2015) *CRSI Mill Database*. Schaumburg, IL.

[7] BS 4449:2005+A2:2009 (2005). "Steel for the reinforcement of concrete. Weldable reinforcing steel. Bar, coil and decoiled product. Specification ", BSI.ISBN: 978 0 580 64585 3

[8] G.T. Van Rooyen (1986). "The embrittlement of hardened, tempered low-alloy steel by strain aging." *Journal of the South African Institute of Minining Metallurgy*, vol. 86, no. 2. (1986): 67-72

[9] Hopkins, D., and Poole, R. (2008). "Grade 500E Reinforcing Steel: Tests on Micro-alloy and Quenched and Tempered samples available in New Zealand." Department of Building and Housing, Wellington, New Zealand, 11.

[10] Rashid M.S. (1976). "Strain Aging Kintetics of Vanadium or Titanium Strengthened High-Strength Low-Alloy Steels." Metallurgical Transactions A, vol. 7A, (1976): 497-503.